European Journal of Medicinal Chemistry 297 (2025) 117899

Contents lists available at ScienceDirect

European Journal of Medicinal Chemistry

journal homepage: www.elsevier.com/locate/ejmech

Research paper

Rational optimization of D3R/GSK-3β dual target-directed ligands as potential treatment for bipolar disorder: Design, synthesis, X-ray crystallography, molecular dynamics simulations, *in vitro* ADME, and *in vivo* pharmacokinetic studies

R.M.C. Di Martino [a,1,*], D. Russo [b,2], I. Penna [b,3], S. Demuro [a,c,4,5], A. Dalle Vedove [d], R. Spagnuolo [e,6], G. Ottonello [f], S.M. Bertozzi [f], M. Summa [g], J. Desantis [h], A. Valeri [i], L. Pruccoli [j], S.K. Tripathi [a], A. Tarozzi [j], P. Storici [k], S. Girotto [a,2], R. Bertorelli [g], A. Armirotti [f], G. Cruciani [h], T. Bandiera [b,7], A. Cavalli [a,c,8], G. Bottegoni [e,l,**]

[a] Computational and Chemical Biology, Istituto Italiano di Tecnologia, via Morego 30, 16163, Genova (GE), Italy
[b] D3 PharmaChemistry, Istituto Italiano di Tecnologia, via Morego 30, 16163, Genova (GE), Italy
[c] Department of Pharmacy and Biotechnology, University of Bologna, via Belmeloro 6, 40126, Bologna (BO), Italy
[d] Area Science Park, Padriciano 99, Trieste, Italy
[e] Department of Biomolecular Sciences, University of Urbino, Campus Scientifico Enrico Mattei, via Ca' Le Suore 2/4, 61029, Urbino (PU), Italy
[f] Analytical Chemistry Facility, Istituto Italiano di Tecnologia, via Morego 30, 16163, Genova (GE), Italy
[g] Translational Pharmacology Facility, Istituto Italiano di Tecnologia, via Morego 30, 16163, Genova (GE), Italy
[h] Department of Chemistry, Biology and Biotechnology, University of Perugia, via dell'Elce di Sotto 8, 06123, Perugia (PG), Italy
[i] Molecular Horizon srl, via Montelino 20, 06084, Bettona (PG), Italy
[j] Department for Life Quality Studies, University of Bologna, Corso d'Augusto 237, 47921, Rimini (RN), Italy
[k] Protein Targets for Drug Discovery Lab, Structural Biology, Elettra Sincrotrone Trieste, SS 14 Km 163.5 in AREA Science Park, Basovizza, Trieste, Italy
[l] School of Pharmacy, University of Birmingham, Edgbaston, B15 2TT, Birmingham, UK

ARTICLE INFO

Keywords:
Dopamine D3 receptor (D3R)
Glycogen synthase kinase-3β (GSK-3β)
Dual target-directed ligands
Multi-target compounds
Molecular dynamics
Bipolar disorder

ABSTRACT

Bipolar disorder is a complex neuropsychiatric condition with a significant unmet medical need, as current treatments lack disease-modifying properties and multimodal therapeutic effects. To overcome the limitations of single-target drugs, we designed dual-target ligands that combine partial agonism at the dopamine D3 receptor (D3R) with inhibition of glycogen synthase kinase-3β (GSK-3β). We previously identified ARN24161 (**1**) as a promising prototype, demonstrating partial agonism at D3R (EC_{50} = 10.1 nM, % Eff. = 26.3) and GSK-3β inhibition (IC_{50} = 561 nM). However, its drug-like properties remained suboptimal. To optimize this compound, we initiated a multidisciplinary refinement campaign, leveraging computational modeling and crystallographic data to fine-tune the balance between D3R and GSK-3β activity, reduce P-glycoprotein (P-gp) affinity, and improve the pharmacokinetic profile. This effort led to the identification of ARN25297 (**5**), a moderately balanced dual-target ligand that exhibits partial agonism at D3R (EC_{50} = 13.1 nM, % Eff. = 17.1) and potent

* Corresponding author. Computational and Chemical Biology, Istituto Italiano di Tecnologia, via Morego 30, 16163, Genova (GE), Italy
** Corresponding author. Department of Biomolecular Sciences, University of Urbino, Campus Scientifico Enrico Mattei, via Ca' Le Suore 2/4, 61029, Urbino, PU, Italy.
E-mail addresses: rita.dimartino@uniupo.it (R.M.C. Di Martino), giovanni.bottegoni@uniurb.it (G. Bottegoni).
[1] Present address: Department of Pharmaceutical Sciences, University of Piemonte Orientale, via Largo Donegani 2, 28100, Novara (NO), Italy
[2] Present address: Structural Biophysics Facility, Istituto Italiano di Tecnologia, via Morego 30, 16163, Genova (GE)
[3] Present address: Medicinal Chemistry and Technologies for Drug Discovery and Delivery Facility, Istituto Italiano di Tecnologia, via Morego 30, 16163, Genova (GE), Italy
[4] Present address: Department of Medicine and Division of Endocrinology, Stanford University, Stanford, CA 94305, USA
[5] Present address: Medicinal Chemistry Knowledge Center, Sarafan ChEM-H, Stanford University, Stanford, CA 94305, USA
[6] Present address: Department of Pharmacy and Biotechnology, University of Bologna, via Belmeloro 6, 40126, Bologna (BO), Italy
[7] Present address: Istituto Italiano di Tecnologia, via Morego 30, 16163, Genova (GE)
[8] Present address: CECAM, EPFL, Avenue Forel 3, CH - 1015, Lausanne, Switzerland

https://doi.org/10.1016/j.ejmech.2025.117899
Received 3 March 2025; Received in revised form 31 May 2025; Accepted 20 June 2025
Available online 25 June 2025

GSK-3β inhibition (IC_{50} = 47.0 nM). Notably, ARN25657 (**16**) emerged as the most well-balanced candidate, demonstrating enhanced D3R partial agonism (EC_{50} = 15.2 nM, % Eff. = 37.7) alongside strong GSK-3β inhibition (IC_{50} = 19.3 nM). Compound **16** also exhibited the lowest P-gp inhibition and significant improvements in *in vitro* ADME properties compared to prototype **1**, while maintaining a balanced dual target profile. Although the PK profile of **16** remained comparable to that of prototype **1**, these findings lay the groundwork for further lead optimization and structural refinement, driving future *in vivo* proof-of-concept toward innovative therapeutic strategies for bipolar disorder and related neuropsychiatric conditions.

1. Introduction

Bipolar disorder (BD) is an umbrella term for complex neuropsychiatric disorders characterized by biphasic mood episodes of mania or hypomania and depression, which are expressed as changes in energy levels and behaviour [1]. The early onset, chronic nature, high prevalence (approximately 1 %), and lack of optimal treatment make these conditions among the world's most disabling [2]. In the last 30 years, the conventional concept of BD has transformed into a collection of interrelated disorders [1]. Understanding the pathophysiology of these disorders poses a significant challenge for contemporary research in psychiatry and neuroscience [3]. The dopamine (DA) hypothesis has highlighted the essential role of disrupted DA signaling in mesocorticolimbic circuits during both the manic and depressive phases of the disorder. From a molecular standpoint, elevated levels of DA receptors of the D2/3 subtypes (D2/D3Rs) result in hyperdopaminergia, contributing to mania. Conversely, a compensatory rise in DA transporter (DAT) levels decreases the DA tone, leading to depressive states [4]. Furthermore, the compromised activity of the versatile Ser/Thr kinase glycogen synthase kinase-3β (GSK-3β) within the signaling pathways implicated in neurodevelopment and the regulation of functions and structures within the nervous system (such as Wnt and neurotrophic factor signaling pathways) has been associated with the initiation and advancement of several psychiatric disorders, including BD [5–7]. Notably, in conditions of hyperdopaminergia, the activation of D2-like receptors not only modulates G protein/cAMP-dependent signaling but also initiates the Akt/GSK-3β signaling cascade via a non-canonical mechanism. This novel signaling pathway includes the

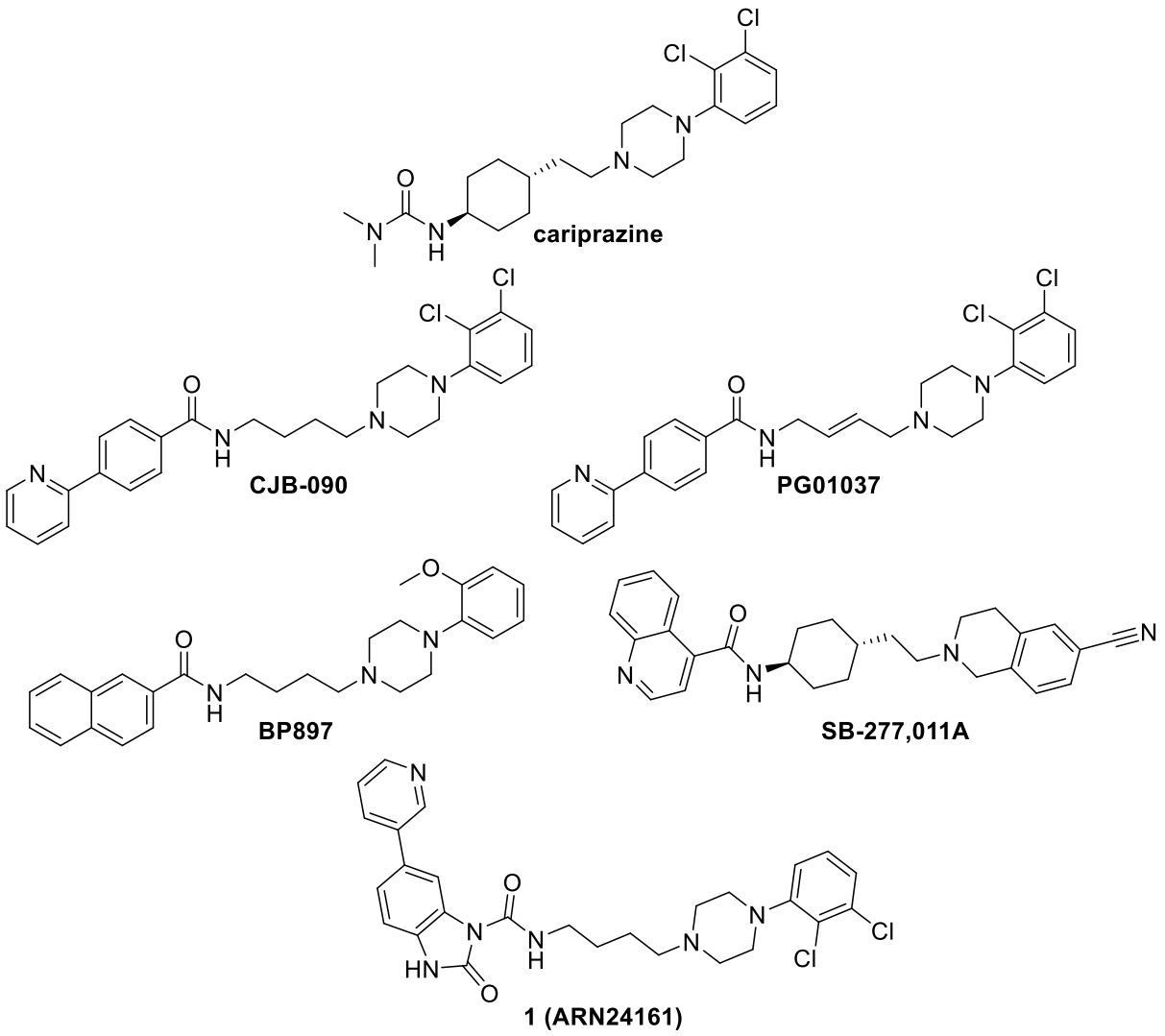

Fig. 1. Structures of representative potent and selective/preferred D3R partial agonists and antagonists, as well as structure of D3R partial agonist/GSK-3β inhibitor **1** (ARN24161).

involvement of the multifunctional scaffolding protein β-arrestin2, which has clinical implications in G protein-coupled receptor (GPCR) desensitization. This mechanism may play a significant role in mediating the antimanic effects of both mood stabilizers and antipsychotic drugs [8–10]. The latter serve as foundational elements in BD treatment and have gained approval from the US Food and Drug Administration (FDA) for use in monotherapy or combination therapy [11].

Among mood stabilizers, lithium stands as a first-line treatment for acute manic or mixed episodes, exhibiting very high efficacy in maintenance treatment [12,13]. Lithium is a direct inhibitor of GSK-3β, while also operating through an indirect mechanism that disrupts the D2R-mediated β-arrestin 2/Akt/GSK-3 signaling pathway. This pathway is distinct from G protein-dependent mechanisms, through which the D2R (and to a lesser extent the D3R) heighten GSK-3β activity [8,11,14].

Atypical antipsychotic agents are DA partial agonists and antagonists acting via the canonical G-protein dependent pathway [15,16]. Among them, cariprazine (Fig. 1), a D3R-preferring D2/D3R partial agonist approved in 2015 (D3R: EC_{50} = 2.09 nM (70.9 % E_{max}); D2R: EC_{50} = 3.16 nM (30 % E_{max}), has demonstrated efficacy on both positive and negative symptoms of BD [11,17–19]. Several studies have proposed a significant role for cariprazine's mild partial agonism/antagonism in the β-arrestin 2/Akt/GSK-3 signaling pathway, potentially mediating its antimanic properties [8,10].

Despite proven efficacy in clinical trials, single-target medications for BD are frequently affected by issues of tolerability and the occurrence of adverse effects, particularly when used for long-term maintenance [20]. In this framework, D3R partial agonists may be more effective and safer than full agonists or antagonists [21,22]. Therefore, there is a significant need for innovative research to illuminate novel disease-modifying and multifunctional treatments. Considering this context, the separate yet interrelated roles of D3R and GSK-3β in cognition and mood regulation have guided our attention to the multi-target-directed ligand (MTDL) approach as a practical polypharmacological solution. This approach aims at addressing the limitations of conventional single-target agents providing patients with substantial advantages [23–25].

We have recently reported the rational development of first-in-class D3R partial agonists/GSK-3β inhibitors relying on the combination of a 2,3-dichlorophenyl piperazine [26], a primary pharmacophore (PP) of potent and selective/preferred D3R partial agonists and antagonists (Fig. 1) [27–30] with a 2-oxo-2,3-dihydro-1*H*-benzimidazole moiety (found in potent GSK-3β ATP-competitive inhibitors) [31,32], through a four-methylene aliphatic linker, this latter still part of the D3R PP. A preliminary computer-assisted structure-activity relationship (SAR) study led us to the discovery of ARN24161 (**1**, Fig. 1), a promising prototype, in which the insertion of a 3-pyridine moiety at 6-position of the 2-oxo-benzimidazole increased the activity against the enzyme up to 561 nM, while retaining the partial agonism at D3R in the two-digit nanomolar range (EC_{50} = 10.1 nM, % Eff. = 26.3). Docking simulations confirmed the crucial role of the basic *N* piperazine atom for targeting Asp110$^{(3.32)}$ at the orthosteric binding pocket (OBP) of D3R and the 2-oxo-benzimidazole framework for engaging both the specificity binding pocket (SBP) of the GPCR and the hinge region in the ATP-binding pocket of the enzyme. Notably, the 3-pyridine seemed to fit in a strongly hydrophobic region of the kinase binding pocket likely capturing an additional H-bond with Lys85. In *in vitro* ADME and preliminary PK studies in mouse, compound **1** showed suboptimal drug-like properties: i) limited stability against metabolic reactions of phase 1 when incubated in mouse liver microsomes (MLM, $t_{1/2}$ = 18 min), ii) low oral bioavailability and iii) low brain exposure after oral administration. Notably, a 17-fold increase in brain penetration was observed after **1** co-administration with elacridar, a well-known P-gp inhibitor. This result suggested a potential interference of **1** with this ATP-dependent efflux transporter, which we further corroborated in a P-gp antagonism cell-based assay, in which derivative **1** showed inhibition of the P-gp-mediated acetoxymethyl calcein efflux by 48 % and 70 % at 1 and 10 μM, respectively [26].

In this study, we present our investigation supported by computational modeling and macromolecular crystallography to expand, starting from **1**, our understanding of the SAR for this class of compounds. The aim is to elucidate the structural components that contribute to a balanced activity profile involving GSK-3β and D3R, along with improvements in *in vitro* ADME and *in vivo* PK properties.

2. Results and discussion

2.1. Design

To better understand the structural factors influencing GSK-3β affinity and to home in on specific modifications to the scaffold of **1**, we conducted co-crystallization experiments of the compound with the enzyme. GSK-3β-**1** crystals were diffracted to a resolution of about 3.5 Å (PDB ID: 9HUK, Fig. 2), revealing unassigned positive electron density in the ATP-binding site. Upon density enhancement, the density was found to be compatible with **1** (see also Fig. S1A and B in the Supporting Information for the electron density maps). In agreement with the previously reported model of the bound conformation of **1** (orange structure in Fig. 2) [26], the 2-oxo-2,3-dihydro-1*H*-benzimidazole moiety, besides the exocyclic NH of the urea function, engaged the hinge region of the enzyme establishing three H-bonding interactions with the backbone of Val135 and Asp133. Furthermore, an additional H-bond was observed between the 3-pyridine of **1** and the side-chain amino group of Lys85. According to the docking model prediction, the arylpiperazine moiety of **1** appears to prefer a folded conformation away from the external solvent-accessible part of the enzyme pocket.

We performed an extensive SAR exploration around **1** to identify more promising dual D3R/GSK-3β modulators, increasing activity at GSK-3β, while retaining nanomolar affinity for D3R with partial agonist efficacy. Insights that we previously gained through the analysis of extended molecular dynamics (MD) simulations aimed at rationalizing the experimentally observed efficacies of *O*-aryl carbamate derivatives were instrumental to this goal [33]. Additionally, a deeper understanding of the structural basis for both selectivity and efficacy at D3R [16], along with the successful application of the multi-target paradigm to develop dual-target D3R ligands [34,35], significantly supported our optimization campaign. We designed and synthesized two different series of analogs by inserting tailored modifications in three different areas of the scaffold of **1** (Fig. 3): 1) 6-position of the 2-oxo-benzimidazole; 2) the pendant aryl ring on the PP; 3) the central spacer. Particular attention was directed to fine-tuning some physicochemical properties (*e.g.*,

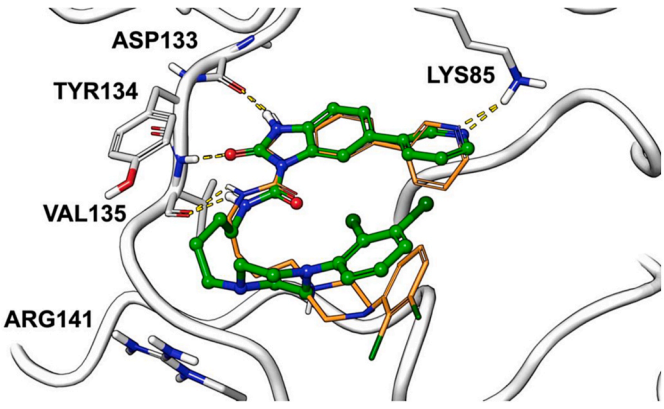

Fig. 2. X-ray structure of GSK-3β-**1** complex. **1** is reported in green carbon atoms. Relevant residues are reported in ball and stick representation and labeled explicitly. Yellow dash lines highlight H-bonds. The previously reported pose of **1** predicted by ligand docking is reported in thin orange sticks for comparison. (For interpretation of the references to color in this figure legend, the reader is referred to the Web version of this article.)

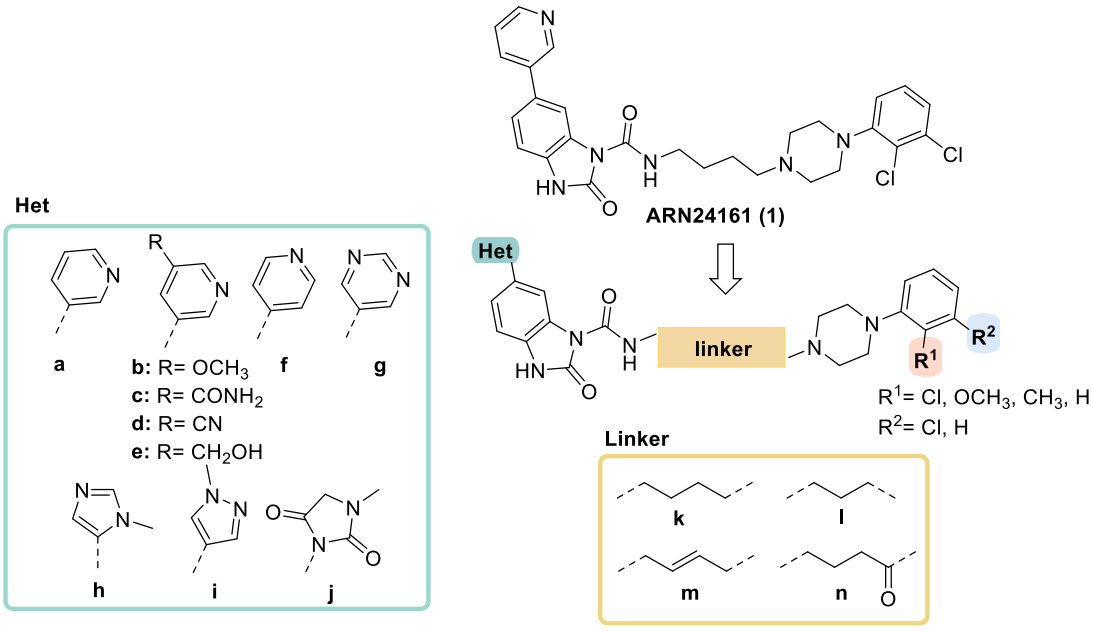

Fig. 3. Exploration of the chemical space around compound **1** (ARN24161).

logD, TPSA and pKa) to reduce the overall lipophilicity and basicity, as they are key determinants of drug-likeness and CNS permeability [36], as well as P-gp inhibition [37,38]. Furthermore, this was also crucial as MTDLs tend to grow in size and lipophilicity during the optimization process [39,40].

In series I, taking advantage of the essential role of the 3-pyridine in conferring affinity for GSK-3β, we addressed one structural modification at time on the 3-pyridine group, keeping constant both the linker and the PP of **1**. Three different strategies were applied: 1) incorporation of different groups (*i.e.*, methoxy (**2**), carbamoyl (**3**), cyano (**4**), and hydroxymethylene (**5**)) at 5-position; 2) shift of the *N* atom of the pyridine moiety from position 3 to 4 (**6**); 3) replacement of the 3-pyridine with other 5- and 6-membered nitrogen heterocycles (*i.e.*, pyrimidine (**7**), *N*-methylimidazole (**8**), *N*-methylpyrazole (**9**), and *N*-methylhydantoin (**10**)).

In series II, we devised 2-oxo-6-(pyridin-3-yl)-2,3-dihydro-1*H*-benzo[*d*]imidazole-1-carboxamide analogs that rely on a 3-methylene units' spacer (**11**) and a (*E*)-2-butenyl one (**12**) and different hexatomic aryl moieties on the piperazine (*i.e.*, phenyl (**13**), 2-methoxyphenyl (**14**) and 2-methylphenyl (**15**)). Furthermore, we also investigated the effect of combining two modifications at time on the central spacer and on the PP of **1**. Two novel phenylpiperazine derivatives were designed, which only differ in the chemical nature of the spacer: a propyl analog (**16**) and a (*E*)-2-butenyl derivative **17**. Finally, being aware of the detrimental effect of the piperazine basicity for GSK-3β inhibition given the proximity of the guanidine group of different Arg residues (*i.e.*, Arg141 and Arg144), we rationally designed analog **18**, where an amide function was incorporated at position 1 of the piperazine. Since the removal of this basic *N* piperazine atom results in a predictable loss of activity at D3R, we devised this compound as a tool to study GSK-3β inhibition.

2.2. Chemistry

The multistep synthetic protocol to access compound **1** analogs is depicted in Scheme 1. It was devised for controlling the regiochemistry of the key urea formation reaction between *in-house* prepared isocyanates **19**–**27** and *N-tert*-butoxycarbonyl (Boc)-5-heteroaryl-2-oxobenzimidazoles **28**–**37a**. The urea synthesis reaction was carried out under an Argon (Ar) atmosphere in dry CH_2Cl_2 at rt, affording *N*-Boc protected derivatives **38**–**54** in fair to excellent yields (48 %-quant.). A subsequent Boc deprotection was performed using TFA in dry CH_2Cl_2 or HCl (4 N) in 1,4-dioxane, followed by an alkaline work-up. The resulting products were then subjected to a final salification step using either HCl (1.25 or 3 N) in CH_3OH or HCl (4 N) in 1,4-dioxane, yielding the title compounds as HCl salts. Apart from derivative **15**, which was prepared as free base (74 %), and the hydrochloride salt **18** (86 %), all other compounds **2**–**14**, **16**, and **17** were isolated as trihydrochloride salts in good to very good yields (69–90 %).

Isocyanates **19**–**27** were freshly prepared by reacting amines **55**–**63** with triphosgene at 0 °C in dry CH_2Cl_2, in the presence of dry Et_3N, and under an Ar atmosphere. The resulting suspension of freshly prepared isocyanates was added dropwise to a stirred solution of the appropriate *N*-Boc-5-heteroaryl-2-oxobenzimidazole (Scheme 1).

A Gabriel-type synthesis gave amines **55**–**63** and two different synthetic routes were successful devised to access phthalimide intermediates **74**–**82**, depending on the chemical nature of the central linker (Scheme 2). Alkylation of commercially available arylpiperazines (**70**–**73**) with haloalkyl- (**64** and **65**) and haloalkenyl- (**68**) phthalimides, using potassium carbonate, as a base, under reflux and a further deprotection by hydrazine monohydrate treatment in CH_3OH at 80 °C, afforded amines **55**–**63** in fair to quantitative yields (53 %-quant.). (*E*)-2-(4-chlorobut-2-en-1-yl)isoindoline-1,3-dione (**68**) was, in turn, prepared *via* monosubstitution of (*E*)-1,4-dichloro-2-butene (**67**) with potassium phthalimide (**66**) in dry DMF at rt [41,42]. Lastly, acylation of 2,3-dichlorophenyl piperazine hydrochloride (**70**) with commercially available 4-(1,3-dioxoisoindolin-2-yl)butanoyl chloride (**69**) in dry pyridine and in the presence of dry Et_3N, as a base, followed by a hydrazine-mediated deprotection, afforded amine **63** (56 %).

N-Boc-5-heteroaryl-2-oxobenzimidazoles **28**–**37a** were prepared according to the synthetic procedure reported in Scheme 3. Likewise prototype **1**, Boc monoprotection at position 1 of 5-bromo-1,3-dihydro-2*H*-benzo[*d*]imidazole-2-one (**83**) afforded regioisomer of interest **84** [26], after flash chromatography purification; a further Pd-catalyzed Suzuki coupling reaction of this latter with *in-house* prepared boronate **85** (Scheme 4) and commercially available pyrimidin-5-ylboronic acid **86** gave **28** and **33**, respectively. The same protocol was not feasible to access intermediates **29**–**32a**, and **34**–**37a** due to the low stability of the Boc protecting group under aqueous basic conditions of the Suzuki coupling reaction. Therefore, the reactions' order was inverted by performing the Suzuki reaction between **83** and the appropriate

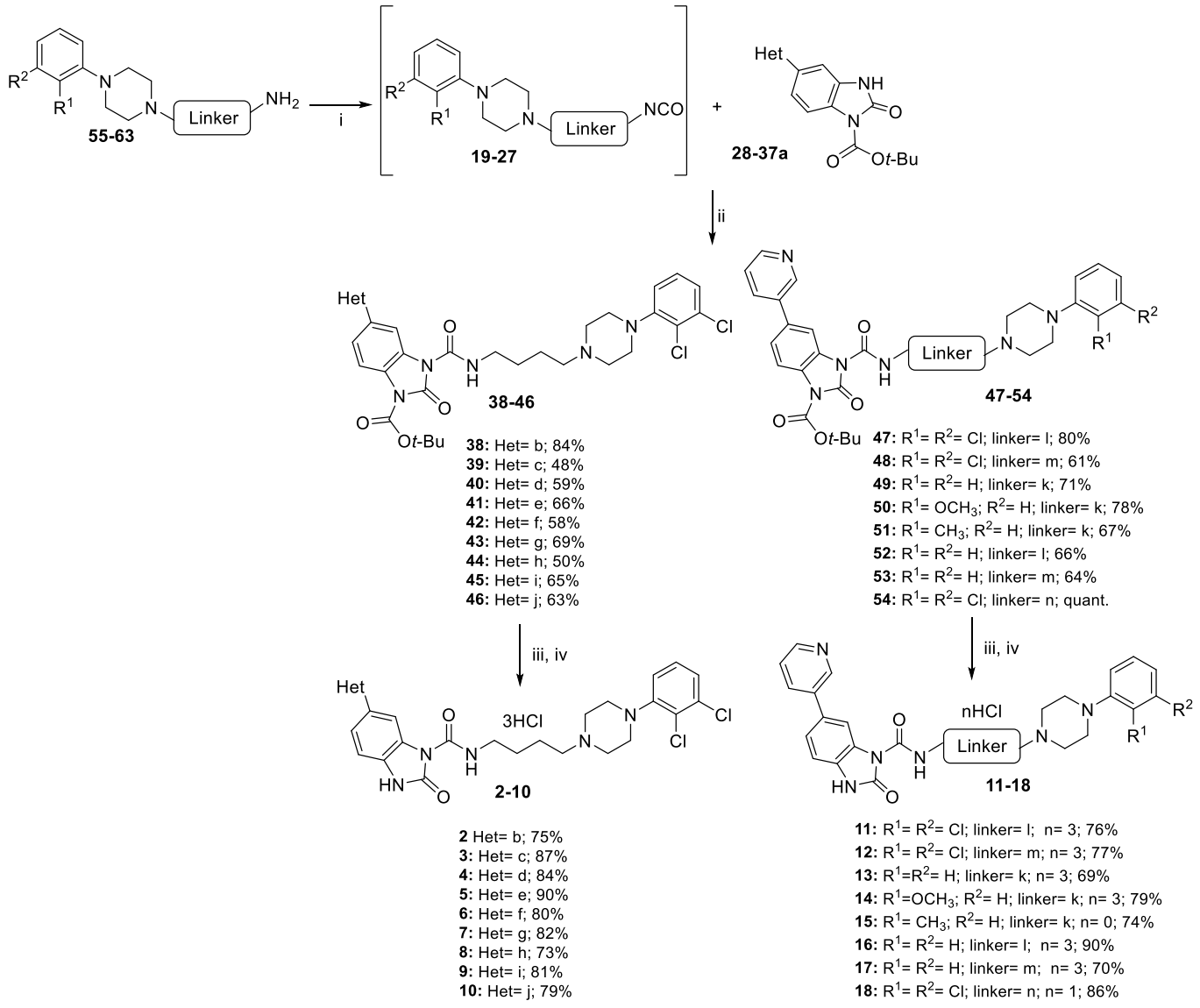

Scheme 1. Preparation of the final compounds of series I (**2**–**10**) and series II (**11**–**18**).[a]
[a]Reagents and conditions. i) triphosgene, dry Et_3N, dry CH_2Cl_2, 0 °C, Ar, 1 h and 30 min; ii) dry CH_2Cl_2, 0 °C to rt, Ar, 1 h and 20 min-2 days; iii) TFA, dry CH_2Cl_2, 0 °C to rt, 2 h-overnight (work-up with saturated aq $NaHCO_3$ solution), 54–92 %; iv) HCl (4 N) in 1,4-dioxane or HCl (1.25 or 3 N) in CH_3OH, 1,4-dioxane or CH_3OH, rt, 1 h.

commercially available boronic acids/boronic acid pinacol esters first, followed by the Boc monoprotection one. All desired intermediates were isolated as couples of regioisomers a and b, which were carefully separated through flash chromatography and whose regiochemistry was confirmed by 2D-NMR experiments including 2D-NOESY. Boronate esters **85** and **94** were, in turn, prepared with excellent yields through Miyaura borylation reaction starting from the corresponding bromines **95** and **96**, respectively (Scheme 4).

In Scheme 5, the multistep synthesis to access *N*-methylhydantoin intermediate **97** is depicted. First, Boc protection of *N*-methylglicine **98** by using Boc anhydride yielded **99**, which was then reacted with 5-amino-1,3-dihydro-2*H*-benzo[*d*]imidazole-2-one **100** under classical conditions of amide coupling reaction. TFA-mediated cleavage of the Boc protecting group of amide **101**, followed by SCX purification, gave **102** as a free base. Lastly, a CDI mediated cyclization afforded 1-methyl-3-(2-oxo-2,3-dihydro-1*H*-benzo[*d*]imidazole-5-yl)imidazolidine-2,4-dione (**97**).

2.3. Biological evaluation

All synthesized compounds were tested for their inhibitory activity against GSK-3β and partial agonism at D3R in a TR-FRET enzymatic assay and in a cAMP HTRF cell-based functional assay, respectively. Compounds with percentage efficacy (% Eff.) less than 20 were also assessed in a cAMP functional antagonism assay (see Tables 1 and 2). As expected, the majority of the tested compounds showed partial agonism at D3R with EC_{50} values in the low nanomolar range (1.1 nM ≤ EC_{50} ≥ 15.2 nM; 10.3 ≤ % Eff. ≥41.1). In series I, the replacement of the 3-pyridine moiety of prototype **1** with a 1-methylpyrazol-4-yl group (**9**) led to a slightly higher partial agonist (EC_{50} = 2.8 nM). In series II, a similar effect was observed with 2-methoxyphenyl analog **14** bearing a shorter aliphatic chain (EC_{50} = 1.1 nM) than **1**.

While insertion of unsaturation in the central linker (**12**) led to a predictable shift of activity from partial agonism to antagonism at D3R (IC_{50} = 29.2 nM), the combined removal of the chlorine atoms on the pendant phenyl ring (**17**) restored the partial agonism at the receptor with potency in the low nanomolar range (EC_{50} = 6.0 nM).

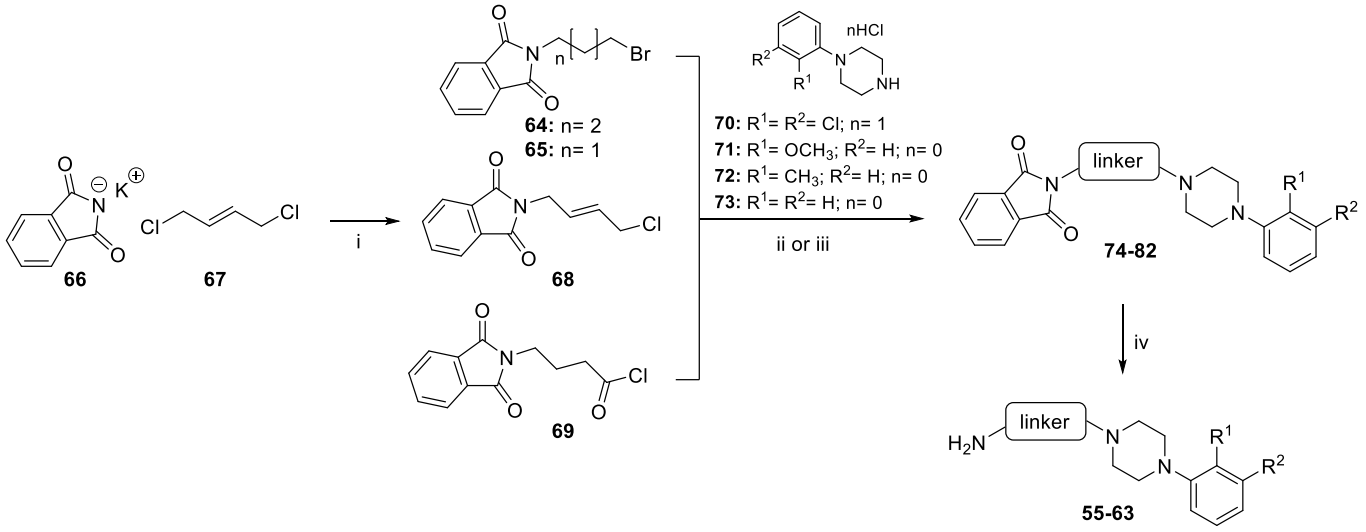

Scheme 2. Different synthetic routes for the preparation of phenylpiperazine-based amines **55**–**63**.[a]
[a]Reagents and conditions. i) dry DMF, rt, Ar, overnight, 72 %; ii) dry CH_3CN, K_2CO_3, 85 °C, 6 h, 83 %−quant.; iii) dry Et_3N, dry pyr, rt, 20 h, 69 %; iv) $NH_2NH_2{\cdot}H_2O$, CH_3OH, 80 °C, 2 h, then HCl (2 N), 1 h, 53 %−quant.

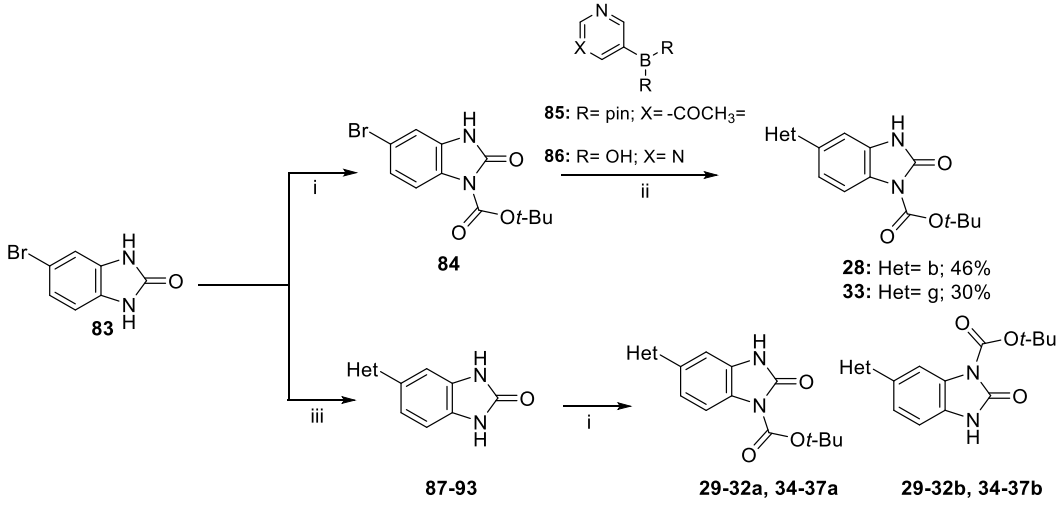

Scheme 3. Synthetic procedure to access *N*-Boc-5-heteroaryl-2-oxobenzimidazoles **28**–**37a**.
[a]Reagents and conditions: i) $(Boc)_2O$, NaH (60 % in mineral oil), dry DMF, rt, Ar, 3 h and 45 min-4 days, 11–43 %; ii) $PdCl_2(dppf){\cdot}CH_2Cl_2$, CH_3COOK, dry 1,4-dioxane, 80–90 °C (MW), Ar, 9–14 h; iii) aryl/heteroarylboronic acid, $PdCl_2(dppf){\cdot}CH_2Cl_2$, aq K_2CO_3 (2 M), 1,4-dioxane/H_2O (4:1) or dry DMF, 80–120 °C (MW), Ar, 1 h–3 h and 30 min, 55–98 %.

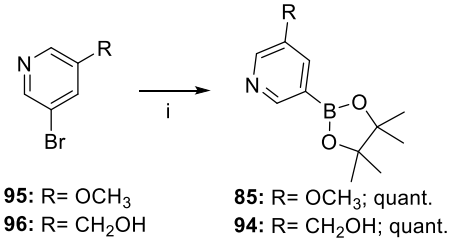

Scheme 4. Preparation of boronates **85** and **94**.[a]
[a]Reagents and conditions: i) bis(pinacolato)diboron, $PdCl_2(dppf){\cdot}CH_2Cl_2$, CH_3COOK, 1,4-dioxane, 85–160 °C (conventional heating or MW), Ar, 15 min-2 h.

Unpredictably, 5-cyano-3-pyridyl derivative (**4**) and 4-pyridyl compound (**6**) did not show agonism at D3R, but only antagonism with potency in the high nanomolar range (IC_{50} = 198.4 and 142.0 nM, respectively). A similar outcome was observed when we removed the aromaticity of the substituent at 6-position of the 2-oxobenzimidazole moiety (**10**) although a slightly more potent D3R antagonist (IC_{50} = 56.8 nM) was discovered. On the contrary, the installation of a 2-tolyl moiety on the piperazine (**15**) afforded a weak D3R antagonist (IC_{50} = 549.8 nM). The expected drop in potency (IC_{50} = 2769 nM) caused by switching off the basicity of the piperazine (**18**) was experimentally confirmed. All D3R partial agonists with low % efficacy (*i.e.*, **2**, **5**, **7**, **9**, and **11**) also showed antagonism at the same receptor albeit with higher values of IC_{50} ranging from 28.1 to 3790 nM.

Regarding GSK-3β inhibition, the structural modifications explored within both compounds' series provided a large variety of effects on the enzyme activity. A good correlation between higher inhibitory potency and lower values of pKa and logD was observed. In series I, the insertion

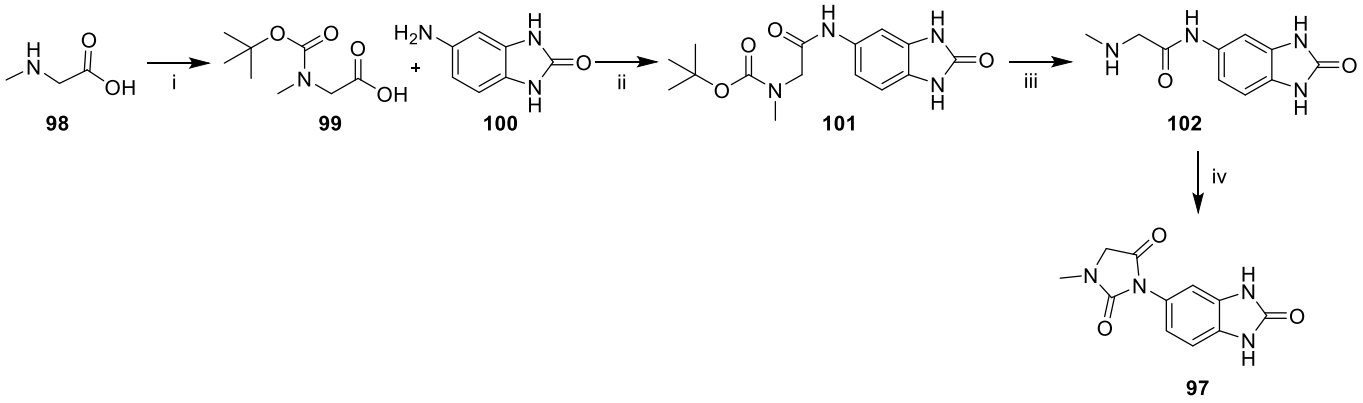

Scheme 5. Multi-step preparation of *N*-1-methyl-3-imidazolidine-2,4-dione intermediate **97**.[a]
[a]Reagent and conditions: i) $(Boc)_2O$, Et_3N, H_2O, rt, overnight, quant.; ii) EDC HCl, dry DMF, rt, overnight, Ar, 65 %; iii) TFA, dry CH_2Cl_2, 0 °C to rt, 4 h, (SCX purification), 96 %; (iv) CDI, DMAP, dry 1,4-dioxane/CH_3CN (7.5:1), 100 °C, overnight, 34 %.

Table 1
Chemical structures and biological data of derivatives of series I.

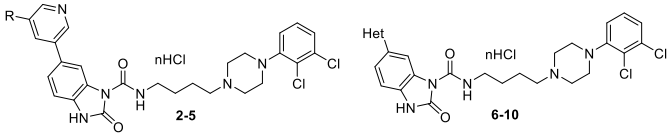

Comp	R/Het	n	logD (pH = 7.4)	TPSA	pKa	D3R[a] EC_{50} (nM)	D3R[b] % Eff.	GSK-3β[a] IC_{50} (nM) or % inh	D3R[c] IC_{50} (nM)
1 (ARN24161)	H	3	3.28	80.28	8.74	10.1 ± 0.4	26.3 ± 2.4	561.0 ± 40.5	
2	OCH_3	3	3.12	89.51	8.74	15.2 ± 0.7	11.0 ± 2.4	284.0 ± 22.6	59.2 ± 8.0
3	$CONH_2$	3	2.13	123.37	8.74	10.3 ± 0.5	22.3 ± 0.8	252.0 ± 17.6	
4	CN	3	3.14	104.1	8.74	n.a.	n.a.	n.d.	198.4 ± 16.2
5 (ARN25297)	CH_2OH	3	2.51	100.5	8.74	13.1 ± 2.1	17.1 ± 0.3	47.0 ± 7.8	37.7 ± 8.8
6		3	3.28	80.28	8.74	n.a.	n.a.	n.i.	142.0 ± 31.0
7		3	2.57	92.64	8.74	9.95 ± 0.03	15.5 ± 1.9	47.5 ± 4.8 % (1 μM)[d]	40.0 ± 7.9
8		3	2.50	83.52	8.74	9.59 ± 1.17	40.6 ± 7.6	138.0 ± 8.3	
9		3	2.93	83.52	8.74	2.8 ± 0.2	23.7 ± 0.5	140.0 ± 27.1	28.1 ± 6.3
10		2	1.53	108.54	8.74	n.a.	n.a.	6160 ± 1120	56.8 ± 10.9

logD values were predicted by using Chemaxon software (https://chemaxon.com).
TPSA values were predicted by using Chemdraw professional 20.0.
[a] EC_{50} and IC_{50} values are reported as a mean of three determinations.
[b] As of 300 nM DA.
[c] As of 10 nM DA.
[d] inh % at 1 μM (the highest dose tested due to poor solubility of compound **7** in the enzymatic assay buffer). n.a.: no activity in the agonism assay. n.i.: no inhibition up to 100 μM (the highest dose tested). n.d.: not determined due to poor compound solubility in the assay buffer.

of a methoxy (**2**) and carbamoyl function (**3**) at position 5 of the 3-pyridine improved the inhibitory activity against the enzyme in the same manner: the IC_{50} halved in the first case. It was reduced by 2.23 times in the second case compared to that of prototype **1**. A 4-fold increase of activity was displayed by the two *N*-methyl 5-memberedheterocycle-based derivatives **8** and **9** (IC_{50} = 138 and 140 nM, respectively), suggesting high enzyme tolerability for both 6-membered and 5-membered heterocycles at position 6 of the 2-oxobenzimidazole moiety. On the contrary, removal of the aromaticity at the same position, like in derivative **10**, had detrimental effects on GSK-3β inhibition (IC_{50} = 6.16 μM), as well as the replacement of the 3-pyridine substituent with a pyrimidine (**7**, 47.5 % inhibition at 1 μM). Furthermore, a loss of enzyme inhibition was observed when we replaced the 3-pyridine substituent of **1** with a 4-pyridine one (**6**). This result confirmed that the nitrogen atom at the 3-position on the heterocycle is optimal for establishing an H-bond with Lys85. The best results in terms of both GSK-3β inhibition and balancing activity at the main targets were achieved by decorating the 3-pyridine ring of **1** with a hydroxymethylene function (**5**). Indeed, in this

Table 2
Chemical structures and biological data of compounds of series II.

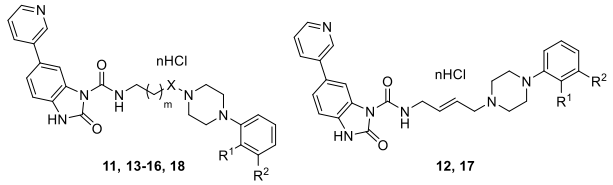

Comp	R^1	R^2	X	m	n	logD (pH = 7.4)	TPSA	pKa	D3R[a] EC_{50} (nM)	D3R[b] % Eff.	GSK-3β[a] IC_{50} (nM)	D3R[c] IC_{50} (nM)
11	Cl	Cl	CH_2	1	3	3.20	80.28	8.26	12.1 ± 1.9	10.3 ± 3.5	123.0 ± 9.9	3790 ± 118.5
12	Cl	Cl	–	–	3	3.99	80.28	7.86	n.a.	n.a.	411.0 ± 101	29.2 ± 2.1
13	H	H	CH_2	2	3	1.91	80.28	8.91	8.5 ± 2.7	41.1 ± 4.8	66.3 ± 11.6	
14	OCH_3	H	CH_2	2	3	1.87	89.51	8.79	1.1 ± 0.2	35.0 ± 6.1	126.0 ± 14.1	
15	CH_3	H	CH_2	2	0	2.41	80.28	8.92	n.a.	n.a.	85.7 ± 15.4	549.8 ± 31.3
16 (ARN25657)	H	H	CH_2	1	3	1.84	80.28	8.43	15.2 ± 2.0	37.7 ± 1.7	19.3 ± 2.7	
17	H	H	–	–	3	2.65	80.28	8.03	6.0 ± 1.1	33.8 ± 3.5	120.0 ± 8.2	
18	Cl	Cl	CO	2	1	3.68	97.35	4.72	n.a.	n.a.	69.3 ± 9.2	2769 ± 250 (partial)

LogD values were predicted by using Chemaxon software (https://chemaxon.com).
TPSA values were predicted by using Chemdraw professional 20.0.
[a] EC_{50} and IC_{50} values are reported as a mean of three determinations.
[b] As of 300 nM DA.
[c] As of 10 nM DA. n.a.: no activity in the agonism assay.

latter compound, we boosted the inhibitory potency against the enzyme down to 47.0 nM, obtaining a quite-balanced dual D3R partial agonist/GSK-3β inhibitor. On the contrary, decoration of the 3-pyridine ring with a cyano group afforded derivative **4**, whose IC_{50} value could not be measured because of its poor solubility in the assay buffer.

In series II, the rigidification of the central linker (**12**) by introduction of a double bond gave a slightly more potent GSK-3β inhibitor (IC_{50} = 411 nM) compared to **1**, while a 4-fold increase of enzyme inhibition (IC_{50} = 120 nM) was observed with the unsubstituted phenylpiperazine derivative **17**, bearing a trans 2-butene as central linker. A similar effect (IC_{50} value around 120 nM) was observed reducing by one methylene unit the length of the central spacer (**11**) and with 2-methoxypheylpiperazine derivative **14**. A progressive and significant increase of GSK-3β inhibition was observed with 2-tolyl-based analog (**15**) and phenylpiperazine-based compound **13** (6.5-fold and 8.5-fold increase, respectively). Moreover, removing the piperazine basicity in derivative **18** led to the expected increase in GSK-3β inhibition (IC_{50} = 69.3 nM), highlighting that the Coulombic repulsion between the protonated guanidine groups of surrounding arginine residues (Arg141 and Arg144) and the piperazine moiety in **1** and its analogs is detrimental to activity. Of note, the combination of two favorable modifications for GSK-3β inhibition, namely a 3-methylene units' linker and an unsubstituted simple phenyl ring on the piperazine (**16**), boosted the inhibitory activity against the enzyme (IC_{50} = 19.3 nM). Indeed, **16** (ARN25657) turned out to be the best well-balanced dual D3R/GSK-3β modulator (EC_{50} = 15.2 nM/IC_{50} = 19.3 nM).

2.4. *In vitro* ADME profiling and P-gp inhibition

Bearing in mind the metabolic vulnerability of prototype **1** when incubated with MLM, we assessed some balanced D3R/GSK-3β modulators for *in vitro* ADME properties including liver microsome stability (Ph1 and Ph2) in both mouse (M) and human (H), as well as plasma stability in both species. As reported in Table 3, similar to our prototype, all derivatives showed good stability in both H- and M-plasma, against Ph2 metabolic biotransformation in both MLM and HLM, and Ph1 metabolic reactions in HLM. Regarding MLM (Ph1) stability, we successfully overcame the liability of **1** ($t_{1/2}$= 18 min) by simply replacing the 3-pyridine moiety with a *N*-methylimidazole (**8**, $t_{1/2}$= >60 min) and by combing the three methylene units' central spacer with a phenylpiperazine as a PP, while retaining the 3-pyridine on the 2-oxobenzimidazole group (**16**, $t_{1/2}$ = 55 min). On the contrary, single modifications as the introduction of a hydroxymethyl function at position 5 of the 3-pyridine ring (**5**, $t_{1/2}$ = 18 min) and the length reduction of the central linker from four to three methylene units (**11**, $t_{1/2}$ = 20 min) did not improve MLM stability. Finally, the two phenylpiperazine-based derivatives (**13** and **17**) displayed lower stability ($t_{1/2}$ = 9 min) compared to compound **1**, suggesting a higher susceptibility of the terminal phenyl

Table 3
In vitro stability and P-gp inhibition studies on selected dual D3R/GSK-3β modulators.

Comp	MLM (Ph1) $t_{1/2}$ (min)	MLM (Ph2) $t_{1/2}$ (min)	HLM (Ph1) $t_{1/2}$ (min)	HLM (Ph2) $t_{1/2}$ (min)	M-plasma $t_{1/2}$ (min)	H-plasma $t_{1/2}$ (min)	P-gp inh. (%)
1 (ARN24161)	18 ± 2	>60	>60	>60	>120	>120	47.9 (1 μM) 69.8 (10 μM)
5 (ARN25297)	18 ± 1	45 ± 2	>60	>60	>120	103	1.3 (1 μM) 35.3 (10 μM)
8	>60	>60	>60	>60	>120	92 ± 8	8.6 (1 μM) 79.7 (10 μM)
11	20 ± 4	>60	>60	>60	88 ± 1	79 ± 6	n.d.
13	9 ± 1	36 ± 3	>60	>60	>120	>120	5.2 (1 μM) 56.1 (10 μM)
16 (ARN25657)	55 ± 9	>60	>60	>60	>120	>120	4.2 (1 μM) 10.9 (10 μM)
17	9 ± 3	51 ± 9	>60	>60	>120	>120	n.d.

ring to undergo Ph1 biotransformations in MLM.

The keystone of our optimization strategy was to decrease the overall lipophilicity and to slightly reduce the basicity for fine-tuning GSK-3β affinity [7], as well as P-gp inhibition while preserving affinity and proper efficacy at D3R. Therefore, we also investigated the effect of some tailored modifications on inhibition of P-gp-mediated acetoxymethyl calcein efflux in MDR1-MDCKII cells, which is measured as a proxy for P-gp interaction. All compounds were tested at 1 and 10 μM, and verapamil was used as a reference compound. As shown in Table 3, a desired reduction in P-gp inhibition was observed as the logD of the tested molecules decreased; the positive trend was clearer at 10 μM than it was at 1 μM. The replacement of the 3-pyridine moiety of **1** with a *N*-methylimidazole ring (**8**) lowered logD value from 3.28 to 2.50 leading to a drop in P-gp inhibition at 1 μM concentration (8.6 %). The insertion of a hydroxymethyl function on the 3-pyridine (**5**) significantly reduced P-gp inhibition at both tested concentrations. Very good results in terms of both logD and P-gp inhibition were also obtained when we replaced the pendant 2,3-dichlorophenyl ring of **1** with a simple phenyl moiety (**13**). Of note, the best well-balanced dual D3R partial agonist/GSK-3β inhibitor **16** displayed the lowest logD (1.84) as well as the lowest percentage of inhibition (10.9 %) of the ATP-dependent efflux transporter at 10 μM concentration among the tested compounds.

To better understand the metabolism operated by human Cytochromes P450, we decided to carry out a metabolite identification (MetID) study in HLM. Samples were analyzed by LC-MS/MS and raw data were processed by using the Mass-MetaSite protocol and WebMetabase software (Mass-Analytica™) [43,44] for automatic metabolite identification and structure elucidation. We studied prototype **1**, the quite balanced hydroxymethyl-derivative **5** and the best well-balanced analog **16**. Each compound was tested at 5 μM and the percentage of remaining compound as well as the percentage of metabolites formed were monitored at different incubation times (*i.e.*, 0.5, 15, 30, and 60 min, see Supporting Information for more details).

All three tested derivatives underwent both aromatic and nonaromatic hydroxylation reactions as well as *N*-dealkylation, as depicted in Figs. 4–6. Remarkably, the 2,3-dichlorophenylpiperazine was found as the most abundant metabolite of both **1** (M6, Fig. 4 and Fig. S2A and B in the Supporting Information) and **5** (M6, Fig. 5 and Fig. S2C and D in the Supporting Information), while an aliphatic hydroxylation reaction product (M3, Fig. 6 and Fig. S2E and F in the Supporting Information) was identified as the predominant metabolite of **16**.

2.5. GSK-3β inhibition in cells

To confirm the ability of compounds **5** (ARN25297) and **16** (ARN25657) to induce GSK-3β inhibition in a cellular context, neuronal SH-SY5Y cells were treated with the compounds at the concentrations of 0.5–1 μM and 1–5 μM, respectively, for 3 h. A preliminary *in vitro* cytotoxicity assessment in SH-SY5Y cells was performed to identify non-cytotoxic concentration ranges for both compounds (Fig. S3 in the Supporting Information). At the end of incubation, phospho-GSK-3α/β (Ser21/9) levels and total GSK-3β protein were analyzed by western blotting. As shown in Fig. 7A, compound **5** significantly inhibits GSK-3β activity, reflected by an increase in the inactive phospho-GSK-3α/β (Ser21/9) form, only at the concentration of 1 μM, with no effect observed at 0.5 μM. In contrast, compound **16** significantly inhibits GSK-3β activity at all tested concentrations in a dose-dependent manner (Fig. 7B). Interestingly, compound **16** showed a stronger activity compared to **5** at the same concentration of 1 μM (Fig. 7C).

2.6. In vivo PK studies

On the basis of *in vitro* ADME profile, logD and P-gp inhibition data, as well as inhibition of GSK-3β activity in SH-SY5Y cells, **16** (ARN25657)

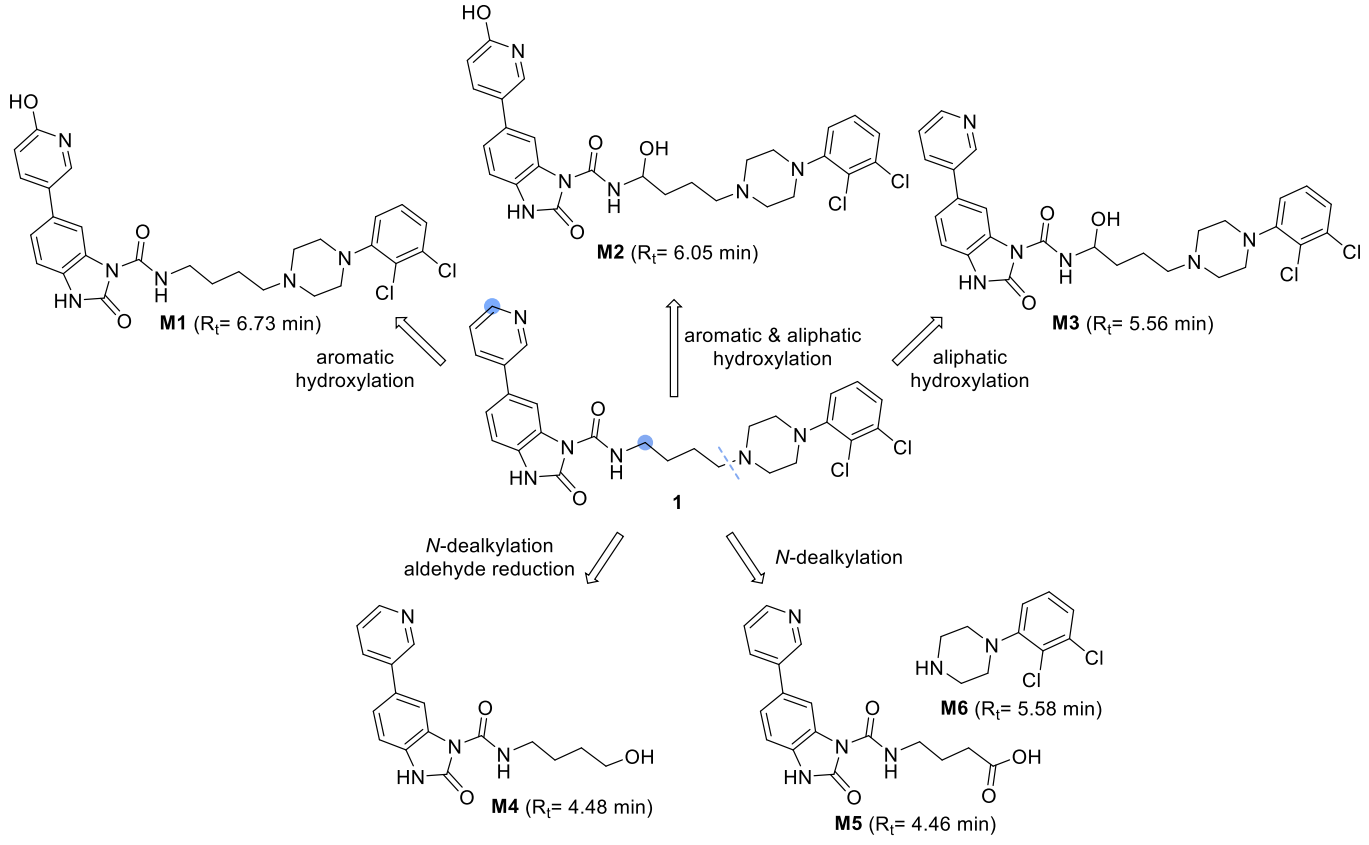

Fig. 4. Experimental sites of metabolism for prototype **1**.

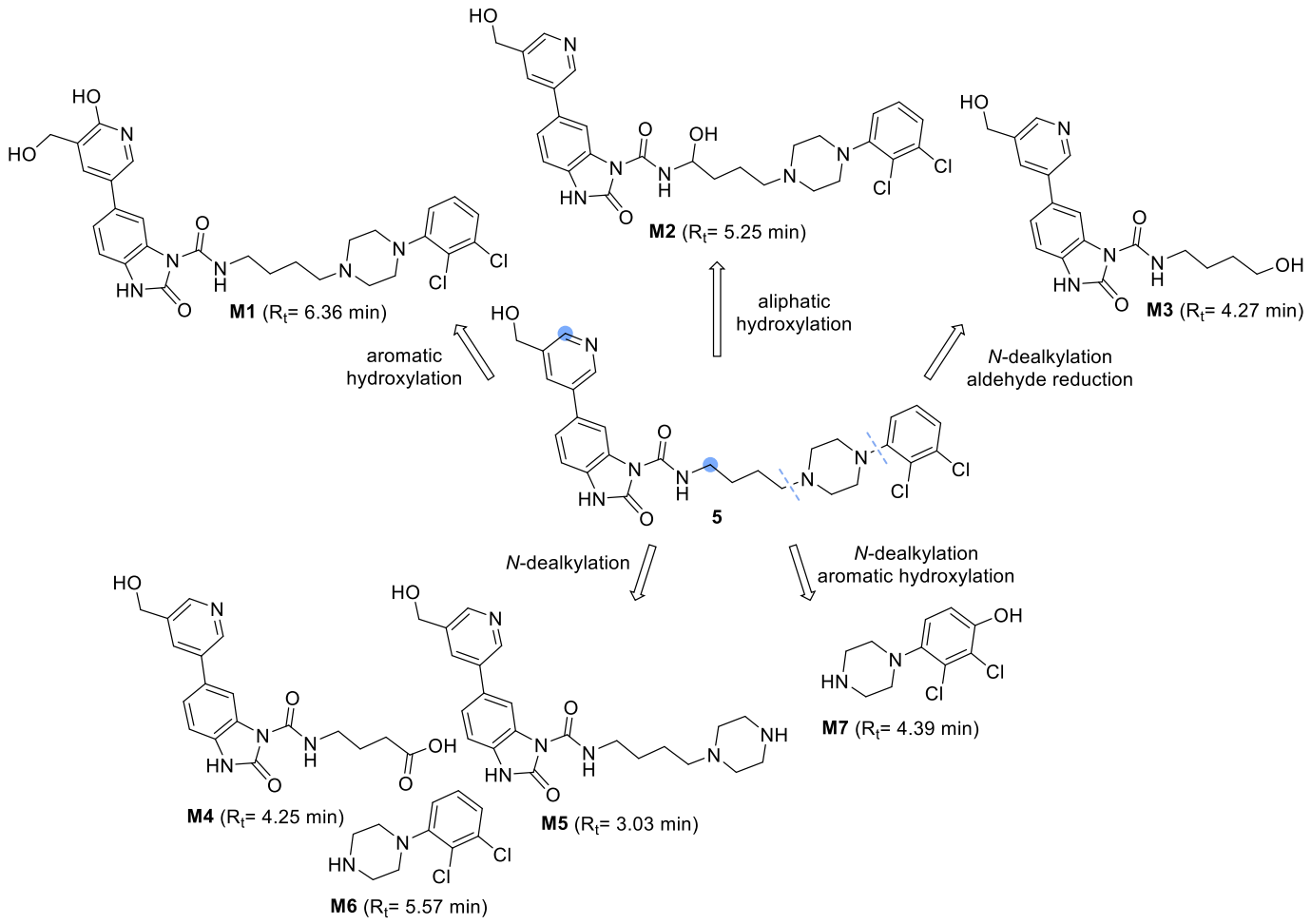

Fig. 5. Experimental sites of metabolism for compound **5**.

and **5** (ARN25297), as a back-up compound, were selected for *in vivo* pharmacokinetic (PK) study on C57BL/6J mice following both intravenous (I.V.) and oral (P.O.) administration at 3 and 10 mg/kg, respectively (Fig. 8). During the PK studies, both tested compounds proved to be well tolerated with no acute treatment-related toxicity. Compounds **16** and **5** displayed a C_{max} of 1429 ng/mL and 1677 ng/mL at 5 min after I.V. administration, respectively, and were still detectable after 4 h at a concentration of 3 ng/mL and 21 ng/mL, respectively. The profile of **16** declined within the first hour, and hereafter a half-life of ca. 40 min was observed. The back-up compound showed a decline within the first 30 min, followed by the elimination phase with a half-life of ca. 1 h.

After P.O. administration, **16** reached the maximum concentration (C_{max} = 678 ng/mL) within 15 min, faster than **5** (C_{max} = 76 ng/mL and T_{max} = 30 min), and both compounds remained detectable after 4 h with concentrations of 9 ng/mL and 2 ng/mL, respectively. Furthermore, in line with their mouse microsomal stability data, compound **16** showed a relatively high clearance (CL = 368 ml/min/kg), while **5** displayed a very high clearance (CL = 1566 ml/min/kg). Oral bioavailability was also estimated at 15 % for **16** and only 4 % for **5**. Conversely, after I.V. administration, both compounds **16** and **5** exhibited a moderate clearance (60 and 58 ml/min/kg, respectively).

In summary, compound **16** displayed a PK profile comparable to prototype **1** and marginally superior to the back-up compound **5** [26]. Unfortunately, despite having addressed the affinity for P-gp, low brain exposure was observed for compound **16** after both I.V. and P.O. administration (see Table S2 in the Supporting Information). Compound **5** was only detected in a low amount in the brain after I.V. administration (see Table S2 in the Supporting Information). These data suggest that the limited brain exposure displayed by **1** could not be completely explained by P-gp affinity. Further studies will be required to identify the structural determinants associated with poor brain exposure.

2.7. Off-target data

Despite low brain exposure levels, we decided to investigate the polypharmacological profile of **16** by assessing its activity on closely related targets selected on the basis of compound structure, mechanism of action, and putative therapeutic applications, in line with previous studies [41]. Competitive binding experiments using membrane preparations from different human recombinant cell lines were performed to assess binding affinities of **16** for some selected GPCRs (Table 5). Activity was measured by assessing the inhibition of binding of a radioactively labeled ligand specific to each target, with compound **16** tested at concentrations of 10 nM and 100 nM, respectively. As expected, **16** exhibited high affinity for D3R (68 % inhibition of binding of (+)-butaclamol; K_i = 1.5 nM) at 100 nM. High binding affinity for D2R at the lowest concentration (80 % inhibition of [^{3}H]7-OH-DPAT binding; K_i = 1 nM) was also observed. This is somewhat unexpected considering how compounds from this series consistently match the pharmacophoric features for D3R selectivity over D2R [45], with the pyridine-substituted benzimidazol-2-one moiety binding at the SBP of D3R, as predicted by docking simulations [26].

Moreover, compound **16** turned out to exhibit high selectivity for D3R over endocannabinoid receptor CB1 and both serotonergic receptor subtypes 5-HT_{1A} and 5-HT_{2C} at both tested concentrations. Interestingly, a high binding affinity for the serotonergic receptor subtype 5-HT_{2A} (85

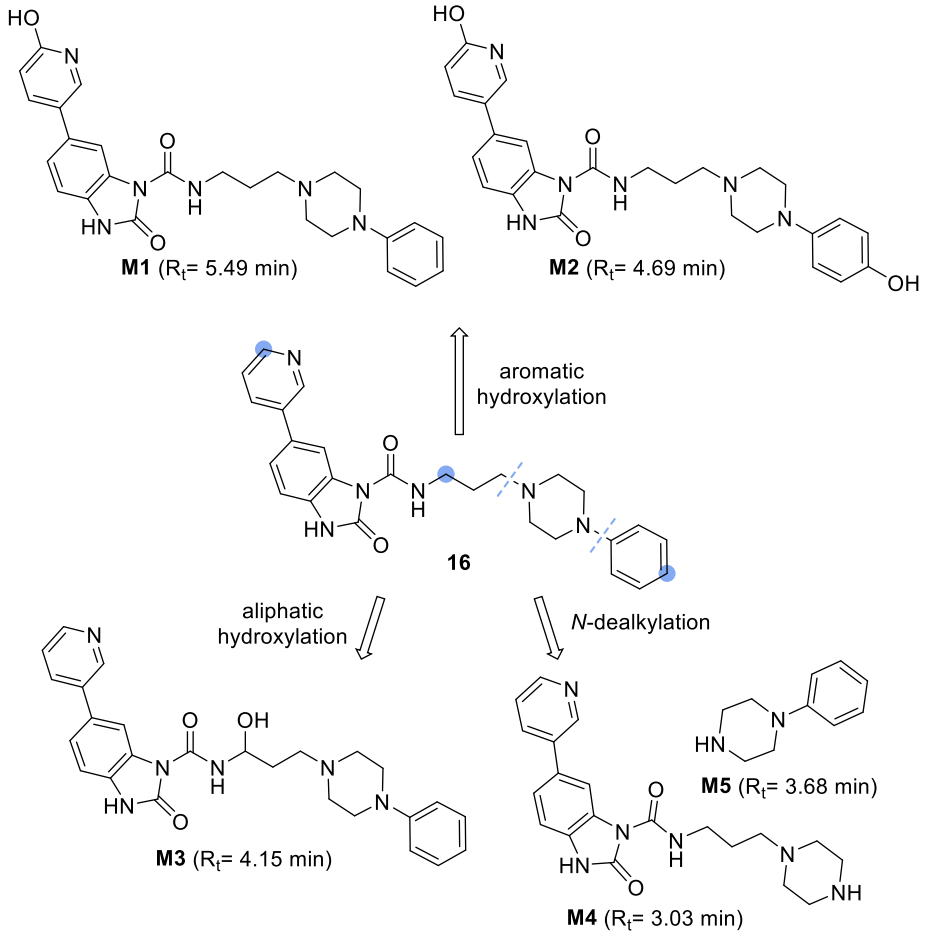

Fig. 6. Experimental sites of metabolism for compound **16**.

% inhibition of the binding of [^{125}I](±)DOI) was observed for **16** even when tested at 10 nM concentration. Given the sought pharmacological profile, a certain level of promiscuity could be regarded as a positive feature rather than a drawback. For example, the high affinity of aripiprazole for 5-HT$_{2A}$ likely contributes to the atypical antipsychotic ability to improve negative symptoms while reducing antipsychotic-induced extrapyramidal symptoms [46,47].

Furthermore, the GSK-3β selectivity of **16**, at 0.1 and 10 μM concentrations, was assessed in a KinaseProfiler assay over a focused panel of protein kinases (Table 6). Of note, **16** exhibited excellent GSK-3β selectivity over FYN, PKA and CDK5/p35. On the contrary, no selectivity was observed toward phylogenetically similar kinases GSK-3α [53,54] and DYRK1A [55,56], which, according to the available literature [57], have not been related explicitly to mood disorders.

2.8. X-ray crystal structures and MD simulations

To better rationalize GSK-3β activity, crystal structures of two more compounds were solved in complex with the kinase. These include the dual derivative **11** (ARN25423) that displays fairly well-balanced activities at the two targets (Fig. 9A and Fig. S1C and D of the Supporting Information for the electron density maps) and analog **16**, the one endowed with the most balanced profile in the series (Fig. 9B and Fig. S1E and F of the Supporting Information for the electron density maps), both bearing the same 2-oxo-6-(3-pyridyl)-3*H*-benzimidazole-1-carboxamide core but different tails with respect to prototype **1**. As expected, in **11** and **16**, the core engaged the hinge region of the enzyme in the same way as **1**, establishing the typical donor-acceptor-donor H-binding pattern of type I kinase inhibitors. The 3-pyridine substituent still contacted Lys85. However, in both cases, the phenyl-piperazine tail adopted a more open conformation, pointing toward the bulk of the solvent, without establishing any obvious additional interaction that could justify the increased inhibitory potency of **11** and **16**. Increased flexibility with respect to the hinge-binding core, likely contributes to the less defined electron density observed for the tail of the molecules.

To rationalize this increase in potency and evaluate the flexibility of the aryl-piperazine tail, we conducted extended MD simulations on the two co-crystallized derivatives and, for baseline comparison, on **1**. For each system, we generated three independent trajectories of 1 μs each.

In the first replica, compound **1** predominantly adopted a closed conformation throughout the trajectory, only temporarily transitioning to an open conformation, with the piperazine-bearing side chain adopting a rearrangement similar to that displayed by **11** and **16** in the crystallographic structures (Fig. 10A). In the second replica, **1** explored an open conformation early in the trajectory and, due to a concurrent partial collapse of the glycine-rich loop affecting the external region of the binding pocket, the closed state was never fully recovered, with the side chain constantly oscillating between an open conformation and a more closed one (Fig. S4A in the Supporting Information). In the third replica, **1** always maintained a closed conformation, with only minor changes in the orientation of the 2,3-dichlorophenyl ring (Fig. S4B in the Supporting Information). Considering a predicted pKa value equal to 7.44 ± 0.76 for the piperazine nitrogen in **1**, we also simulated the protonated species. Also in this case, the molecule mostly adopted a closed state similar to the one adopted in the neutral species. Only toward the end of the simulation, the protonated nitrogen and the carbonyl oxygen formed an intramolecular hydrogen bond (Fig. S4C in the Supporting Information). Compound **11** started the simulation

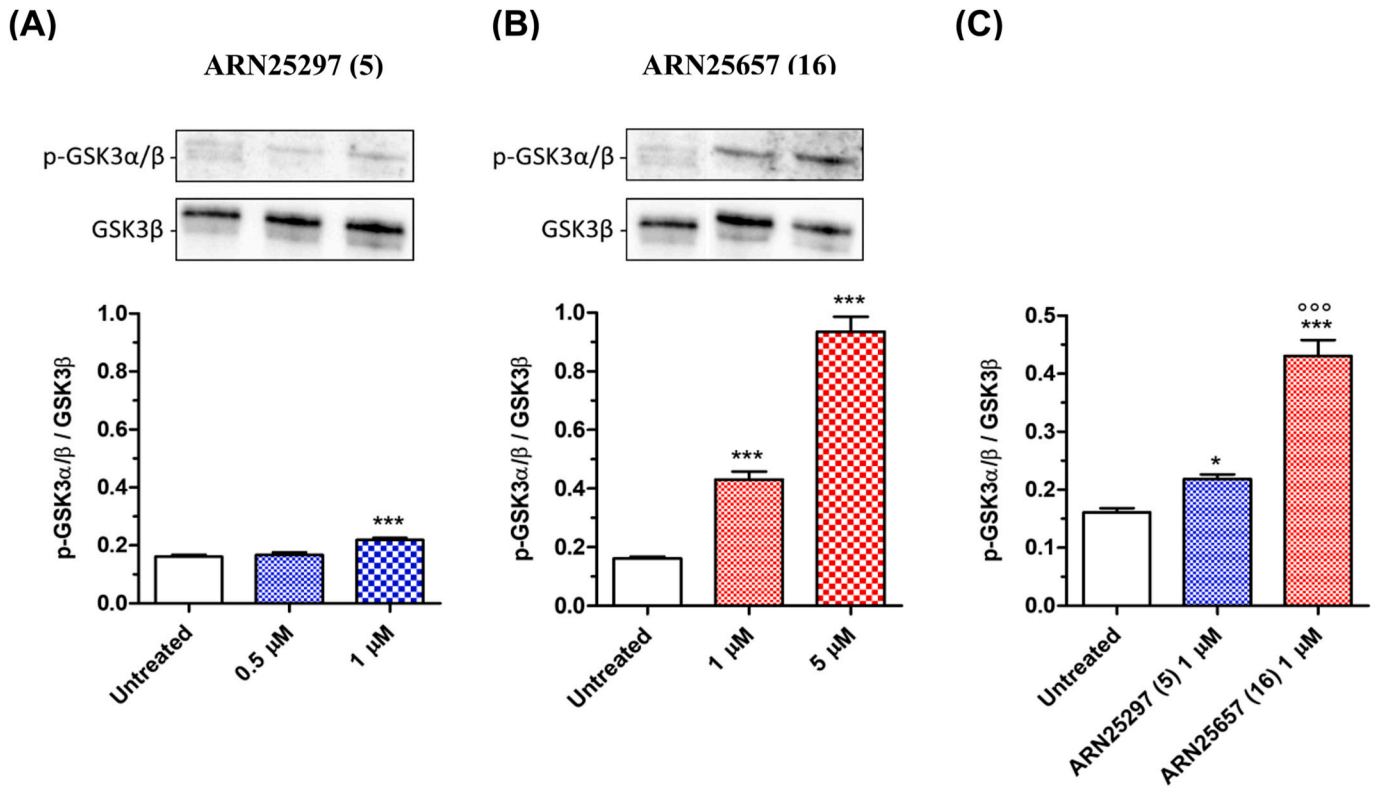

Fig. 7. Effects of compound **5** (ARN25297) and **16** (ARN25657) on GSK-3β activity in SH-SY5Y cells. Cells were incubated with compound **5** (0.5–1 μM) **(A)** or **16** (1–5 μM) **(B)** for 3 h. At the end of incubation, the phosphorylation of GSK-3α/β on Ser21/9 (inactive GSK-3α/β form) was determined by western blotting; **(C)** comparison between the two compounds at the concentration of 1 μM. Data are expressed as ratio between phospho-GSK-3α/β and total GSK-3β levels normalized against β-Actin and reported as mean ± SD of three independent experiments (*$p < 0.05$ and ***$p < 0.001$ *vs.* untreated cells; °$p < 0.001$ *vs.* cells treated with **5** at one-way ANOVA with Bonferroni post hoc test).

retaining the crystallographic open conformation but, after 100 ns, adopted a close conformation resembling the crystallographic pose of **1**. It maintained this rearrangement for 350 ns before returning to the initial state (first replica, Fig. 10B). A similar behavior could be consistently observed in the other two replicas (Figure S5A and Figure S5B in the Supporting Information). Compound **16** never adopted a closed conformation (Fig. 10C). This was consistent across all replicas (Figure S6A and Figure S6B in the Supporting Information). The protonated species of **11** (predicted pKa 7.06 ± 0.76) and **16** (predicted pKa 7.23 ± 0.81) retained an open conformation, with the side chain exploring different rearrangements but always pointing toward the solvent (Figure S5C and Figure S6C in the Supporting Information).

The common 2-oxo-6-(3-pyridyl)-3*H*-benzimidazole-1-carboxamide core was always stable, forming four tight interactions with the enzyme that never experienced any significant variation across 12 μs of aggregated simulated time. The only significant contribution to the calculated RMSD came from the phenyl-piperazine tail, with crystal structures capturing the most stable rearrangement among several possible ones. The inhibitory activity correlated with the propensity to adopt an open conformation. This propensity was, in turn, likely affected by the length of the linker and the nature of the phenyl ring substituents. Compounds **1** and **11** can be observed exploring both open and closed states in plain MD trajectories, suggesting that the energetic barrier to cross between these states is relatively low. Conversely, **16**, possessing a short, and thus less flexible linker and a naked, less hydrophobic, and less bulky distal portion, is never observed adopting a closed conformation. Further modelling studies will be required to quantitatively characterize binding free energy profiles.

2.9. Concluding remarks and future work

In this study, we have reported our multidisciplinary effort to optimize prototype **1**, aiming at achieving a well-balanced activity on both D3R and GSK-3β, at designing out affinity for P-gp while, ideally, obtaining an improved PK profile. We focused on decreasing the overall lipophilicity and slightly reducing the basicity, with the goal of fine-tuning GSK-3β affinity and P-gp inhibition, while preserving partial agonism in the low nanomolar range at D3R.

A computer- and crystallography-assisted SAR study was carried out leading to the design of 17 new derivatives. In series I, we discovered compound **5** (ARN25297) as an interesting quite-balanced D3R partial agonist/GSK-3β inhibitor (D3R: $EC_{50} = 13.1$ nM, % Eff. = 17.1; GSK-3β: $IC_{50} = 47.0$ nM), and in series II our optimization campaign resulted in compound **16** (ARN25657), which shows a balanced partial agonism at D3R ($EC_{50} = 15.2$ nM, % Eff. = 37.7) and very good GSK-3β inhibition ($IC_{50} = 19.3$ nM). Both compounds, featuring logD values lower than **1**, did not display P-gp inhibition when tested at 1 μM concentration. Among them, derivative **16** showed the lowest percentage of P-gp inhibition at 10 μM (10.9 % *vs.* 69.8 % of compound **1**) and exhibited a significant improvement in MLM stability ($t_{1/2} = 55$ min), overcoming another key liability of **1**. To elucidate the metabolism in HLM, we performed a Mass-MetaSite MetID study that led to: i) characterizing metabolic soft spots and ii) the identification of M3 ($R_t = 4.15$ min) as the predominant metabolite for compound **16**. Furthermore, an acceptable kinase and GPCR polypharmacological profile was also observed for **16**, which significantly inhibited GSK-3β activity in SH-SY5Y cells at 1 μM concentration. Overall, **16** undoubtedly emerged as the most interesting D3R partial agonist/GSK-3β inhibitor endowed with a well-balanced activity in the low nanomolar range and drug-like properties.

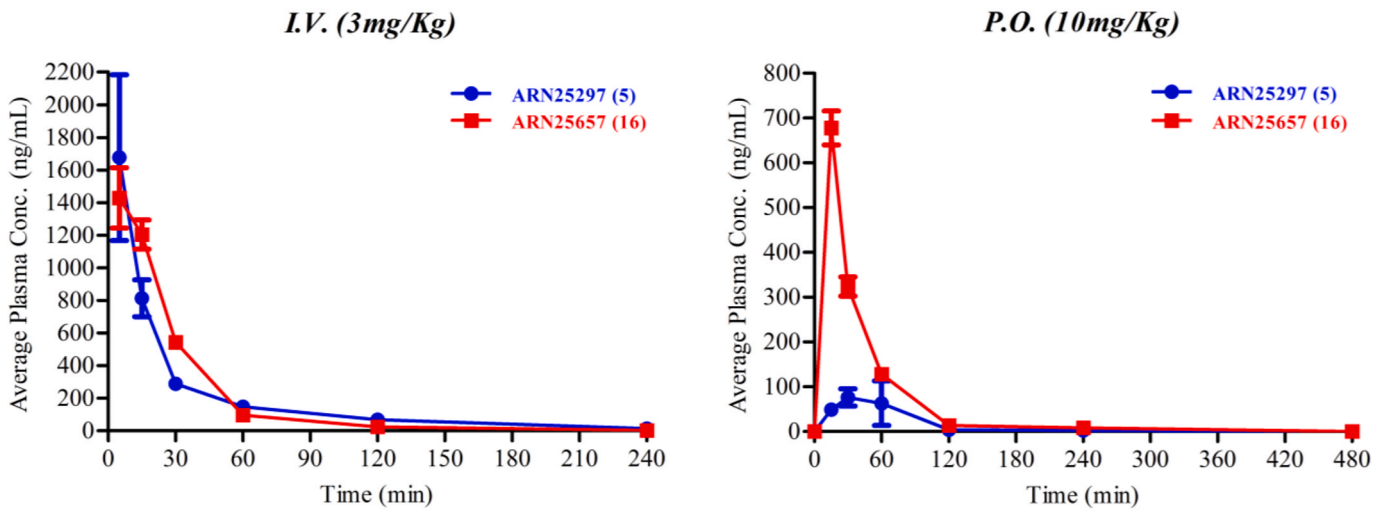

PK Parameters	ARN25297 (5)		ARN25657 (16)	
	I.V.	*P.O.*	*I.V.*	*P.O.*
Cmax (ng/mL)	1677	76	1429	678
Tmax (min)	5	30	5	15
AUC (min*ng/mL)	49587	5836	49493	24957
$t_{½}$ (min)	58	154	38	180
V_D (L/Kg)	4.9	347.0	3.3	95.6
CL (mL/min/Kg)	58	1566	60	368
F (%)	**4**		**15**	

Fig. 8. Mouse PK profiles of **5** (ARN25297) and **16** (ARN25657) following intravenous (I.V.) and oral (P.O.) administration at 3 and 10 mg/kg, respectively, and the corresponding observed and calculated PK parameters.

Table 5
Off-target binding affinities of the best well-balanced dual D3R/GSK-3β modulator **16**.

Target	Source	Ligand	% Inh. of control specific binding (10 nM)	% Inh. of control specific binding (100 nM)	Detection method
D2S(h) (agonist radioligand)	human recombinant (HEK293 cells)	[^{3}H]7-OH-DPAT	79.5	96.6	scintillation counting [48]
D3(h) (antagonist radioligand)	human recombinant (CHO cells)	(+)-butaclamol	12.6	68.0	scintillation counting [49]
CB1(h) (agonist radioligand)	human recombinant (Chem-RBL cells)	[^{3}H]CP-55,940	−31.6	−6.9	scintillation counting [50]
5-HT$_{1A}$(h) (agonist radioligand)	human recombinant (HEK-293 cells)	[^{3}H]8-OH-DPAT	−1.1	28.3	scintillation counting [51]
5-HT$_{2A}$(h) (agonist radioligand)	human recombinant (HEK-293 cells)	[^{125}I](±)DOI	84.6	96.0	scintillation counting [52]
5-HT$_{2C}$(h) (agonist radioligand)	human recombinant (HEK-293 cells)	[^{125}I](±)DOI	−18.8	−0.9	scintillation counting [52]

Table 6
GSK-3β selectivity of **16** over a small panel of protein kinases in radiometric enzymatic assays.

Protein kinase	% Inh (0.1 μM)	% Inh (10 μM)	Selectivity ratio (*vs.* GSK-3β at 0.1 μM)
GSK-3β (h)	48	100	1
GSK-3α (h)	72	100	1.5
FYN (h)	0	16	0
DYRK1A (h)	55	99	1.1
PKA (h)	5	1	0.1
CDK5/p35 (h)	0	72	0

In summary, the optimization campaign yielded valuable insights. Although compounds **16** and **5** did not show improved PK profiles compared to **1**, the results of our study prove that potent and balanced activities at D3R and against GSK-3β can be engineered within a merged dual-target compound [25,40]. Driven by the insights gained here, future studies will focus on more significant structural variations within the original scaffold to achieve optimal brain penetration. This pursuit will aim at creating a new chemical class of D3R/GSK-3β modulators with enhanced PK properties, potentially providing innovative treatments for BD and related neuropsychiatric conditions, as well as addressing psychostimulant-induced behaviors involved in the maintenance of drug-seeking [58,59].

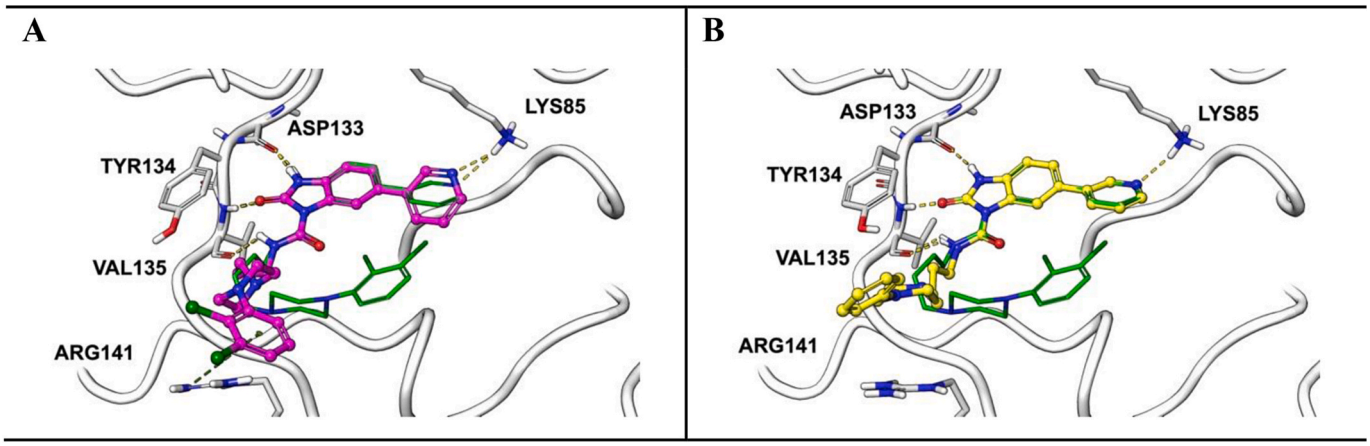

Fig. 9. X-ray crystal structures of A) GSK-3β-**11** (PDB ID: 9HUL) and B) GSK-3β-**16** complexes (PDB ID: 9HV3). The structures of **11** and **16** are reported in magenta and yellow, respectively. Relevant residues are reported in ball and stick representation and labeled explicitly. Yellow dash lines highlight H-bonds. The crystallographic pose of **1** is reported in green sticks for comparison. (For interpretation of the references to color in this figure legend, the reader is referred to the Web version of this article.)

3. Experimental methods

3.1. Chemistry

3.1.1. General information

Solvents and reagents were obtained from commercial suppliers and were used without further purification. For simplicity, solvents and reagents were indicated as follows: 1,1′-bis(diphenylphosphino)ferrocene] dichloropalladium(II) complex with dichloromethane ($PdCl_2(dppf)\cdot CH_2Cl_2$), 4-dimethylaminopyridine (DMAP), acetic acid (AcOH), acetonitrile (CH_3CN), ammonium acetate (NH_4OAc), chloroform ($CHCl_3$), cyclohexane (Cy), dichloromethane (CH_2Cl_2), diethyl ether (Et_2O), dimethylsulfoxide (DMSO), di-*tert*-butyl dicarbonate $(Boc)_2O$, ethanol (EtOH), ethyl acetate (EtOAc), formic acid (HCOOH), hydrazine monohydrate ($NH_2NH_2\cdot H_2O$), hydrochloric acid (HCl), methanol (CH_3OH), *N*-(3-dimethylaminopropyl)-*N*′-ethylcarbodiimide hydrochloride (EDC·HCl), *N*,*N*-carbonyldiimidazole (CDI), *N*,*N*-diisopropylethylamine (DIPEA), *N*,*N*-dimetilacetammide (DMA), *N*,*N*-dimethylformamide (DMF), potassium acetate (CH_3COOK), potassium carbonate (K_2CO_3), pyridine (pyr), room temperature (rt), sodium bicarbonate ($NaHCO_3$), sodium hydride (NaH), sodium hydroxide (NaOH), sodium sulfate (Na_2SO_4), triethylamine (Et_3N), trifluoroacetic acid (TFA), water (H_2O).

Thin-layer chromatography analyses were performed using precoated Supelco silica gel on TLC Al foils 0.2 mm and visualized by UV (254 nm).

Chromatographic separations were performed on silica gel columns by flash method (Kieselgel 40, 0.040–0.063 mm, Merck). Automated column chromatography purifications were done using a Teledyne ISCO apparatus (CombiFlash® Rf) with pre-packed silica gel columns of different sizes (from 4 g until 40 g). Mixtures of increasing polarity of Cy and EtOAc or CH_2Cl_2 and CH_3OH or CH_2Cl_2 and EtOH or $CHCl_3$ and CH_3OH were used as eluents.

Reactions involving microwave irradiation were performed using a CEM Discover SP focused microwave reactor.

NMR experiments were run on a Bruker Avance III 400 system (400.13 MHz for ^1H, and 100.62 MHz for ^{13}C), equipped with a BBI probe and Z-gradients and on a Bruker Avance III 600 MHz spectrometer (600 MHz for ^1H, and 151 MHz for ^{13}C), equipped with a 5 mm CryoProbe™ QCI $^1H/^{19}F–^{13}C/^{15}N–D$ quadruple resonance, a shielded z-gradient coil and the automatic sample changer SampleJet™ NMR system. Spectra were acquired at 300 K, using deuterated dimethylsulfoxide (DMSO-d_6) or deuterated chloroform ($CDCl_3$) as solvent. Chemical shifts for ^1H and ^{13}C spectra were recorded in parts per million using the residual non-deuterated solvent as the internal standard (for DMSO-d_6: 2.50 ppm, ^1H; 39.52 ppm, ^{13}C). Data are reported as follows: chemical shift (ppm), multiplicity (indicated as: br, broad signal; s, singlet; d, doublet; t, triplet; q, quartet; p, quintet; m, multiplet and combinations thereof), coupling constants (*J*) in Hertz (Hz) and integrated intensity.

Ultra-performance liquid chromatography-mass spectrometry (UPLC-MS) analyses were run on a Waters ACQUITY UPLC-MS system consisting of a single quadrupole detector (SQD) mass spectrometer equipped with an electrospray ionization interface (ESI) and a photodiode array detector (PDA) from Waters Inc. (Milford, MA, USA). PDA range was 210–400 nm. The analyses were performed on an ACQUITY UPLC BEH C_{18} (50x2.1 mmID, particle size 1.7 μm) with a VanGuard BEH C_{18} pre-column (5x2.1 mmID, particle size 1.7 μm) (for method A and B) and an ACQUITY UPLC HSS T3 (50x2.1 mmID, particle size 1.8 μM) with a VanGuard HSS T3 pre-column (5x2.1 mmID, particle size 1.8 μM) (for method C). The mobile phase was 10 mM NH_4OAc in H_2O at pH 5 adjusted with AcOH (A) and 10 mM NH_4OAc in $CH_3CN–H_2O$ (95:5) at pH 5 (B) with 0.5 mL/min as flow rate. Electrospray ionization in positive and negative mode was applied in the mass scan range 100–750 Da. Different analytical methods were applied depending on the LogD of the compounds. For method A (generic), the mobile phase B was increased from 5 % to 95 % in 2.5 min. For method B (apolar), the mobile phase B was increased from 50 % to 100 % in 2.5 min. For method C (polar), the mobile phase B was increased from 0 % to 50 % in 2.5 min.

The QC analyses of final compounds were performed on a Waters ACQUITY UPLC-MS system as described above. Electrospray ionization in positive and negative mode was applied in the mass scan range 110–750 Da and the PDA range was 210–400 nm. The analyses were run on an ACQUITY UPLC BEH C_{18} column (100x2.1 mmID, particle size 1.7 μm) with a VanGuard BEH C_{18} pre-column (5x2.1 mmID, particle size 1.7 μm), using 10 mM NH_4OAc in H_2O at pH 5 adjusted with AcOH (A) and 10 mM NH_4OAc in $CH_3CN–H_2O$ (95:5) at pH 5 (B) as mobile phase. A linear gradient was applied increasing the mobile phase B from 10 % to 90 % in 6 min (method D) with 0.5 mL/min as flow rate.

High-resolution mass spectrometry (HRMS) for accurate mass measurements was performed on a Sciex TripleTOF High-resolution LC-MS using a Waters UPLC ACQUITY chromatographic system (from Waters Inc., Milford, MA, USA) coupled to a TripleTOF 5600+ Mass Spectrometer (from Sciex, Warrington, UK) equipped with a DuoSpray Ion source. The analyses were run on an ACQUITY UPLC BEH C_{18} column (50x2.1mmID, particle size 1.7 μm), using H_2O + 0.1 % HCOOH (A) and CH_3CN + 0.1 % HCOOH as mobile phase.

Compounds were named using the naming algorithm developed by CambridgeSoft Corporation and used in ChemDraw professional 20.0.

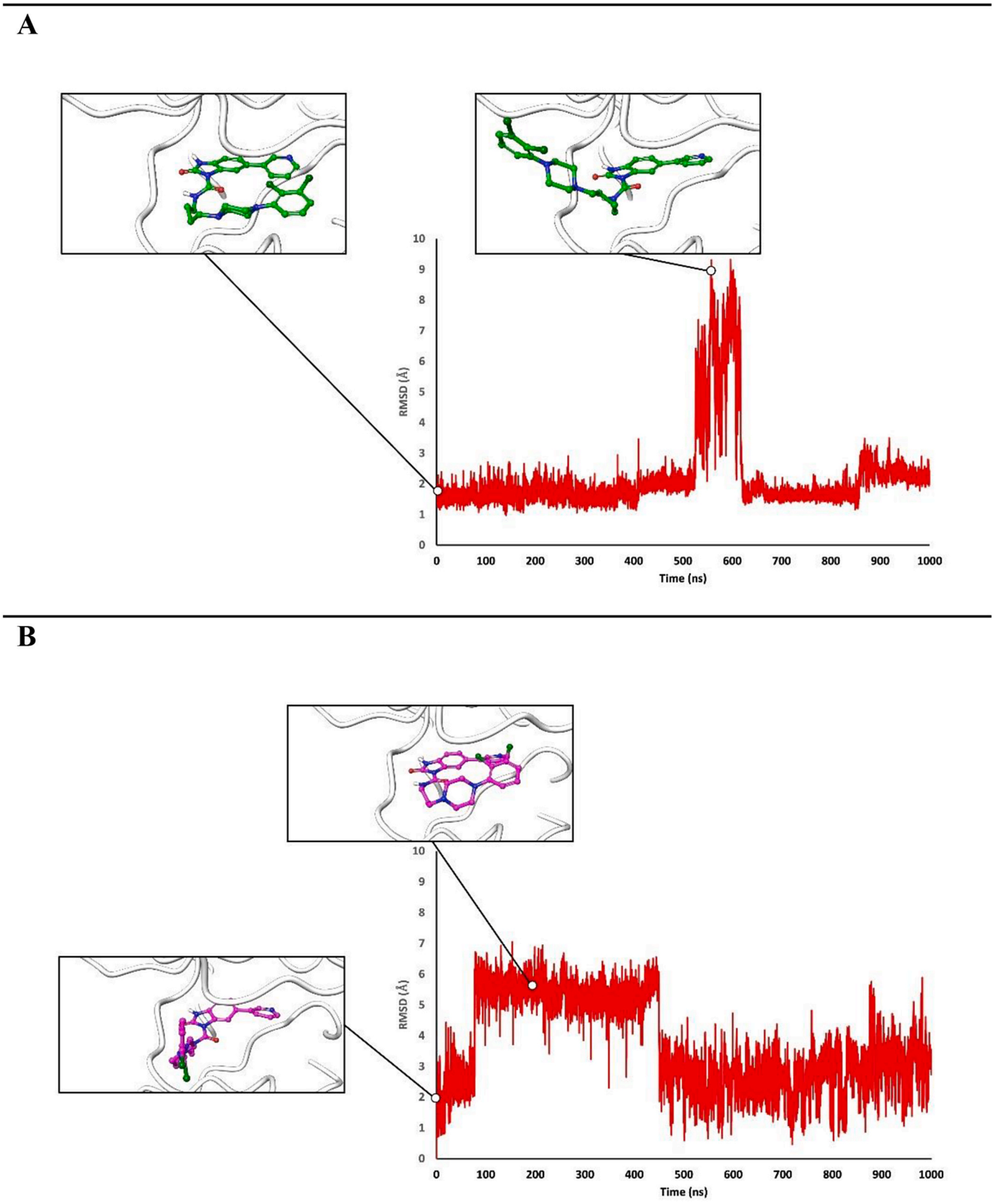

Fig. 10. Root mean square deviation (RMSD) plots of ligand non-hydrogen atoms as a function of time from MD simulations of compounds **1** (A), **11** (B) and **16** (C). RMSD is calculated with respect to the starting conformation after superimposition of the protein backbone atoms. In the insets, the conformation adopted by the ligand in relevant snapshots discussed in the text is reported explicitly.

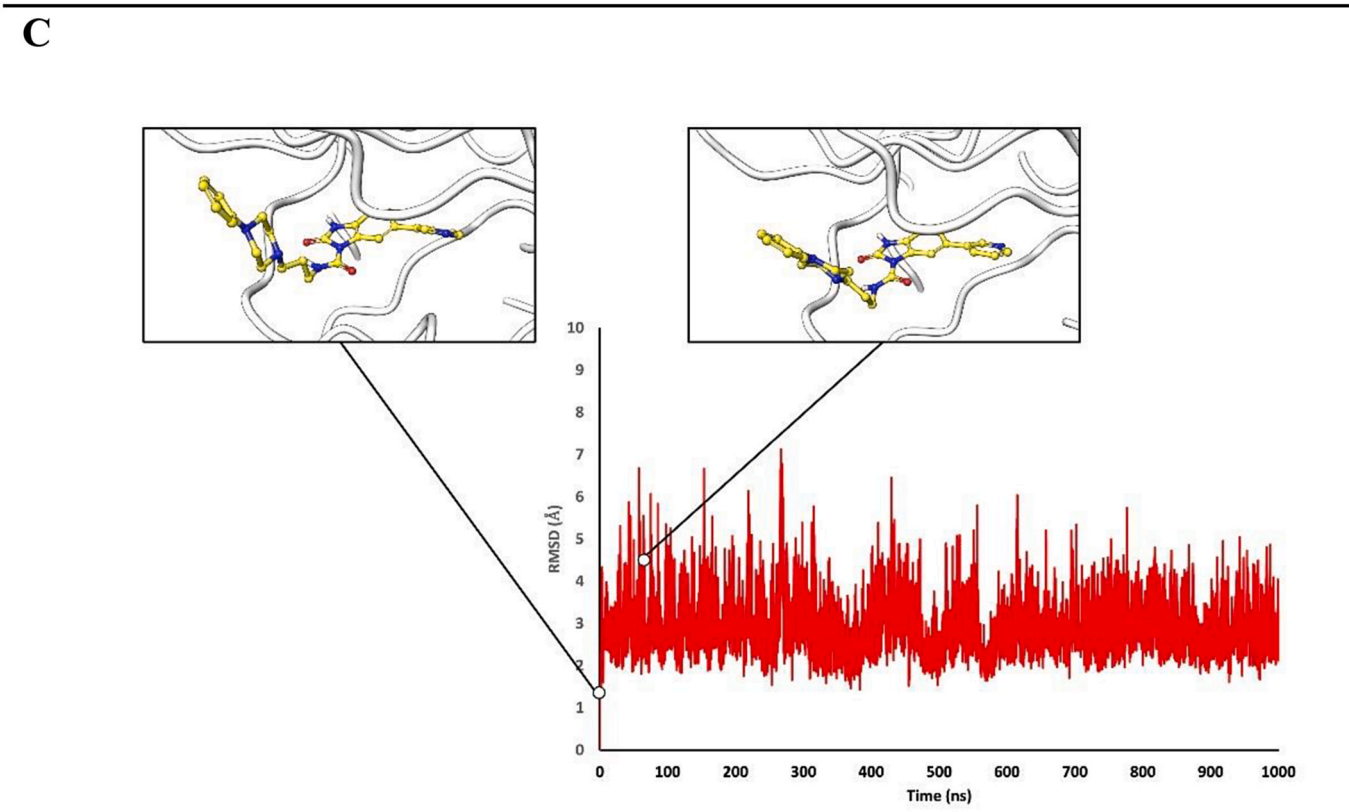

Fig. 10. (*continued*).

All final compounds displayed ≥95 % UV purity at 215 nm as determined by UPLC-MS analysis.

3.1.1.1. General procedure A: synthesis of phthalimide intermediates 74-82. Phthalimide analogs were prepared by applying a synthetic procedure adapted from that reported by De Simone et al. [41,42] A stirred mixture of the appropriate *N*-aryl piperazine or *N*-aryl piperazine hydrochloride (1 mmol), *N*-(haloalkyl/alkenyl)phthalimide (1.1 mol equiv) and K_2CO_3 (2.5 mol equiv) in CH_3CN (1.87 mL) was heated at 85 °C for 6 h. Upon completion, the cooled suspension was filtered under *vacuum*; the obtained residue was washed several times with acetone and the resultant filtrate was concentrated to dryness. The isolated product was pure enough to be used in the next synthetic step without further purification.

3.1.1.2. General procedure B: synthesis of amines 55-63. Amine derivatives were synthetized following a procedure adapted from that reported by De Simone et al. [41,42] To a solution/suspension of the proper phthalimide intermediate (1 mmol) in CH_3OH (2.9 mL), $NH_2NH_2{\cdot}H_2O$ (50–60 %, 2.4 mol equiv) was added dropwise and the resulting mixture was heated at 80 °C for 2 h. Then, aqueous HCl solution (2 N, 0.36 mL) was added to the hot suspension and the heating was prolonged for additional 1 h. The cooled mixture was filtrated under *vacuum*, the residue was washed with fresh CH_3OH, and the collected filtrate was evaporated to dryness. The obtained crude product was suspended in H_2O and the pH was adjusted up 8 using aqueous NaOH solution (2 N). Extraction with CH_2Cl_2 and further evaporation under reduced pressure afforded an oily product, which was purified by typical silica gel flash chromatography or was employed in the next synthetic step without further purification.

3.1.1.3. General procedure C: Suzuki-coupling reaction for intermediates 28, 33 and 87-93. $PdCl_2(dppf){\cdot}CH_2Cl_2$ (0.10–0.24 mol equiv) and the appropriate base (4.0–5.0 mol equiv) were sequentially added to a degassed mixture of the appropriate boronic acid or boronate ester (1.3–3.0 mol equiv) and bromine derivative (1 mmol) in dry 1,4-dioxane or dry DMF (0.1 M). The resulting mixture was heated at 80–120 °C for 1–14 h under MW irradiation. Upon completion, the resulting mixture was partitioned between EtOAc and water. If needed, the pH of the aqueous phase was corrected to 6–7 using HCl solution (2 N) and the separated aqueous phase was extracted with fresh EtOAc (x3). The combined organic phase was dried over Na_2SO_4, concentrated under reduced pressure, and purified by normal phase silica gel flash chromatography.

3.1.1.4. General procedure D: synthesis of N-Boc protected regioisomers of interest 29a-32a and 34a-37a. To a stirred solution of 5-aryl/heteroaryl-1,3-dihydrobenzoimidazol-2-one (1 mmol) in dry DMF or in a dry DMF/DMA mixture (2–20 mL), NaH (60 % dispersion in mineral oil, 1 mol equiv) was added portionwise at rt under an Ar atmosphere. After about 1 h, a solution of $(Boc)_2O$ (1 mol equiv) in dry DMF (0.1 M) was added dropwise and the resulting mixture was stirred for additional 3–4 days. If needed, K_2CO_3 (1.0 or 1.2 mol equiv) alone or together with 5-aryl/heteroaryl-1,3-dihydrobenzoimidazol-2-one (1.0 mol equiv) was added to the reaction mixture to aid the formation of the title regioisomer. Upon completion, the reaction mixture was poured into H_2O and extracted with EtOAc (x3). Adjusting the pH of the aqueous phase to 6–7 was sometimes necessary to facilitate extraction of the synthetized regioisomers into the organic phase. The combined organic phases were washed with brine, dried over Na_2SO_4 and evaporated under reduced pressure. Purification of the resulting crude product by silica gel flash chromatography afforded the pure regioisomer of interest.

3.1.1.5. General procedure E: synthesis of N-Boc protected urea-based derivatives 38-54. To a dry CH_2Cl_2 solution (0.1 M) of the appropriate amine (1.1–3.0 mol equiv), cooled down to 0 °C, a solution of triphosgene (0.7–1.8 mol equiv) in dry CH_2Cl_2 (0.1 M) was added dropwise under an Ar atmosphere. The resulting mixture was allowed to stir at 0 °C for about 1 h. Then, dry Et_3N (5.6–15.0 mol equiv) was added and the resulting mixture was stirred at 0 °C for extra 30 min. The suspension of the freshly prepared isocyanate was added dropwise to a stirred solution of the proper *tert*-butyl 5-aryl-2-oxo-3*H*-benzimidazole-1-carboxylate or *tert*-butyl 5-(3-methyl-2,5-dioxoimidazolidin-1-yl)-2-oxo-3*H*-benzimidazole-1-carboxylate (1 mmol) in dry CH_2Cl_2 or in a dry mixture of CH_2Cl_2/DMF (10 mL) at 0 °C under an Ar atmosphere. The resulting mixture was warmed to rt and was stirred for 2 h-3 days at the same temperature under an inert atmosphere. Then, the reaction mixture was diluted with fresh CH_2Cl_2, washed with a saturated aqueous solution of $NaHCO_3$, dried over Na_2SO_4 and concentrated to dryness. The title *N*-Boc protected urea derivatives were isolated pure by flash chromatography purification on silica gel.

3.1.1.6. General procedure F: N-Boc deprotection reaction to prepare urea-based compounds as free bases. The appropriate *N*-Boc protected urea-based compound (1 mmol) was treated with TFA (10–30 mol equiv) in CH_2Cl_2 (10 mL) at 0 °C. The resulting reaction mixture was warmed to rt and stirred for 2 h-overnight at the same temperature. At the end of the reaction, addition of cold Et_2O gave a precipitate, which was filtered under *vacuum*, dissolved in a saturated aqueous solution of $NaHCO_3$ and extracted with EtOAc (x2). The separated organic phase was dried over Na_2SO_4, and concentrated under reduced pressure to give a crude product, which was pure enough to be used in the next synthetic step without further purification.

3.1.1.7. General procedure G: preparation of hydrochloride salts 2–14 and 16-18. A solution (4 N) of HCl in 1,4-dioxane or a solution (1.25 or 3 N) of HCl in CH_3OH (10 mol equiv) was added dropwise to a suspension of the apposite free base (1 mmol) in 1,4-dioxane or CH_3OH (0.1 M). The resulting mixture was allowed to stir at rt for 1 h, and, then was evaporated under reduced pressure. Treatment of the obtained residue with Et_2O afforded a precipitate, which was collected by filtration, washed with fresh Et_2O (x2), and dried in vacuo.

3.1.1.7.1. (E)-2-(4-Chlorobut-2-en-1-yl)isoindoline-1,3-dione (68). To a solution of *trans*-1,4-dichloro-2-butene **67** (2.70 g, 21.60 mmol) in dry DMF (10 mL) purged with Ar, potassium phthalimide salt **66** (2.00 g, 10.80 mmol) was added and the resulting mixture was allowed to stir at rt overnight. The reaction mixture was poured into H_2O obtaining the precipitation of a white solid that was filtered under *vacuum* and dried. Purification by normal phase silica gel flash chromatography by employing a gradient 2–30 % of EtOAc in Cy gave the title phthalimide intermediate **68** (1.8 g, 72 %) as a white powder. UPLC-MS: t_R = 2.05 min (method A). MS (ESI) *m/z*: 236.0 $(M + H)^+$; $C_{12}H_{11}ClNO_2$ $(M + H)^+$ calcd: 236.0. ^{1}H NMR (400 MHz, $CDCl_3$) δ 7.89–7.84 (m, 2H), 7.75–7.70 (m, 2H), 5.90–5.85 (m, 2H), 4.32–4.30 (m, 2H), 4.03–4.01 (m, 2H).

3.1.1.7.2. 2-(4-(4-(2,3-Dichlorophenyl)piperazin-1-yl)butyl)isoindoline-1,3-dione (74). Phthalimide **74** was prepared according to general procedure A and in line with refs. [26,41].

3.1.1.7.3. 2-(3-(4-(2,3-Dichlorophenyl)piperazin-1-yl)propyl)isoindoline-1,3-dione (75). Phthalimide **75** was prepared according to general procedure A and in line with refs. [26,41].

3.1.1.7.4. (E)-2-(4-(4-(2,3-Dichlorophenyl)piperazin-1-yl)but-2-en-1-yl)isoindoline-1,3-dione (76). Phthalimide **76** was prepared according to general procedure A and in line with ref. [41].

3.1.1.7.5. 2-(4-(4-Phenylpiperazin-1-yl)butyl)isoindoline-1,3-dione (77). Phthalimide **77** was prepared according to general procedure A using *N*-(4-bromobutyl)phthalimide **65** (1.70 g, 6.16 mmol), 1-phenylpiperazine **73** (1.0 g, 6.16 mmol), K_2CO_3 (1.71 g, 12.34 mmol) and 10 mL of CH_3CN (10 mL). The reaction mixture was heated overnight to afford intermediate **77** (2.0 g, 89 %) as a yellow powder. UPLC-MS: t_R = 1.78 min (method A). MS (ESI) *m/z*: 364.1 $(M + H)^+$; $C_{22}H_{26}N_3O_2$ $(M + H)^+$ calcd: 364.2. ^{1}H NMR (400 MHz, DMSO-d_6) δ 7.97–7.75 (m, 4H), 7.28–7.13 (m, 2H), 6.99–6.84 (m, 2H), 6.75 (tt, *J* = 7.4 and 1.4 Hz, 1H), 3.60 (t, *J* = 7.0 Hz, 2H), 3.09–3.07 (m, 4H), 2.49 (s, 4H), 2.37–2.28 (m, 2H), 1.63 (p, *J* = 7.1 Hz, 2H), 1.47 (p, *J* = 7.3 Hz, 2H).

3.1.1.7.6. 2-(4-(4-(2-Methoxyphenyl)piperazin-1-yl)butyl)isoindoline-1,3-dione (78). Phthalimide **78** was prepared according to general procedure A and in line with ref. [41].

3.1.1.7.7. 2-(4-(4-(o-Tolyl)piperazin-1-yl)butyl)isoindoline-1,3-dione (79). Phthalimide **79** was prepared according to general procedure A and in line with ref. [41].

3.1.1.7.8. 2-(3-(4-Phenylpiperazin-1-yl)propyl)isoindoline-1,3-dione (80). Phthalimide **80** was prepared according to general procedure A and in line with ref. [41].

3.1.1.7.9. (E)-2-(4-(4-Phenylpiperazin-1-yl)but-2-en-1-yl)isoindoline-1,3-dione (81). Phthalimide **81** was prepared according general procedure A by using **68** (0.418 g, 1.773 mmol), 1-phenylpiperazine **73** (0.262 g, 1.612 mmol), K_2CO_3 (0.557 g, 4.031 mmol) and 9.8 mL of CH_3CN to afford **81** (0.583 g, quant.) as yellow powder. UPLC-MS: t_R = 1.87 min (method A). MS (ESI) *m/z*: 362.0 $(M + H)^+$; $C_{22}H_{24}N_3O_2$ $(M + H)^+$ calcd: 362.2. ^{1}H NMR (400 MHz, DMSO-d_6) δ 7.94–7.80 (m, 4H), 7.26–7.15 (m, 2H), 6.95–6.84 (m, 2H), 6.75 (tt, *J* = 7.2 and 1.0 Hz, 1H), 5.75–5.55 (m, 2H), 4.20 (dd, *J* = 5.1 and 1.2 Hz, 2H), 3.12–3.05 (m, 4H), 2.98–2.89 (m, 2H), 2.47–2.41 (m, 4H).

3.1.1.7.10. 2-(4-(4-(2,3-Dichlorophenyl)piperazin-1-yl)-4-oxo-butyl) isoindoline-1,3-dione (82). A mixture of 1-(2,3-dichlorophenyl)piperazine hydrochloride **70** (0.510, 1.87 mmol), 4-(1,3-dioxoisoindol-2-yl) butanoyl chloride **69** (0.489 g, 1.85 mmol) and dry Et_3N (0.26 mL, 1.87 mmol) in dry pyridine (6.70 mL) was stirred for 20 h at rt. At the end of the reaction, the crude reaction mixture was poured into H_2O and was stirred for 1 h. The resulting precipitate was filtered under *vacuum* and was dried to give **82** (0.56 g, 69 %) as a light-yellow powder. UPLC-MS: t_R = 2.43 min (method A). MS (ESI) *m/z*: 446.4/448.4/450.4 $(M + H)^+$; $C_{22}H_{22}Cl_2N_3O_3$ $(M + H)^+$ calcd: 446.1/448.1/450.1. ^{1}H NMR (400 MHz, $CDCl_3$): δ 7.87–7.82 (m, 2H), 7.74–7.69 (m, 2H), 7.22–7.12 (m, 2H), 6.93 (dd, *J* = 7.6 and 1.9 Hz, 1H), 3.79 (t, *J* = 6.6 Hz, 2H), 3.76 (t, *J* = 5.1 Hz, 2H), 3.61 (t, *J* = 5.0 Hz, 2H), 3.08–2.96 (m, 4H), 2.43 (t, *J* = 7.3 Hz, 2H), 2.17–1.99 (m, 2H).

3.1.1.7.11. 4-(4-(2,3-Dichlorophenyl)piperazin-1-yl)butan-1-amine (55). Amine **55** was prepared according to general procedure B, following the method described in refs. [26,41].

3.1.1.7.12. 3-(4-(2,3-Dichlorophenyl)piperazin-1-yl)propan-1-amine (56). Amine **56** was prepared according to general procedure B, following the method described in ref. [41].

3.1.1.7.13. (E)-4-(4-(2,3-Dichlorophenyl)piperazin-1-yl)but-2-en-1-amine (57). Amine **57** was prepared according to general procedure B, following the method described in ref. [41].

3.1.1.7.14. 4-(4-Phenylpiperazin-1-yl)butan-1-amine (58). Amine **58** was prepared according to general procedure B, following the method described in ref. [41].

3.1.1.7.15. 4-(4-(2-Methoxyphenyl)piperazin-1-yl)butan-1-amine (59). Amine **59** was prepared according to general procedure B, following the method described in ref. [41].

3.1.1.7.16. 4-(4-(o-Tolyl)piperazin-1-yl)butan-1-amine (60). Amine **60** was prepared according to general procedure B, following the method described in ref. [41].

3.1.1.7.17. 3-(4-Phenylpiperazin-1-yl)propan-1-amine (61). Amine **61** was prepared according to general procedure B, following the method described in ref. [41].

3.1.1.7.18. (E)-4-(4-Phenylpiperazin-1-yl)but-2-en-1-amine (62). Amine **62** was prepared according to general procedure B heating $NH_2NH_2{\cdot}H_2O$ (0.15 mL, 3.04 mmol) and phthalimide intermediate **81** (0.566 g, 1.27 mmol) in CH_3OH (8 mL) for 3 h. In this case, aqueous HCl solution was not added to the hot solution. The cooled suspension was filtrated under *vacuum*; the obtained filtrate was concentrated under

reduced pressure to give a residue that was then treated with CH_2Cl_2. Lastly, *vacuum* filtration of the resulting suspension followed by evaporation of the obtained filtrate to dryness afforded title amine **62** (0.383 g, quant.) as a pale-yellow oil. UPLC-MS: $t_R = 1.35$ min (method A). MS (ESI) *m/z*: 232.1 $(M + H)^+$; $C_{14}H_{22}N_3$ $(M + H)^+$ calcd: 232.1. ^{1}H NMR (400 MHz, $CDCl_3$): δ 7.28–7.23 (m, 2H), 6.97–6.89 (m, 2H), 6.85 (td, J = 7.2 and 1.1 Hz, 1H), 5.86–5.70 (m, 2H), 3.40 (d, J = 4.8 Hz, 2H), 3.26–3.16 (m, 4H), 3.05 (d, J = 5.6 Hz, 2H), 2.67–2.59 (m, 4H).

3.1.1.7.19. 4-Amino-1-(4-(2,3-dichlorophenyl)piperazin-1-yl)butan-1-one (63). In agreement with the general procedure B, $NH_2NH_2{\cdot}H_2O$ (0.15 mL, 3.04 mmol) and phthalimide intermediate **82** (0.566 g, 1.27 mmol) were heated in EtOH (8 mL) for 3 h. In this case, aqueous HCl solution was not added to the hot solution. The cooled suspension was filtrated under *vacuum*; the obtained filtrate was concentrated under reduced pressure to give a residue that was then treated with CH_2Cl_2. A *vacuum* filtration of the resulting suspension followed by evaporation of the obtained filtrate to dryness afforded a residue. Purification by of the crude reaction mixture by normal phase silica gel flash chromatography by employing a gradient 0.1–8.0 % of NH_3 solution (1 N in CH_3OH) in CH_2Cl_2 afforded amine **63** (0.226 g, 56 %) as a colorless oil. UPLC-MS: $t_R = 1.69$ min (method A). MS (ESI) *m/z*: 316.4/318.4/320.4 $(M + H)^+$; $C_{14}H_{20}Cl_2N_3O$ $(M + H)^+$ calcd: 316.1/318.1/320.1. ^{1}H NMR (400 MHz, $CDCl_3$): δ 7.24–7.12 (m, 2H), 6.92 (dd, J = 7.7 and 1.8 Hz, 1H), 3.80 (t, J = 5.0 Hz, 2H), 3.66 (t, J = 5.1 Hz, 2H), 3.01 (dt, J = 9.7 and 4.9 Hz, 4H), 2.78 (t, J = 6.9 Hz, 2H), 2.45 (t, J = 7.4 Hz, 2H), 1.81 (p, J = 7.1 Hz, 2H).

3.1.1.7.20. tert-Butyl 5-bromo-2-oxo-2,3-dihydro-1H-benzo[d]imidazole-1-carboxylate (84). Regioisomer **84** was obtained in line with the synthetic procedure described in ref. [26].

3.1.1.7.21. tert-Butyl 5-(5-methoxypyridin-3-yl)-2-oxo-2,3-dihydro-1H-benzo[d]imidazole-1-carboxylate (28). General procedure C was followed using **85** (1.24 g, 3.90 mmol), **84** (0.305 g, 0.974 mmol), $PdCl_2$(dppf)·CH_2Cl_2 (0.239 g, 0.292 mmol) and CH_3COOK (0.765 g, 7.792 mmol) in dry 1,4-dioxane (9.8 mL). The reaction mixture was heated at 80 °C for 9 h. Purification of the crude product by chromatography using a gradient 0.05–3 % of CH_3OH in CH_2Cl_2 afforded **28** (167 mg, 46 %) as a beige powder. UPLC-MS: $t_R = 1.82$ min (method A). MS (ESI) *m/z*: 342.1 $(M + H)^+$; $C_{18}H_{20}N_3O_4$ $(M + H)^+$ calcd: 342.1. ^{1}H NMR (400 MHz, DMSO-d_6): δ 9.59 (br s, 1H), 8.48 (s, 1H), 8.31 (d, J = 2.6 Hz, 1H), 7.83 (d, J = 8.8 Hz, 1H), 7.39 (s, 1H), 7.35 (dt, J = 4.8 and 2.3 Hz, 2H), 3.95 (s, 3H), 1.71 (s, 9H).

3.1.1.7.22. tert-Butyl 2-oxo-5-(pyrimidin-5-yl)-2,3-dihydro-1H-benzo[d]imidazole-1-carboxylate (33). General procedure C was followed using **86** (0.890 g, 7.185 mmol), **84** (0.500 g, 1.597 mmol), $PdCl_2$(dppf)·CH_2Cl_2 (0.391 g, 0.479 mmol) and CH_3COOK (1.411 g, 14.373 mmol) in dry 1,4-dioxane (16 mL). The reaction mixture was heated at 90 °C for 14 h. Purification of the crude product by chromatography using a gradient 0.3–3 % of CH_3OH in CH_2Cl_2 afforded **33** (150 mg, 30 %) as a beige powder. UPLC-MS: $t_R = 1.62$ min (method A). MS (ESI) *m/z*: 313.2 $(M + H)^+$; $C_{16}H_{17}N_4O_3$ $(M + H)^+$ calcd: 313.1. ^{1}H NMR (400 MHz, DMSO-d_6): δ 9.17 (s, 1H), 9.11 (s, 2H), 7.76 (d, J = 8.4 Hz, 1H), 7.50 (dd, J = 8.4 and 1.9 Hz, 1H), 7.37 (d, J = 1.8 Hz, 1H), 1.61 (s, 9H).

3.1.1.7.23. 5-(2-Oxo-2,3-dihydro-1H-benzo[d]imidazole-5-yl)nicotinamide (87). General procedure C was followed twice in parallel by using **83** (0.243 g, 1.14 mmol), 5-(4,4,5,5-tetramethyl-1,3,2-dioxaborolan-2-yl)nicotinamide (0.368 g, 1.48 mmol), $PdCl_2$(dppf)·CH_2Cl_2 (0.112 g, 0.137 mmol) and aq K_2CO_3 (2 M, 2.28 mL) in dry DMF (12 mL). The reaction mixture was heated at 110 °C for 2 h. Upon completion, the two reaction mixtures were combined and worked up together. Purification of the crude product by chromatography using a gradient 0.1–20 % of CH_3OH in CH_2Cl_2 afforded **87** (422.0 mg, 73 %) as a grey-brown powder. UPLC-MS: $t_R = 1.53$ min (method C); MS (ESI) *m/z*: 255.1 $(M + H)^+$; $C_{13}H_{11}N_4O_2$ $(M + H)^+$ calcd: 255.1. ^{1}H NMR (400 MHz, DMSO-d_6): δ 8.94 (t, J = 2.4 Hz, 2H), 8.40 (t, J = 2.2 Hz, 1H), 8.25 (s, 1H), 7.62 (s, 1H), 7.36 (dd, J = 8.1 and 1.8 Hz, 1H), 7.29 (d, J = 1.7 Hz, 1H), 7.06 (d, J = 8.1 Hz, 1H).

3.1.1.7.24. 5-(2-Oxo-2,3-dihydro-1H-benzo[d]imidazole-5-yl)nicotinonitrile (88). General procedure C was followed twice in parallel by using **83** (0.229 g, 1.074 mmol), 5-cyanopyridine-3-boronic acid (0.317 g, 2.148 mmol), $PdCl_2$(dppf)·CH_2Cl_2 (0.105 g, 0.129 mmol) and aq K_2CO_3 (2 M, 2.69 mL) in dry 1,4-dioxane (10.7 mL). The reaction mixture was heated at 120 °C for 1 h and 30 min. Upon completion, the two reaction mixtures were combined, diluted with CH_3OH and filtered through a celite pad. Washing of the latter with mixtures of CH_3CN/water (1:1, 2x50 mL) and MeOH/acetone (1:1, 2x50 mL) and concentration of the collected filtrates to dryness afforded **88** (430.0 mg, 85 %) as a light grey powder, which was pure enough to be used in the next synthetic step without any further purification. UPLC-MS: $t_R = 1.28$ min (method A). MS (ESI) *m/z*: 237.0 $(M + H)^+$; $C_{13}H_9N_4O$ $(M + H)^+$ calcd: 237.1. ^{1}H NMR (400 MHz, $MeOD_4$): δ 9.08 (s, 1H), 8.86 (s, 1H), 8.45 (s, 1H), 7.43–7.41 (m, 2H), 7.42 (d, J = 9.2 Hz, 2H).

3.1.1.7.25. 5-(5-(Hydroxymethyl)pyridin-3-yl)-1,3-dihydro-2H-benzo[d]imidazole-2-one (89). General procedure C was followed eleven times in parallel by using **83** (0.301 g, 1.414 mmol), **94** (0.662 g, 2.828 mmol), $PdCl_2$(dppf)·CH_2Cl_2 (0.207 g, 0.255 mmol) and aq K_2CO_3 (2 M, 3.54 mL) in dry 1,4-dioxane (14.1 mL). The reaction mixture was heated at 120 °C for 2 h and 30 min. Upon completion, the reaction mixtures were combined and worked up together. Purification of the crude product by chromatography using a gradient 0.1–20 % of CH_3OH in CH_2Cl_2 afforded **89** (2.4 g, 64 %) as a light-pink powder. UPLC-MS: $t_R = 1.57$ min (method C). MS (ESI) *m/z*: 242.0 $(M + H)^+$; $C_{13}H_{12}N_3O_2$ $(M + H)^+$ calcd: 242.1. ^{1}H NMR (400 MHz, DMSO-d_6): δ 10.74 (s, 1H), 10.77 (s, 1H), 8.69 (d, J = 2.3 Hz, 1H), 8.45 (d, J = 2.0 Hz, 1H), 7.90 (t, J = 2.2 Hz, 1H), 7.28 (dd, J = 8.1 and 1.8 Hz, 1H), 7.20 (d, J = 1.7 Hz, 1H), 7.04 (d, J = 8.0 Hz, 1H), 5.36 (t, J = 5.8 Hz, 1H), 4.60 (d, J = 5.7 Hz, 2H).

3.1.1.7.26. 5-(Pyridin-4-yl)-1,3-dihydro-2H-benzo[d]imidazole-2-one (90). General procedure C was followed twice in parallel by using **83** (0.250 g, 1.174 mmol), 4-pyridylboronic acid (0.288 g, 2.347 mmol), $PdCl_2$(dppf)·CH_2Cl_2 (0.115 g, 0.141 mmol) and aq K_2CO_3 (2 M, 2.35 mL) in dry 1,4-dioxane (12 mL). The reaction mixture was heated at 120 °C for 3 h. Upon completion, the two reaction mixtures were combined and worked up together. Purification of the crude product by chromatography using a gradient 0.1–10 % of EtOH in CH_2Cl_2 afforded **90** (271.0 mg, 55 %) as a light-yellow powder. UPLC-MS: $t_R = 1.79$ min (method C). MS (ESI) *m/z*: 212.1 $(M + H)^+$; $C_{12}H_{10}N_3O$ $(M + H)^+$ calcd: 212.1. ^{1}H NMR (400 MHz, DMSO-d_6): δ 10.80 (s, 2H), 8.62–8.50 (m, 2H), 7.69–7.58 (m, 2H), 7.40 (dd, J = 8.1 and 1.8 Hz, 1H), 7.30 (d, J = 1.7 Hz, 1H), 7.05 (d, J = 8.1 Hz, 1H).

3.1.1.7.27. 5-(1-Methyl-1H-imidazole-5-yl)-1,3-dihydro-2H-benzo[d]imidazole-2-one (91). General procedure C was followed twice in parallel by using **83** (0.238 g, 1.117 mmol), 1-methyl-1*H*-imidazole-5-boronic acid pinacol ester (0.465 g, 2.234 mmol), $PdCl_2$(dppf)·CH_2Cl_2 (0.164 g, 0.201 mmol) and aq K_2CO_3 (2 M, 2.23 mL) in dry 1,4-dioxane (11.2 mL). The reaction mixture was heated at 120 °C for 3 h. Upon completion, the two reaction mixtures were combined and worked up together. Purification of the crude product by chromatography using a gradient 0.2–9 % of CH_3OH in CH_2Cl_2 afforded **91** (270.0 mg, 56 %) as a pale-purple powder. UPLC-MS: $t_R = 1.21$ min (method C). MS (ESI) *m/z*: 215.1 $(M + H)^+$; $C_{11}H_{11}N_4O$ $(M + H)^+$ calcd: 215.1. ^{1}H NMR (400 MHz, DMSO-d_6): δ 10.69 (s, 2H), 7.64 (d, J = 1.1 Hz, 1H), 7.08–6.86 (m, 4H), 3.62 (s, 3H).

3.1.1.7.28. 5-(1-Methyl-1H-pyrazol-4-yl)-1,3-dihydro-2H-benzo[d]imidazole-2-one (92). General procedure C was followed twice in parallel by using **83** (0.312 g, 1.465 mmol), 1-methyl-1*H*-pyrazole-4-boronic acid (0.368 g, 2.929 mmol), $PdCl_2$(dppf)·CH_2Cl_2 (0.120 g, 0.147 mmol) and aq Cs_2CO_3 (2 M, 3.66 mL) in dry 1,4-dioxane (14.7 mL). The reaction mixture was heated at 120 °C for 1 h. Upon completion, the two reaction mixtures were combined and worked up together. Purification of the crude product by chromatography using a gradient 0.2–10 % of CH_3OH in CH_2Cl_2 afforded **92** (460.0 mg, 73 %) as a beige powder. UPLC-MS: $t_R = 1.12$ min (method A). MS (ESI) *m/z*: 215.1 $(M + H)^+$; $C_{11}H_{11}N_4O$ $(M + H)^+$ calcd: 215.1. ^{1}H NMR (400 MHz, DMSO-d_6):

δ 10.59 (s, 1H), 10.54 (s, 1H), 8.01 (s, 1H), 7.73 (d, $J = 0.9$ Hz, 1H), 7.12 (dd, $J = 8.0$ and 1.7 Hz, 1H), 7.04 (d, $J = 1.6$ Hz, 1H), 6.88 (d, $J = 8.0$ Hz, 1H), 3.84 (s, 3H).

3.1.1.7.29. 5-(Pyridin-3-yl)-1,3-dihydro-2H-benzo[d]imidazole-2-one (93). General procedure C was followed ten times in parallel by using **83** (0.300 g, 1.408 mmol), 3-pyridynilboronic acid (0.519 g, 4.224 mmol), $PdCl_2(dppf)\cdot CH_2Cl_2$ (0.276 g, 0.338 mmol) and aq K_2CO_3 (2 M, 4.22 mL) in dry 1,4-dioxane (14.1 mL). The reaction mixture was heated at 120 °C for 3 h and 30 min. Upon completion, the two reaction mixtures were combined and worked up together. Purification of the crude product by chromatography using a gradient 0.1–16 % of EtOH in CH_2Cl_2 afforded **93** (2.9 g, 98 %) as a light-pink powder. UPLC-MS: t_R = 1.19 min (method A). MS (ESI) *m/z*: 212.0 $(M + H)^+$; $C_{12}H_{10}N_3O$ $(M + H)^+$ calcd: 212.1. ^{1}H NMR (400 MHz, DMSO-d_6): δ 10.77 (s, 1H), 10.74 (s, 1H), 8.82 (dd, $J = 2.4$ and 0.9 Hz, 1H), 8.51 (dd, $J = 4.8$ and 1.6 Hz, 1H), 7.99 (ddd, $J = 8.0$, 2.5 and 1.6 Hz, 1H), 7.44 (ddd, $J = 7.9$, 4.8 and 0.9 Hz, 1H), 7.28 (dd, $J = 8.0$ and 1.8 Hz, 1H), 7.21 (d, $J = 1.7$ Hz, 1H), 7.03 (d, $J = 8.0$ Hz, 1H).

3.1.1.7.30. 3-Methoxy-5-(4,4,5,5-tetramethyl-1,3,2-dioxaborolan-2-yl)pyridine (85). A mixture of 3-bromo-5-methoxypyridine **95** (1.0 g, 5.32 mmol) and bis(pinacolato)diboron (2.03 g, 7.98 mmol) in dry 1,4-dioxane (31.61 mL) was degassed for about 5–10 min. To this mixture, $PdCl_2(dppf)\cdot CH_2Cl_2$ (0.434 g, 0.532 mmol) and CH_3COOK (2.61 g, 26.6 mmol) were added and the resulting mixture was heated at 85–90 °C for 2 h under an Ar atmosphere. Then, the heating was stopped and the cooled reaction mixture was portioned between 0.1 M solution of HCl (100 mL) and Et_2O (100 mL). The aqueous phase was separated, neutralized by employing NaOH (2 N) and extracted with EtOAc (3 x 100 mL). The separated organic phase was dried over sodium sulfate and concentrated under reduced pressure. The isolated brown powder (1.36 g, quant.) was pure enough to be used in the next synthetic step without further purification. UPLC-MS: t_R = 1.41 min (method A). MS (ESI) *m/z*: 235.2 $(M + H)^+$; $C_{12}H_{19}BN_2O_2$ $(M + H)^+$ calcd: 235.2. ^{1}H NMR (400 MHz, DMSO-d_6): δ 8.37 (d, $J = 3.1$ Hz, 1H), 8.36 (d, $J = 1.3$ Hz, 1H), 7.45 (dd, $J = 3.2$ and 1.3 Hz, 1H), 3.84 (s, 3H), 1.31 (br s, 12H).

3.1.1.7.31. (5-(4,4,5,5-Tetramethyl-1,3,2-dioxaborolan-2-yl)pyridin-3-yl)methanol (94). The same reaction was performed in parallel five times by using the same reagents amounts. A mixture of (5-bromo-3-pyridyl)methanol **96** (1 g, 5.32 mmol) and bis(pinacolato)diboron (1.62 g, 6.38 mmol) in dry dioxane (14.94 mL) was bubbled with Ar for about 5–10 min; $PdCl_2(dppf)\cdot CH_2Cl_2$ (0.174 g, 0.213 mmol) was added followed by addition of CH_3COOK (1.566 g, 15.96 mmol) under an inert atmosphere. The resulting mixture was heated to 160 °C for 15 min under MW irradiation. The reaction mixtures were combined and filtered through a celite pad; the celite was washed four times with fresh CH_3CN and the collected filtrate was concentrated under reduced pressure. The isolated sticky dark brown powder (9.86 g, quant.) was pure enough to be used in the synthetic step without further purification. UPLC-MS: t_R = 1.41 min (method A). MS (ESI) *m/z*: 236.2 $(M + H)^+$; $C_{12}H_{19}BNO_3$ $(M + H)^+$ calcd: 236.1. ^{1}H NMR (600 MHz, $CDCl_3$): δ 8.86 (br s, 1H), 8.66 (br s, 1H), 8.10 (br s, 1H), 4.73 (s, 2H), 1.35 (br s, 12H).

3.1.1.7.32. tert-Butyl 6-(5-carbamoylpyridin-3-yl)-2-oxo-2,3-dihydro-1H-benzo[d]imidazole-1-carboxylate (29a). Regioisomer **29a** was prepared according to general procedure D by using NaH (0.070 g, 1.741 mmol), $(Boc)_2O$ (0.380 g, 1.741 mmol) and **87** (0.442 g, 1.741 mmol) in a dry DMF/DMA mixture (8.2:1.8, 3.28 mL) overnight. Extra **87** (0.442 g, 1.741 mmol) and K_2CO_3 (0.289 g, 2.088 mmol) were added and the resulting mixture was allowed to stir for an additional 72 h. Purification of the crude product by chromatography using a gradient 0.02–5.0 % of CH_3OH in CH_2Cl_2 afforded **29a** (0.068 g, 11 %) as a white powder. UPLC-MS: t_R = 1.52 min (method A). MS (ESI) *m/z*: 355.2 $(M + H)^+$; $C_{18}H_{19}N_4O_4$ $(M + H)^+$ calcd: 355.1. ^{1}H NMR (400 MHz, DMSO-d_6): δ 8.99 (dd, $J = 4.0$ and 2.1 Hz, 2H), 8.44 (t, $J = 2.1$ Hz, 1H), 8.27 (br s, 1H), 7.76 (d, $J = 8.4$ Hz, 1H), 7.65 (br s, 1H), 7.49 (dd, $J = 8.4$ and 1.9 Hz, 1H), 7.36 (d, $J = 1.7$ Hz, 1H), 1.61 (s, 9H). A 2D-NOESY experiment confirmed the compound regiochemistry; diagnostic NOE contact: H-7 (doublet signal at 7.76 ppm) *vs.* $3CH_3$ (Boc, singlet signal at 1.61 ppm); (see Supporting Information).

3.1.1.7.33. tert-Butyl 5-(5-cyanopyridin-3-yl)-2-oxo-2,3-dihydro-1H-benzo[d]imidazole-1-carboxylate (30a). Regioisomer **30a** was prepared according to general procedure D by using NaH (0.070 g, 1.756 mmol), $(Boc)_2O$ (0.383 g, 1.756 mmol) and **88** (0.415 g, 1.756 mmol) in a dry DMF/DMA mixture (9.8:0.2, 12.96 mL) for 72 h. Purification of the crude product by chromatography using a gradient 0.0–3.0 % of CH_3OH in CH_2Cl_2 afforded **30a** (0.094 g, 16 %) as a white powder. UPLC-MS: t_R = 1.88 min (method A). MS (ESI) *m/z*: 337.1 $(M + H)^+$; $C_{18}H_{17}N_4O$ $(M + H)^+$ calcd: 337.1. ^{1}H NMR (400 MHz, DMSO-d_6): δ 9.15 (d, $J = 2.3$ Hz, 1H), 8.97 (d, $J = 1.9$ Hz, 1H), 8.62 (t, $J = 2.1$ Hz, 1H), 7.74 (d, $J = 8.4$ Hz, 1H), 7.50 (dd, $J = 8.4$ and 1.9 Hz, 1H), 7.39 (d, $J = 1.8$ Hz, 1H), 1.60 (s, 9H). A 2D-NOESY experiment confirmed the compound regiochemistry; diagnostic NOE contact: H-7 (doublet signal at 7.74 ppm) *vs.* $3CH_3$ (Boc, singlet signal at 1.60 ppm); (see Supporting Information).

3.1.1.7.34. tert-Butyl 5-(5-(hydroxymethyl)pyridin-3-yl)-2-oxo-2,3-dihydro-1H-benzo[d]imidazole-1-carboxylate (31a). Regioisomer **31a** was prepared according to general procedure D, which was carried out in parallel three times by using NaH (0.134 g, 3.341 mmol), $(Boc)_2O$ (0.729 g, 3.341 mmol) and **89** (0.806 g, 3.341 mmol) in dry DMF (40 mL) for 4 h. Extra K_2CO_3 (0.554 g, 4.009 mmol) was added and the resulting mixture was allowed to stir for an additional 72 h. Purification of the crude product by chromatography using a gradient 0.05–7.5 % of EtOH in CH_2Cl_2 afforded **31a** (1.39 g, 41 %) as a white powder. UPLC-MS: t_R = 1.48 min (method A). MS (ESI) *m/z*: 342.1 $(M + H)^+$; $C_{18}H_{20}N_3O_4$ $(M + H)^+$ calcd: 342.1. ^{1}H NMR (400 MHz, DMSO-d_6): δ 8.73 (d, $J = 2.3$ Hz, 1H), 8.50 (d, $J = 1.9$ Hz, 1H), 7.95 (t, $J = 2.2$ Hz, 1H), 7.73 (d, $J = 8.4$ Hz, 1H), 7.40 (dd, $J = 8.4$ and 1.9 Hz, 1H), 7.26 (d, $J = 1.8$ Hz, 1H), 4.61 (s, 2H), 1.60 (s, 9H). A 2D-NOESY experiment confirmed the compound regiochemistry; diagnostic NOE contact: H-7 (doublet signal at 7.73 ppm) *vs.* $3CH_3$ (Boc, singlet signal at 1.60 ppm); (see Supporting Information).

3.1.1.7.35. tert-Butyl 2-oxo-5-(pyridin-4-yl)-2,3-dihydro-1H-benzo[d]imidazole-1-carboxylate (32a). Regioisomer **32a** was prepared according to general procedure D by using NaH (0.052 g, 1.278 mmol), $(Boc)_2O$ (0.279 g, 1.278 mmol) and **90** (0.270 g, 1.278 mmol) in a dry DMF/DMA mixture (8.9:1.1, 10.2 mL) for 4 days. Purification of the crude product by chromatography using a gradient 15 %–45 % of EtOAc in Cy afforded **32a** (0.103 g, 26 %) as a white powder. UPLC-MS: t_R = 1.75 min (method A). MS (ESI) *m/z*: 312.2 $(M + H)^+$; $C_{17}H_{18}N_3O_3$ $(M + H)^+$ calcd: 312.1. ^{1}H NMR (400 MHz, DMSO-d_6): δ 8.63–8.60 (m, 2H), 7.75 (d, $J = 8.4$ Hz, 1H), 7.70–7.65 (m, 2H), 7.52 (dd, $J = 8.5$ and 1.9 Hz, 1H), 7.35 (d, $J = 1.8$ Hz, 1H), 1.60 (s, 9H). A 2D-NOESY experiment confirmed the compound regiochemistry; diagnostic NOE contact: H-7 (doublet signal at 7.75 ppm) *vs.* $3CH_3$ (Boc, singlet signal at 1.60 ppm); (see Supporting Information).

3.1.1.7.36. tert-Butyl 5-(1-methyl-1H-imidazole-5-yl)-2-oxo-2,3-dihydro-1H-benzo[d]imidazole-1-carboxylate (34a). Regioisomer **34a** was prepared according to general procedure D by using NaH (0.050 g, 1.256 mmol), $(Boc)_2O$ (0.274 g, 1.256 mmol) and **91** (0.269 g, 1.256 mmol) in a dry DMF/DMA mixture (9:1, 10.0 mL) for 4 days. Purification of the crude product by chromatography using a gradient 0.05 %–7.5 % of EtOH in CH_2Cl_2 afforded **34a** (0.156 g, 40 %) as a light-pink powder. UPLC-MS: t_R = 1.54 min (method A). MS (ESI) *m/z*: 315.2 $(M + H)^+$; $C_{16}H_{19}N_4O_3$ $(M + H)^+$ calcd: 315.1. ^{1}H NMR (400 MHz, DMSO-d_6): δ 7.69 (d, $J = 7.7$ Hz, 1H), 7.68 (s, 1H), 7.18 (dd, $J = 8.4$ and 1.7 Hz, 1H), 7.03 (dd, $J = 8.7$ and 1.5 Hz, 2H), 3.66 (s, 3H), 1.60 (s, 9H). A 2D-NOESY experiment confirmed the compound regiochemistry; diagnostic NOE contact: H-7 (doublet signal at 7.69 ppm) *vs.* $3CH_3$ (Boc, singlet signal at 1.60 ppm); (see Supporting Information).

3.1.1.7.37. tert-Butyl 5-(1-methyl-1H-pyrazol-4-yl)-2-oxo-2,3-dihydro-1H-benzo[d]imidazole-1-carboxylate (35a). Regioisomer **35a** was prepared according to general procedure D by using NaH (0.073 g, 1.836 mmol), $(Boc)_2O$ (0.401 g, 1.836 mmol) and **92** (0.393 g, 1.836 mmol) in dry DMF (22.1 mL) overnight. Extra 2.203 mmol of K_2CO_3

(0.305 g) was added and the resulting mixture was allowed to stir 48 h. Purification of the crude product by chromatography using a gradient 0.02 %–3.0 % of CH_3OH in CH_2Cl_2 afforded **35a** (0.249 g, 43 %) as a white powder. UPLC-MS: $t_R = 1.62$ min (method A). MS (ESI) *m/z*: 315.2 $(M + H)^+$; $C_{16}H_{19}N_4O_3$ $(M + H)^+$ calcd: 315.1. ^1H NMR (400 MHz, DMSO-d_6): δ 8.10 (d, $J = 0.8$ Hz, 1H), 7.81 (d, $J = 0.8$ Hz, 1H), 7.59 (d, $J = 8.4$ Hz, 1H), 7.26 (dd, $J = 8.4$, 1.7 Hz, 1H), 7.11 (d, $J = 1.6$ Hz, 1H), 3.85 (s, 3H), 1.59 (s, 9H). A 2D-NOESY experiment confirmed the compound regiochemistry; diagnostic NOE contact: H-7 (doublet signal at 7.59 ppm) *vs.* $3CH_3$ (Boc, singlet signal at 1.59 ppm); (see Supporting Information).

3.1.1.7.38. tert-Butyl 5-(3-methyl-2,5-dioxo-imidazolidin-1-yl)-2-oxo-2,3-dihydro-1H-benzo[d]imidazole-1-carboxylate (36a). Regioisomer **36a** was prepared according to general procedure D by using NaH (0.036 g, 0.898 mmol), $(Boc)_2O$ (0.196 g, 0.898 mmol) and **97** (0.221 g, 0.898 mmol) in dry DMF (7.14 mL) overnight. Extra 0.898 mmol of K_2CO_3 (0.124 g) was added and the resulting mixture was allowed to stir for an additional 48 h. Purification of the crude product by chromatography using a gradient 0.02 %–10.0 % of EtOH in CH_2Cl_2 afforded **36a** (0.050 g, 16 %) as a white powder. UPLC-MS: $t_R = 1.63$ min (method A). MS (ESI) *m/z*: 347.1 $(M + H)^+$; $C_{16}H_{19}N_4O_5$ $(M + H)^+$ calcd: 347.1. ^1H NMR (400 MHz, DMSO-d_6): δ 7.67 (d, $J = 8.4$ Hz, 1H), 7.04–6.97 (m, 2H), 4.08 (s, 2H), 2.92 (s, 3H), 1.59 (s, 9H). A 2D-NOESY experiment confirmed the compound regiochemistry; diagnostic NOE contact: H-7 (doublet signal at 7.67 ppm) *vs.* $3CH_3$ (Boc, singlet signal at 1.59 ppm); (see Supporting Information).

3.1.1.7.39. tert-Butyl 2-oxo-5-(pyridin-3-yl)-2,3-dihydro-1H-benzo[d]imidazole-1-carboxylate (37a). Regioisomer **37a** was prepared according to general procedure D, which was carried out in parallel three times by using NaH (0.177 g, 4.427 mmol), $(Boc)_2O$ (0.966 g, 4.427 mmol) and **93** (0.935 g, 4.427 mmol) in a dry DMF/DMA mixture (9.1:0.9, 56.4 mL) overnight. Extra 4.427 mmol of K_2CO_3 (0.124 g) was added and the resulting mixture was allowed to stir for an additional 48 h. Purification of the crude product by chromatography using a gradient 0.0 %–3.0 % of EtOH in CH_2Cl_2 afforded **37a** (1.04 g, 25 %) as a white powder. UPLC-MS: $t_R = 1.84$ min (method A). MS (ESI) *m/z*: 312.0 $(M + H)^+$; $C_{17}H_{18}N_3O_3$ $(M + H)^+$ calcd: 312.1. ^1H NMR (400 MHz, DMSO-d_6): δ 8.88–8.86 (m, 1H), 8.56 (dd, $J = 4.8$ and 1.6 Hz, 1H), 8.05 (ddd, $J = 7.9$, 2.5 and 1.6 Hz, 1H), 7.74 (d, $J = 8.4$ Hz, 1H), 7.48 (ddd, $J = 7.9$, 4.7 and 0.9 Hz, 1H), 7.43 (dd, $J = 8.4$ and 1.9 Hz, 1H), 7.28 (d, $J = 1.8$ Hz, 1H), 1.61 (s, 9H). A 2D-NOESY experiment confirmed the compound regiochemistry; diagnostic NOE contact: H-7 (doublet signal at 7.74 ppm) *vs.* $3CH_3$ (Boc, singlet signal at 1.61 ppm); (see Supporting Information).

3.1.1.7.40. N-(tert-Butoxycarbonyl)-N-methylglycine (99). To a solution of *N*-methylglycine **98** (1 g, 11.225 mmol) in H_2O (75 mL), $(Boc)_2O$ (2.45 g, 11.225 mmol) and Et_3N (4.69 mL, 33.675 mmol) were added sequentially. The reaction mixture was stirred at rt overnight. 1 N solution of HCl (64 mL) was added and the aqueous layer was extracted with EtOAc (3x75 mL). The combined organic phase was separated, dried over Na_2SO_4 filtered and concentrated under reduced pressure affording **99** (2.12 g, quant.) as a colorless oil, which was pure enough to be used in the next step without further purification. ^1H NMR (400 MHz, $CDCl_3$, 1:1 mixture of rotamers): δ 8.47 (br s, 2H), 4.02 (s, 2H), 3.94 (s, 2H), 2.93 (s, 6H), 1.47 (s, 9H), 1.43 (s, 9H).

3.1.1.7.41. tert-Butyl methyl(2-oxo-2-((2-oxo-2,3-dihydro-1H-benzo[d]imidazole-5-yl)amino)ethyl) carbamate (101). To a solution of 5-amino-1,3-dihydro-2*H*-benzimidazol-2-one **100** (0.431 g, 2.90 mmol) and **99** (0.601 g, 3.179 mmol) in dry DMF (7.9 mL), bubbled with Ar for about 10 min, EDC·HCl (0.609 g, 3.179 mmol) and DMAP (0.388 g, 3.179 mmol) were added under an inert atmosphere. The reaction mixture was stirred at rt overnight. DMF was evaporated under reduced pressure and the resulting residue was purified by normal phase silica gel chromatography by using a gradient 0.04–5 % of CH_3OH in CH_2Cl_2 affording **101** (607.0 mg, 65 %) as a white powder. UPLC-MS $t_R = 2.21$ min (method C). MS (ESI) *m/z*: 321.1 $(M + H)^+$; $C_{15}H_{21}N_4O_4$ $(M + H)^+$ calcd: 321.2. ^1H NMR (400 MHz, DMSO-d_6, 1:0.9 mixture of rotamers): δ 10.53 (br s, 1H), 10.46 (br s, 1H), 9.77 (br s, 1H), 9.74 (br s, 1H), 7.42 (d, $J = 2.0$ Hz, 2H), 6.99 (d, $J = 8.2$ Hz, 2H), 6.82 (d, $J = 8.3$ Hz, 2H), 3.93 (s, 2H), 2.90 (s, 2H), 2.87 (s, 3H), 2.84 (s, 3H), 1.41 (s, 9H), 1.33 (s, 9H).

3.1.1.7.42. 2-(Methylamino)-N-(2-oxo-2,3-dihydro-1H-benzo[d]imidazole-5-yl)acetamide (102). To a suspension of **101** (0.600 g, 1.873 mmol) in dry CH_2Cl_2 (18.7 mL), cooled down to 0 °C, TFA (1.45 mL, 18.73 mmol) was added dropwise. The reaction mixture was stirred at rt for 4 h. Cool Et_2O was added until a white solid precipitated, which was then filtered under *vacuum* and dried. Purification of the obtained solid via strong cation exchange (SCX) chromatography by using a NH_3 solution (0.1 N) in CH_3OH gave **102** (395.0 mg, 96 %) as a white powder. UPLC-MS: $t_R = 1.78$ min (method A). MS (ESI) *m/z*: 221.0 $(M + H)^+$; $C_{10}H_{13}N_4O_2$ $(M + H)^+$ calcd: 221.1. ^1H NMR (400 MHz, DMSO-d_6): δ 10.52 (br s, 1H), 10.45 (br s, 1H), 9.62 (br s, 1H), 7.49 (d, $J = 1.9$ Hz, 1H), 7.03 (dd, $J = 8.3$ and 2.0 Hz, 1H), 6.82 (d, $J = 8.3$ Hz, 1H), 3.17 (d, $J = 4.2$ Hz, 2H), 2.30 (s, 3H).

3.1.1.7.43. 1-Methyl-3-(2-oxo-2,3-dihydro-1H-benzo[d]imidazole-5-yl)imidazolidine-2,4-dione (97). To a suspension of **102** (0.366 g, 1.662 mmol) in a dry mixture of 1,4-dioxane/CH_3CN (8.2:1.8, 32 mL), in a closed system (pressure tube) under an Ar atmosphere, CDI (0.404 g, 2.493 mmol) and DMAP (0.061 g, 0.499 mmol) were sequentially added. The resultant mixture was heated at 100 °C overnight. The heating was stopped and the cooled mixture was evaporated under reduced pressure obtaining a crude product, which was purified by normal phase neutral Al_2O_3 gel chromatography by using a gradient 0.02–10 % of CH_3OH in CH_2Cl_2. A final treatment with CH_3OH (5 mL) afforded the title intermediate **97** (140.0 mg, 34 %) as a pale-yellow powder. UPLC-MS: $t_R = 1.00$ min (method A). MS (ESI) *m/z*: 247.0 $(M + H)^+$; $C_{11}H_{11}N_4O_3$ $(M + H)^+$ calcd: 247.1. ^1H NMR (400 MHz, DMSO-d_6): δ 10.74 (s, 2H), 6.97 (d, $J = 8.1$ Hz, 1H), 6.88–6.74 (m, 2H), 4.07 (s, 2H), 2.92 (s, 3H).

3.1.1.7.44. tert-Butyl 3-((4-(4-(2,3-dichlorophenyl)piperazin-1-yl) butyl)carbamoyl)-5-(5-methoxy pyridin-3-yl)-2-oxo-2,3-dihydro-1H-benzo [d]imidazole-1-carboxylate (38). *N*-Boc protected urea **38** was prepared according to general procedure E reacting freshly prepared isocyanate **19** (0.488 mmol, 1.7 mol equiv) in dry CH_2Cl_2 (4.9 mL) with **28** (0.100 g, 0.293 mmol) in dry CH_2Cl_2 (2.9 mL) for 1 h and 30 min. To aid reaction completion, additional freshly prepared isocyanate **19** (0.244 mmol, 0.8 mol equiv) in dry CH_2Cl_2 (2.5 mL) was added to the reaction solution, which was stirred for additional 1 h and 30 min. Isocyanate **19** was, in turn, prepared using amine **55** (0.148 g, 0.488 mmol), triphosgene (0.060 g, 0.195 mmol) and dry Et_3N (0.23 mL, 1.628 mmol), the first time, and amine **55** (0.075 g, 0.244 mmol), triphosgene (0.030 g, 0.098 mmol) and dry Et_3N (0.11 mL, 0.814 mmol), the second time. Purification by normal phase silica gel chromatography by employing a gradient 0.05–4 % of EtOH in $CHCl_3$ afforded **38** (164.0 mg, 84 %) as sticky white semisolid. UPLC-MS: $t_R = 1.74$ min (method B). MS (ESI) *m/z*: 669.3/671.2/673.2 $(M + H)^+$; $C_{33}H_{39}Cl_2N_6O_5$ $(M + H)^+$ calcd: 669.2/671.2/673.2. ^1H NMR (400 MHz, $CDCl_3$): δ 8.69 (t, $J = 5.7$ Hz, 1H), 8.57 (d, $J = 1.8$ Hz, 1H), 8.47 (d, $J = 1.9$ Hz, 1H), 8.30 (d, $J = 2.8$ Hz, 1H), 7.94 (d, $J = 8.5$ Hz, 1H), 7.46 (dd, $J = 8.5$ and 1.9 Hz, 1H), 7.39 (dd, $J = 2.8$ and 1.9 Hz, 1H), 7.21–7.09 (m, 2H), 6.96 (dd, $J = 7.0$ and 2.5 Hz, 1H), 3.92 (s, 3H), 3.48 (q, $J = 6.4$ Hz, 2H), 3.11 (br s, 4H), 2.78–2.44 (m, 6H), 1.71 (br s, 13 H).

3.1.1.7.45. tert-Butyl 5-(5-carbamoylpyridin-3-yl)-3-((4-(4-(2,3-dichlorophenyl)piperazin-1-yl)butyl) carbamoyl)-2-oxo-2,3-dihydro-1H-benzo[d]imidazole-1-carboxylate (39). *N*-Boc protected urea **39** was prepared according to general procedure E reacting freshly prepared isocyanate **19** (0.275 mmol, 1.5 mol equiv) in dry CH_2Cl_2 (2.8 mL) with **29a** (0.065 g, 0.183 mmol) in dry CH_2Cl_2 (1.8 mL) overnight. The morning after, additional freshly prepared isocyanate **19** (0.275 mmol, 1.5 mol equiv) in dry CH_2Cl_2 (2.8 mL) was added to the reaction solution, which was stirred for 2 days. Isocyanate **19** was, in turn, prepared using amine **55** (0.083 g, 0.275 mmol), triphosgene (0.049 g, 0.165 mmol) and dry Et_3N (0.19 mL, 1.37 mmol) both times. Purification by

normal phase silica gel chromatography by employing a gradient 0.1–10 % of EtOH in $CHCl_3$ afforded **39** (60.0 mg, 48 %) as a white powder. UPLC-MS: t_R = 2.27 min (method A). MS (ESI) *m/z*: 682.2/684.2/686.2 $(M + H)^+$; $C_{33}H_{38}Cl_2N_7O_5$ $(M + H)^+$ calcd: 682.2/684.2/686.2. ^{1}H NMR (400 MHz, $CDCl_3$): δ 8.99 (dd, *J* = 13.8 and 2.1 Hz, 2H), 8.65 (t, *J* = 5.7 Hz, 1H), 8.58 (d, *J* = 1.9 Hz, 1H), 8.37 (t, *J* = 2.2 Hz, 1H), 7.94 (d, *J* = 8.5 Hz, 1H), 7.48 (dd, *J* = 8.5 and 1.9 Hz, 1H), 7.18–7.08 (m, 2H), 6.94 (dd, *J* = 6.9, 2.7 Hz, 1H), 6.60 (br s, 1H), 6.09 (br s, 1H), 3.46 (d, *J* = 6.0 Hz, 2H), 3.08 (s, 4H), 2.68 (br s, 4H), 2.50 (s, 2H), 1.69 (br s, 11H), 1.60 (br s, 2H).

3.1.1.7.46. tert-Butyl 5-(5-cyanopyridin-3-yl)-3-((4-(4-(2,3-dichlorophenyl)piperazin-1-yl)butyl) carbamoyl)-2-oxo-2,3-dihydro-1H-benzo[d] imidazole-1-carboxylate (40). *N*-Boc protected urea **40** was prepared according to general procedure E reacting freshly prepared isocyanate **19** (0.357 mmol, 1.5 mol equiv) in dry CH_2Cl_2 (3.6 mL) with **30a** (0.080 g, 0.238 mmol) in dry CH_2Cl_2 (2.4 mL) overnight. The morning after, additional freshly prepared isocyanate **19** (0.119 mmol, 0.5 mol equiv) in dry CH_2Cl_2 (1.19 mL) was added to the reaction solution, which was stirred for 2 h and 15 min. Isocyanate **19** was, in turn, prepared using amine **55** (0.108 g, 0.357 mmol), triphosgene (0.064 g, 0.214 mmol) and dry Et_3N (0.25 mL, 1.785 mmol), the first time, and amine **55** (0.036 g, 0.119 mmol), triphosgene (0.011 g, 0.036 mmol) and dry Et_3N (0.083 mL, 0.595 mmol), the second time. Purification by normal phase silica gel chromatography by employing a gradient 0.05–3.5 % of EtOH in CH_2Cl_2 afforded **40** (93.0 mg, 59 %) as a pale-yellow powder. UPLC-MS: t_R = 1.83 min (method B). MS (ESI) *m/z*: 664.3/666.2/668.2 $(M + H)^+$; $C_{33}H_{36}Cl_2N_7O_4$ $(M + H)^+$ calcd: 664.2/666.2/668.2. ^{1}H NMR (400 MHz, $CDCl_3$): δ 9.06 (d, *J* = 2.3 Hz, 1H), 8.86 (d, *J* = 2.0 Hz, 1H), 8.73 (t, *J* = 5.8 Hz, 1H), 8.55 (d, *J* = 1.9 Hz, 1H), 8.18 (t, *J* = 2.2 Hz, 1H), 8.02 (d, *J* = 8.5 Hz, 1H), 7.47 (dd, *J* = 8.5 and 2.0 Hz, 1H), 7.24 (d, *J* = 1.5 Hz, 1H), 7.19 (t, *J* = 8.0 Hz, 1H), 7.03 (dd, *J* = 7.9 and 1.6 Hz, 1H), 3.75–3.59 (m, 4H), 3.52 (q, *J* = 6.5 Hz, 2H), 3.37 (d, *J* = 12.8 Hz, 2H), 3.16–3.03 (m, 4H), 2.15–2.03 (m, 2H), 1.80 (q, *J* = 7.2 Hz, 2H), 1.71 (s, 9H).

3.1.1.7.47. tert-Butyl 3-((4-(4-(2,3-dichlorophenyl)piperazin-1-yl) butyl)carbamoyl)-5-(5-(hydroxymethyl)pyridin-3-yl)-2-oxo-2,3-dihydro-1H-benzo[d]imidazole-1-carboxylate (41). *N*-Boc protected urea **41** was prepared twice according to general procedure E, which was applied in parallel by reacting freshly prepared isocyanate **19** (2.336 mmol, 1.8 mol equiv) in dry CH_2Cl_2 (23.36 mL) with **31a** (0.386 g, 1.131 mmol) in a dry CH_2Cl_2/DMF mixture (9:1, 12.6 mL) overnight. Isocyanate **19** was, in turn, prepared using amine **55** (0.706 g, 2.336 mmol), triphosgene (0.416 g, 1.402 mmol) and dry Et_3N (1.63 mL, 11.68 mmol). Purification by normal phase silica gel chromatography by employing a gradient 0.02–10 % of EtOH in CH_2Cl_2 afforded **41** (1.0 g, 66 %) as a white powder, after treatment of the isolated solid with EtOH (2x5 mL). UPLC-MS: t_R = 2.55 min (method A). MS (ESI) *m/z*: 669.2/671.2/673.2 $(M + H)^+$; $C_{33}H_{39}Cl_2N_6O_5$ $(M + H)^+$ calcd: 669.2/671.2/673.2. ^{1}H NMR (400 MHz, $CDCl_3$): δ 8.79 (d, *J* = 2.1 Hz, 1H), 8.69 (t, *J* = 5.9 Hz, 1H), 8.62 (s, 1H), 8.57 (d, *J* = 1.8 Hz, 1H), 8.30 (br s, 1H), 7.96 (d, *J* = 8.5 Hz, 1H), 7.53–7.44 (m, 1H), 7.24 (dd, *J* = 8.1 and 1.6 Hz, 1H), 7.19 (t, *J* = 8.2 Hz, 1H), 7.03 (dd, *J* = 8.0 and 1.6 Hz, 1H), 4.87 (s, 2H), 3.74–3.58 (m, 4H), 3.53–3.49 (m, 2H), 3.37 (d, *J* = 12.4 Hz, 2H), 3.18–3.06 (m, 4H), 2.11 (br s, 2H), 1.85–1.74 (m, 2H), 1.71 (s, 9H).

3.1.1.7.48. tert-Butyl 3-((4-(4-(2,3-dichlorophenyl)piperazin-1-yl) butyl)carbamoyl)-2-oxo-5-(pyridin-4-yl)-2,3-dihydro-1H-benzo[d]imidazole-1-carboxylate (42). *N*-Boc protected urea **42** was prepared according to general procedure E reacting freshly prepared isocyanate **19** (0.546 mmol, 1.7 mol equiv) in dry CH_2Cl_2 (3.3 mL) with **32a** (0.102 g, 0.328 mmol) in a dry CH_2Cl_2/DMF mixture (9.2:0.8, 3.3 mL) overnight. Isocyanate **19** was, in turn, prepared using amine **55** (0.165 g, 0.546 mmol), triphosgene (0.097 g, 0.328 mmol) and dry Et_3N (0.38 mL, 2.73 mmol). Purification by normal phase silica gel chromatography by employing a gradient 0.1–5 % of EtOH in CH_2Cl_2 afforded **42** (121.0 mg, 58 %) as a white powder. UPLC-MS: t_R = 1.68 min (method B). MS (ESI) *m/z*: 639.3/641.2/643.1 $(M + H)^+$; $C_{32}H_{37}Cl_2N_6O_4$ $(M + H)^+$ calcd: 639.2/641.2/643.2. ^{1}H NMR (400 MHz, $CDCl_3$): δ 8.71 (t, *J* = 5.3 Hz, 1H), 8.67–8.64 (m, 2H), 8.63 (d, *J* = 1.9 Hz, 1H), 7.97 (d, *J* = 8.5 Hz, 1H), 7.58–7.50 (m, 3H), 7.22–7.13 (m, 2H), 7.02–6.95 (m, 1H), 3.50 (q, *J* = 6.5 Hz, 2H), 3.30 (br s, 4H), 2.89 (br s, 4H), 1.89 (br s, 2H), 1.75 (t, *J* = 3.0 Hz, 2H), 1.70 (s, 9H), 1.60 (br s, 2H).

3.1.1.7.49. tert-Butyl 3-((4-(4-(2,3-dichlorophenyl)piperazin-1-yl) butyl)carbamoyl)-2-oxo-5-(pyrimidin-5-yl)-2,3-dihydro-1H-benzo[d]imidazole-1-carboxylate (43). *N*-Boc protected urea **43** was prepared according to general procedure E reacting freshly prepared isocyanate **19** (0.363 mmol, 1.1 mol equiv) in dry CH_2Cl_2 (3.6 mL) with **33** (0.102 g, 0.327 mmol) in dry CH_2Cl_2 (3.3 mL) for 2 h. Additional freshly prepared isocyanate **19** (0.182 mmol, 0.6 mol equiv) in dry CH_2Cl_2 (1.8 mL) was added to the reaction solution, which was stirred for additional 1 h and 30 min. Isocyanate **19** was, in turn, prepared using amine **55** (0.110 g, 0.363 mmol), triphosgene (0.066 g, 0.218 mmol) and dry Et_3N (0.25 mL, 1.815 mmol), the first time, and amine **55** (0.055 g, 0.182 mmol), triphosgene (0.033 g, 0.109 mmol) and dry Et_3N (0.13 mL, 0.908 mmol), the second time. Purification by normal phase silica gel chromatography by employing a gradient 0.3–3.5 % of CH_3OH in CH_2Cl_2 afforded **43** (145.0 mg, 69 %) as a white powder. UPLC-MS: t_R = 2.53 min (method A). MS (ESI) *m/z*: 640.1/642.1/644.1 $(M + H)^+$; $C_{31}H_{36}Cl_2N_7O_4$ $(M + H)^+$ calcd: 640.1/642.1/644.1. ^{1}H NMR (400 MHz, $CDCl_3$): δ 9.21 (s, 1H), 8.98 (s, 2H), 8.67 (br s, 1H), 8.60 (d, *J* = 1.9 Hz, 1H), 8.01 (d, *J* = 8.5 Hz, 1H), 7.46 (dd, *J* = 8.5 and 1.9 Hz, 1H), 7.15–7.12 (m, 2H), 6.96 (d, *J* = 7.2 Hz, 1H), 3.50–3.46 (m, 2H), 3.11 (br s, 4H), 2.66 (br s, 4H), 2.51 (br s, 2H), 1.73 (br s, 2H), 1.71 (s, 9H), 1.55 (br s, 2H).

3.1.1.7.50. tert-Butyl 3-((4-(4-(2,3-dichlorophenyl)piperazin-1-yl) butyl)carbamoyl)-5-(1-methyl-1H-imidazole-5-yl)-2-oxo-2,3-dihydro-1H-benzo[d]imidazole-1-carboxylate (44). *N*-Boc protected urea **44** was prepared according to general procedure E reacting freshly prepared isocyanate **19** (1.082 mmol, 2.2 mol equiv) in dry CH_2Cl_2 (10.8 mL) with **34a** (0.153 g, 0.487 mmol) in dry CH_2Cl_2 (4.9 mL) for 3 h. Isocyanate **19** was, in turn, prepared using amine **55** (0.327 g, 1.082 mmol), triphosgene (0.193 g, 0.649 mmol) and dry Et_3N (0.75 mL, 5.411 mmol). Purification by normal phase silica gel chromatography by employing a gradient 0.1–8 % of EtOH in CH_2Cl_2 afforded **44** (158.0 mg, 50 %) as a light pink powder. UPLC-MS: R_t = 1.37 min (method B), 642.2/644.2/646.2 $(M + H)^+$; $C_{31}H_{38}Cl_2N_7O_4$ $(M + H)^+$ calcd: 642.2/644.2/646.2. ^{1}H NMR (400 MHz, $CDCl_3$): δ 8.69 (t, *J* = 5.2 Hz, 1H), 8.37 (d, *J* = 1.8 Hz, 1H), 7.91 (d, *J* = 8.4 Hz, 1H), 7.52 (s, 1H), 7.29 (dd, *J* = 8.4 and 1.8 Hz, 1H), 7.23–7.08 (m, 3H), 6.98 (dd, *J* = 7.8 and 1.7 Hz, 1H), 3.70 (s, 3H), 3.48 (q, *J* = 6.4 Hz, 2H), 3.26 (br s, 4H), 2.86 (s, 6H), 1.85 (br s, 2H), 1.75–1.70 (m, 2H), 1.70 (s, 9H).

3.1.1.7.51. tert-Butyl 3-((4-(4-(2,3-dichlorophenyl)piperazin-1-yl) butyl)carbamoyl)-5-(1-methyl-1H-pyrazol-4-yl)-2-oxo-2,3-dihydro-1H-benzo[d]imidazole-1-carboxylate (45). *N*-Boc protected urea **45** was prepared according to general procedure E reacting freshly prepared isocyanate **19** (0.587 mmol, 1.5 mol equiv) in dry CH_2Cl_2 (5.9 mL) with **35a** (0.123 g, 0.391 mmol) in dry CH_2Cl_2 (3.9 mL) for 10 h. Isocyanate **19** was, in turn, prepared using amine **55** (0.177 g, 0.587 mmol), triphosgene (0.102 g, 0.352 mmol) and dry Et_3N (0.41 mL, 2.933 mmol). Purification by normal phase silica gel chromatography by employing a gradient 0.05–4.5 % of CH_3OH in CH_2Cl_2 afforded **45** (163.0 mg, 65 %) as a colorless oil. UPLC-MS: t_R = 1.54 min (method B). MS (ESI) *m/z*: 642.3/644.2/646.3 $(M + H)^+$; $C_{31}H_{38}Cl_2N_7O_4$ $(M + H)^+$ calcd: 642.2/644.2/646.2. ^{1}H NMR (600 MHz, $CDCl_3$): δ 8.72 (t, *J* = 5.6 Hz, 1H), 8.42 (d, *J* = 1.8 Hz, 1H), 7.85–7.74 (m, 2H), 7.66 (s, 1H), 7.35 (dd, *J* = 8.4 and 1.8 Hz, 1H), 7.19–7.07 (m, 2H), 6.97 (dd, *J* = 7.6 and 1.9 Hz, 1H), 3.93 (s, 3H), 3.53–3.43 (m, 2H), 3.15 (br s, 4H), 2.74 (br s, 4H), 2.57 (br s, 2H), 1.71 (br s, 2H), 1.69 (s, 9H), 1.61 (br s, 2H).

3.1.1.7.52. tert-Butyl 3-((4-(4-(2,3-dichlorophenyl)piperazin-1-yl) butyl)carbamoyl)-5-(3-methyl-2,5-dioxoimidazolidin-1-yl)-2-oxo-2,3-dihydro-1H-benzo[d]imidazole-1-carboxylate (46). *N*-Boc protected urea **46** was prepared according to general procedure E reacting freshly prepared isocyanate **19** (0.209 mmol, 1.5 mol equiv) in dry CH_2Cl_2 (2.1 mL) with **36a** (0.048 g, 0.139 mmol) in dry CH_2Cl_2 (1.4 mL) overnight.

Isocyanate **19** was, in turn, prepared using amine **55** (0.063 g, 0.209 mmol), triphosgene (0.038 g, 0.125 mmol) and dry Et_3N (0.15 mL, 1.04 mmol). Purification by normal phase silica gel chromatography by employing a gradient 0.01–4.5 % of EtOH in CH_2Cl_2 afforded **46** (59.0 mg, 63 %) as a colorless oil. UPLC-MS: t_R = 2.49 min (method A). MS (ESI) *m/z*: 674.2/676.2/678.1 $(M + H)^+$; $C_{31}H_{38}Cl_2N_7O_6$ $(M + H)^+$ calcd: 674.2/676.2/678.2. ^{1}H NMR (400 MHz, $CDCl_3$): δ 8.60 (t, *J* = 5.8 Hz, 1H), 8.36 (d, *J* = 2.1 Hz, 1H), 7.92 (d, *J* = 8.7 Hz, 1H), 7.26 (dd, *J* = 8.7 and 2.2 Hz, 1H), 7.21–7.12 (m, 2H), 6.98 (dd, *J* = 7.3 and 2.3 Hz, 1H), 4.04 (s, 2H), 3.45 (q, *J* = 6.4 Hz, 2H), 3.21 (br s, 4H), 3.06 (s, 3H), 2.88–2.66 (m, 6H), 1.77–1.68 (m, 4H), 1.68 (s, 9H).

3.1.1.7.53. tert-Butyl 3-((3-(4-(2,3-dichlorophenyl)piperazin-1-yl) propyl)carbamoyl)-2-oxo-5-(pyridin-3-yl)-2,3-dihydro-1H-benzo[d]imidazole-1-carboxylate (47). *N*-Boc protected urea **47** was prepared according to general procedure E reacting freshly prepared isocyanate **20** (0.321 mmol, 1.7 mol equiv) in dry CH_2Cl_2 (3.2 mL) with **37a** (0.060 g, 0.193 mmol) in dry CH_2Cl_2 (1.93 mL) overnight. Additional freshly prepared isocyanate **20** (0.250 mmol, 1.3 mol equiv) in dry CH_2Cl_2 (2.5 mL) was added to the reaction solution, which was stirred for an additional 1 day. Isocyanate **20** was, in turn, prepared using amine **56** (0.093 g, 0.321 mmol), triphosgene (0.058 g, 0.193 mmol) and dry Et_3N (0.22 mL, 1.608 mmol), the first time, and amine **56** (0.072 g, 0.250 mmol), triphosgene (0.045 g, 0.152 mmol) and dry Et_3N (0.17 mL, 1.220 mmol), the second time. Purification by normal phase silica gel chromatography by employing a gradient 0.0–4.5 % of EtOH in CH_2Cl_2 afforded **47** (97.0 mg, 80 %) as a sticky white powder. UPLC-MS: t_R = 1.88 min (method B). MS (ESI) *m/z*: 625.0/627.0/629.0 $(M + H)^+$; $C_{31}H_{35}Cl_2N_6O_4$ $(M + H)^+$ calcd: 625.2/627.2/629.2. ^{1}H NMR (400 MHz, $CDCl_3$): δ 8.89 (d, *J* = 2.3 Hz, 1H), 8.84 (t, *J* = 6.0 Hz, 1H), 8.62 (d, *J* = 4.9 Hz, 1H), 8.52 (d, *J* = 1.9 Hz, 1H), 7.99 (dd, *J* = 8.6 and 3.0 Hz, 2H), 7.49 (dd, *J* = 8.5 and 1.9 Hz, 1H), 7.44 (dd, *J* = 8.0 and 4.9 Hz, 1H), 7.24 (dd, *J* = 8.0 and 1.6 Hz, 1H), 7.18 (t, *J* = 8.0 Hz, 1H), 7.02 (dd, *J* = 8.0 and 1.6 Hz, 1H), 3.77–3.54 (m, 6H), 3.38 (d, *J* = 12.6 Hz, 2H), 3.20–3.09 (m, 4H), 2.38 (p, *J* = 6.4 Hz, 2H), 1.71 (s, 9H).

3.1.1.7.54. tert-Butyl (E)-3-((4-(4-(2,3-dichlorophenyl)piperazin-1-yl)but-2-en-1-yl)carbamoyl)-2-oxo-5-(pyridin-3-yl)-2,3-dihydro-1H-benzo [d]imidazole-1-carboxylate (48). *N*-Boc protected urea **48** was prepared according to general procedure E reacting freshly prepared isocyanate **21** (0.385 mmol, 2.0 mol equiv) in dry CH_2Cl_2 (3.85 mL) with **37a** (0.060 g, 0.193 mmol) in dry CH_2Cl_2 (1.93 mL) for 2 h and 30 min. Isocyanate **21** was, in turn, prepared using amine **57** (0.116 g, 0.385 mmol), triphosgene (0.069 g, 0.232 mmol) and dry Et_3N (0.27 mL, 1.93 mmol). Purification by normal phase silica gel chromatography by employing a gradient 0.0–5.0 % of CH_3OH in CH_2Cl_2 afforded **48** (75.0 mg, 61 %) as a white powder. UPLC-MS: t_R = 1.81 min (method B). MS (ESI) *m/z*: 637.0/639.0/641.0 $(M + H)^+$; $C_{32}H_{35}Cl_2N_6O_4$ $(M + H)^+$ calcd: 637.2/639.2/641.2. ^{1}H NMR (400 MHz, $CDCl_3$): δ 9.00 (d, *J* = 2.1 Hz, 1H), 8.80 (t, *J* = 5.8 Hz, 1H), 8.69 (d, *J* = 5.6 Hz, 1H), 8.66 (d, *J* = 8.4 Hz, 1H), 8.61 (d, *J* = 2.0 Hz, 1H), 8.10 (d, *J* = 8.5 Hz, 1H), 7.98 (dd, *J* = 8.2 and 5.5 Hz, 1H), 7.52 (dd, *J* = 8.5 and 2.0 Hz, 1H), 7.24 (dd, *J* = 8.0 and 1.6 Hz, 1H), 7.19 (t, *J* = 8.0 Hz, 1H), 7.02 (dd, *J* = 7.8 and 1.6 Hz, 1H), 6.22–6.05 (m, 2H), 4.14 (t, *J* = 5.1 Hz, 2H), 3.69 (t, *J* = 5.9 Hz, 2H), 3.60 (t, *J* = 12.6 Hz, 4H), 3.39 (d, *J* = 12.7 Hz, 2H), 3.12–2.98 (m, 2H), 1.71 (s, 9H).

3.1.1.7.55. tert-Butyl 2-oxo-3-((4-(4-phenylpiperazin-1-yl)butyl)carbamoyl)-5-(pyridin-3-yl)-2,3-dihydro-1H-benzo[d]imidazole-1-carboxylate (49). *N*-Boc protected urea **49** was prepared according to general procedure E reacting freshly prepared isocyanate **22** (0.386 mmol, 2.0 mol equiv) in dry CH_2Cl_2 (3.86 mL) with **37a** (0.060 g, 0.193 mmol) in dry CH_2Cl_2 (1.93 mL) overnight. Additional freshly prepared isocyanate **22** (0.386 mmol, 2.0 mol equiv) in dry CH_2Cl_2 (3.86 mL) was added to the reaction solution, which was stirred for an additional 4 h. Isocyanate **22** was, in turn, prepared twice using amine **58** (0.090 g, 0.386 mmol), triphosgene (0.069 g, 0.232 mmol) and dry Et_3N (0.27 mL, 1.93 mmol). Two sequential purifications by normal phase silica gel chromatography by employing first a gradient 0.0–4.0 % of EtOH in CH_2Cl_2 and then a gradient 0.0–3.0 % of CH_3OH in CH_2Cl_2 afforded the pure **49** (78.0 mg, 71 %) as a light-yellow powder. UPLC-MS: t_R = 2.30 min (method A). MS (ESI) *m/z*: 571.2 $(M + H)^+$; $C_{32}H_{39}N_6O_4$ $(M + H)^+$ calcd: 571.3. ^{1}H NMR (400 MHz, $CDCl_3$): δ 8.87 (d, *J* = 2.1 Hz, 1H), 8.69 (t, *J* = 5.6 Hz, 1H), 8.59 (dd, *J* = 4.8 and 1.6 Hz, 2H), 8.57 (d, *J* = 1.9 Hz, 1H), 7.95 (d, *J* = 8.5 Hz, 1H), 7.91 (ddd, *J* = 7.9, 2.4 and 1.6 Hz, 1H), 7.47 (dd, *J* = 8.5 and 1.9 Hz, 1H), 7.35 (ddd, *J* = 8.0, 4.8 and 0.9 Hz, 1H), 7.28–7.24 (m, 1H), 6.96–6.88 (m, 2H), 6.87 (t, *J* = 7.3 Hz, 1H), 3.48 (q, *J* = 6.3 Hz, 2H), 3.32 (br s, 4H), 2.78 (br s, 4H), 2.61 (br s, 2H), 1.71 (s, 9H), 1.00–0.73 (m, 4H).

3.1.1.7.56. tert-Butyl 3-((4-(4-(2-methoxyphenyl)piperazin-1-yl) butyl)carbamoyl)-2-oxo-5-(pyridin-3-yl)-2,3-dihydro-1H-benzo[d]imidazole-1-carboxylate (50). *N*-Boc protected urea **50** was prepared according to general procedure E reacting freshly prepared isocyanate **23** (0.535 mmol, 1.1 mol equiv) in dry CH_2Cl_2 (5.35 mL) with **37a** (0.150 g, 0.482 mmol) in dry CH_2Cl_2 (4.82 mL) for 4 h. Additional freshly prepared isocyanate **23** (0.535 mmol, 1.1 mol equiv) in dry CH_2Cl_2 (5.35 mL) was added to the reaction solution, which was stirred overnight. Isocyanate **23** was, in turn, prepared twice using amine **59** (0.141 g, 0.535 mmol), triphosgene (0.097 g, 0.321 mmol) and dry Et_3N (0.37 mL, 2.675 mmol). Purification by normal phase silica gel chromatography by employing a gradient 0.0–5.0 % of CH_3OH in $CHCl_3$ afforded the pure **50** (225.0 mg, 78 %) as a sticky white solid. UPLC-MS: t_R = 2.21 min (method A). MS (ESI) *m/z*: 601.4 $(M + H)^+$; $C_{33}H_{41}N_6O_5$ $(M + H)^+$ calcd: 601.3. ^{1}H NMR (400 MHz, $CDCl_3$): δ 8.87 (dd, *J* = 2.4 and 0.9 Hz, 1H), 8.68 (t, *J* = 5.7 Hz, 1H), 8.62–8.57 (m, 2H), 7.95 (d, *J* = 8.5 Hz, 1H), 7.92 (ddd, *J* = 7.9, 2.4 and 1.6 Hz, 1H), 7.47 (dd, *J* = 8.5 and 1.9 Hz, 1H), 7.36 (ddd, *J* = 7.9, 4.8 and 0.9 Hz, 1H), 7.00 (ddd, *J* = 7.9, 6.8 and 2.2 Hz, 1H), 6.96–6.88 (m, 2H), 6.85 (dd, *J* = 8.0 and 1.4 Hz, 1H), 3.86 (s, 3H), 3.50–3.44 (m, 2H), 3.14 (br s, 4H), 2.72 (br s, 4H), 2.52 (br s, 2H), 1.71 (s, 9H), 1.64 (br s, 4H).

3.1.1.7.57. tert-Butyl 2-oxo-5-(pyridin-3-yl)-3-((4-(4-(o-tolyl)piperazin-1-yl)butyl)carbamoyl)-2,3-dihydro-1H-benzo[d]imidazole-1-carboxylate (51). *N*-Boc protected urea **51** was prepared according to general procedure E reacting freshly prepared isocyanate **24** (0.692 mmol, 1.1 mol equiv) in dry CH_2Cl_2 (6.92 mL) with **37a** (0.194 g, 0.623 mmol) in dry CH_2Cl_2 (6.23 mL) overnight. Isocyanate **24** was, in turn, prepared using amine **60** (0.171 g, 0.692 mmol), triphosgene (0.126 g, 0.415 mmol) and dry Et_3N (0.48 mL, 3.460 mmol). Purification by normal phase silica gel chromatography by employing a gradient 2.5–50 % of EtOAc in CH_2Cl_2 afforded the pure **51** (245.0 mg, 67 %) as a white powder. UPLC-MS: t_R = 2.41 min (method A). MS (ESI) *m/z*: 585.4 $(M + H)^+$; $C_{33}H_{41}N_6O_4$ $(M + H)^+$ calcd: 585.3. ^{1}H NMR (400 MHz, $CDCl_3$): δ 8.87 (dd, *J* = 2.4 and 0.9 Hz, 1H), 8.68 (t, *J* = 5.6 Hz, 1H), 8.59 (dd, *J* = 5.1 and 1.8 Hz, 2H), 7.95 (d, *J* = 8.5 Hz, 1H), 7.91 (ddd, *J* = 7.9, 2.4 and 1.7 Hz, 1H), 7.47 (dd, *J* = 8.5 and 1.9 Hz, 1H), 7.36 (ddd, *J* = 7.9, 4.8 and 0.9 Hz, 1H), 7.15 (t, *J* = 7.5 Hz, 2H), 7.02 (dd, *J* = 7.7 and 1.4 Hz, 1H), 6.96 (td, *J* = 7.3 and 1.3 Hz, 1H), 3.48 (q, *J* = 6.5 Hz, 2H), 2.94 (t, *J* = 4.8 Hz, 4H), 2.61 (br s, 4H), 2.46 (t, *J* = 7.2 Hz, 2H), 2.29 (s, 3H), 1.71 (s, 9H), 1.69–1.64 (m, 4H).

3.1.1.7.58. tert-Butyl 2-oxo-3-((3-(4-phenylpiperazin-1-yl)propyl)carbamoyl)-5-(pyridin-3-yl)-2,3-dihydro-1H-benzo[d]imidazole-1-carboxylate (52). *N*-Boc protected urea **52** was prepared twice according to general procedure E reacting freshly prepared isocyanate **25** (2.376 mmol, 1.8 mol equiv) in dry CH_2Cl_2 (23.76 mL) with **37a** (0.411 g, 1.320 mmol) in dry CH_2Cl_2 (13.20 mL) for 4 h. Isocyanate **25** was, in turn, prepared using amine **61** (0.521 g, 2.376 mmol), triphosgene (0.432 g, 1.426 mmol) and dry Et_3N (1.656 mL, 11.88 mmol). Purification by normal phase silica gel chromatography by employing a gradient 0.0–2.0 % of EtOH in $CHCl_3$ afforded the pure **52** (968.0 mg, 66 %) as an off-white powder. UPLC-MS: t_R = 2.42 min (method A). MS (ESI) *m/z*: 557.1 $(M + H)^+$; $C_{31}H_{37}N_6O_4$ $(M + H)^+$ calcd: 557.3. ^{1}H NMR (400 MHz, DMSO-d_6): δ 8.84 (d, *J* = 2.4 Hz, 1H), 8.76 (t, *J* = 5.7 Hz, 1H), 8.59 (dd, *J* = 4.8 and 1.6 Hz, 1H), 8.41 (d, *J* = 2.0 Hz, 1H), 8.04 (dt, *J* = 8.0 and 1.9 Hz, 1H), 7.90 (d, *J* = 8.5 Hz, 1H), 7.62 (dd, *J* = 8.5 and 2.0 Hz, 1H), 7.51 (dd, *J* = 8.0 and 4.8 Hz, 1H), 7.23–7.16 (m, 2H), 6.95–6.87 (m, 2H),

6.75 (t, $J = 7.3$ Hz, 1H), 3.41 (q, $J = 6.5$ Hz, 2H), 3.15 (t, $J = 5.1$ Hz, 4H), 2.53–2.50 (m, 4H), 2.43 (t, $J = 6.8$ Hz, 2H), 1.77 (p, $J = 7.3$ Hz, 2H), 1.57 (s, 9H).

3.1.1.7.59. tert-Butyl (E)-2-oxo-3-((4-(4-phenylpiperazin-1-yl)but-2-en-1-yl)carbamoyl)-5-(pyridin-3-yl)-2,3-dihydro-1H-benzo[d]imidazole-1-carboxylate (53). *N*-Boc protected urea **53** was prepared according to general procedure E reacting freshly prepared isocyanate **26** (0.385 mmol, 2.0 mol equiv) in dry CH_2Cl_2 (3.85 mL) with **37a** (0.060 g, 0.193 mmol) in dry CH_2Cl_2 (1.93 mL) for 2 h. Isocyanate **26** was, in turn, prepared using amine **62** (0.089 g, 0.385 mmol), triphosgene (0.069 g, 0.232 mmol) and dry Et_3N (0.27 mL, 1.93 mmol). Purification by normal phase silica gel chromatography by employing a gradient 0.04–3.0 % of CH_3OH in CH_2Cl_2 afforded the pure **53** (70.0 mg, 64 %) as a beige powder. UPLC-MS: $t_R = 1.13$ min (method B). MS (ESI) *m/z*: 569.1 $(M + H)^+$; $C_{32}H_{37}N_6O_4$ $(M + H)^+$ calcd: 569.3. ^{1}H NMR (400 MHz, $CDCl_3$): δ 8.99 (d, $J = 1.7$ Hz, 1H), 8.81 (t, $J = 5.5$ Hz, 1H), 8.67 (t, $J = 6.5$ Hz, 1H), 8.62 (d, $J = 1.9$ Hz, 1H), 8.10 (d, $J = 8.5$ Hz, 1H), 7.97 (dd, $J = 8.2$ and 5.6 Hz, 1H), 7.77 (br s, 1H), 7.51 (dd, $J = 8.5$ and 1.9 Hz, 1H), 7.36 (dd, $J = 7.9$ and 1.5 Hz, 2H), 7.25–7.23 (m, 1H), 7.14–7.00 (m, 1H), 6.19–6.03 (m, 2H), 4.44 (br s, 1H), 4.14 (t, $J = 5.4$ Hz, 2H), 3.96 (br s, 1H), 3.77 (d, $J = 6.9$ Hz, 1H), 3.69–3.57 (m, 4H), 3.41 (d, $J = 13.1$ Hz, 1H), 3.08–3.02 (m, 2H), 1.71 (s, 9H).

3.1.1.7.60. tert-Butyl 3-((4-(4-(2,3-dichlorophenyl)piperazin-1-yl)-4-oxobutyl)carbamoyl)-2-oxo-5-(pyridin-3-yl)-2,3-dihydro-1H-benzo[d]imidazole-1-carboxylate (54). *N*-Boc protected urea **54** was prepared according to general procedure E reacting freshly prepared isocyanate **27** (0.261 mmol, 1.8 mol equiv) in dry CH_2Cl_2 (2.61 mL) with **37a** (0.045 g, 0.145 mmol) in dry CH_2Cl_2 (1.45 mL) for 1 h and 20 min. Isocyanate **27** was, in turn, prepared using amine **63** (0.083 g, 0.261 mmol), triphosgene (0.048 g, 0.157 mmol) and dry Et_3N (0.18 mL, 1.31 mmol). Purification by normal phase silica gel chromatography by employing a gradient 0.0–2.0 % of CH_3OH in CH_2Cl_2 afforded the pure **54** (95 mg, quant.) as a colorless oil. UPLC-MS: $t_R = 1.66$ min (method B). MS (ESI) *m/z*: 653.0/655.0/657.0 $(M + H)^+$; $C_{32}H_{35}Cl_2N_6O_5$ $(M + H)^+$ calcd: 653.2/655.2/657.2. ^{1}H NMR (400 MHz, $CDCl_3$): δ 8.97 (s, 1H), 8.70–8.62 (m, 3H), 8.50 (s, 1H), 8.06 (d, $J = 8.5$ Hz, 1H), 7.86 (s, 1H), 7.50 (dd, $J = 8.4$ and 1.9 Hz, 1H), 7.22–7.11 (m, 2H), 6.91 (dd, $J = 7.9$ and 1.7 Hz, 1H), 3.81 (br s, 2H), 3.66 (br s, 2H), 3.54 (q, $J = 6.5$ Hz, 2H), 3.02 (br s, 4H), 2.49 (t, $J = 7.2$ Hz, 2H), 2.05 (t, $J = 7.0$ Hz, 2H), 1.71 (s, 9H).

3.1.1.7.61. N-(4-(4-(2,3-Dichlorophenyl)piperazin-1-yl)butyl)-6-(5-methoxypyridin-3-yl)-2-oxo-2,3-dihydro-1H-benzo[d]imidazole-1-carboxamide trihydrogen chloride (2). General procedure F was followed treating *N*-Boc protected urea **38** (0.163 g, 0.243 mmol) with TFA (0.19 mL) in CH_2Cl_2 (2.43 mL) for 5 h to give the corresponding free base (122.0 mg, 88 %) as a white powder. UPLC-MS: $t_R = 2.02$ min (method A). MS (ESI) *m/z*: 569.2/571.2/573.2 $(M + H)^+$; $C_{28}H_{31}Cl_2N_6O_3$ $(M + H)^+$ calcd: 569.2/571.2/573.2. ^{1}H NMR (400 MHz, DMSO-d_6): δ 9.22 (br s, 1H), 8.38 (d, $J = 1.9$ Hz, 1H), 8.21 (dd, $J = 6.7$ and 2.3 Hz, 2H), 7.48 (t, $J = 2.4$ Hz, 1H), 7.41 (dd, $J = 8.2$, 1.9 Hz, 1H), 7.34–7.22 (m, 2H), 7.12 (dd, $J = 6.0$ and 3.6 Hz, 1H), 7.08 (d, $J = 8.2$ Hz, 1H), 3.90 (s, 3H), 2.97 (t, $J = 4.5$ Hz, 6H), 2.55–2.51 (m, 4H), 2.38 (t, $J = 6.8$ Hz, 2H), 1.59–1.53 (m, 4H). General procedure G was followed using the isolated free base (0.121 g, 0.212 mmol) and HCl (4 N) in 1,4-dioxane (0.53 mL) in 1,4-dioxane (3.14 mL), affording the pure salt **2** (108.0 mg, 75 %) as a white powder after lyophilization. ^{1}H NMR (400 MHz, DMSO-d_6): δ 11.98 (s, 1H), 11.17 (br s, 1H), 8.76 (t, $J = 5.8$ Hz, 1H), 8.59 (s, 1H), 8.46 (d, $J = 2.6$ Hz, 1H), 8.34 (d, $J = 1.8$ Hz, 1H), 7.94 (t, $J = 2.28$ Hz, 1H), 7.61 (dd, $J = 8.2$ and 1.9 Hz, 1H), 7.38–7.30 (m, 2H), 7.24 (d, $J = 8.2$ Hz, 1H), 7.19 (dd, $J = 6.9$ and 2.7 Hz, 1H), 3.99 (s, 3H), 3.42–3.32 (m, 6H), 3.24–3.12 (m, 6H), 1.86–1.79 (m, 2H), 1.67–1.59 (m, 2H). ^{13}C NMR (101 MHz, DMSO-d_6): δ 157.2, 154.1, 151.8, 150.0, 139.2, 136.2, 133.2, 132.0, 129.4 (2C), 129.1, 128.6, 126.5, 125.8, 123.7, 120.3, 113.5, 110.5, 57.0, 55.6, 51.5 (2C) 48.1 (2C), 39.2, 26.9, 21.0. UPLC-MS purity (UV at 215 nm): 99.5 %; $t_R = 4.08$ min (method D). MS (ESI) *m/z*: 569.21/571.18/573.65 $(M + H)^+$. HRMS (ESI) *m/z*: calcd for $C_{28}H_{31}Cl_2N_6O_3$ $(M + H)^+$ 569.1824; found: 569.1829.

3.1.1.7.62. 6-(5-Carbamoylpyridin-3-yl)-N-(4-(4-(2,3-dichlorophenyl)piperazin-1-yl)butyl)-2-oxo-2,3-dihydro-1H-benzo[d]imidazole-1-carboxamide trihydrogen chloride (3). General procedure F was followed treating *N*-Boc protected urea **39** (0.059 g, 0.0864 mmol) with TFA (0.07 mL) in CH_2Cl_2 (1.0 mL) for 6 h and 30 min to give the corresponding free base (33.0 mg, 66 %) as a white powder. UPLC-MS: $t_R = 1.85$ min (method A). MS (ESI) *m/z*: 582.2/584.2/586.0 $(M + H)^+$; $C_{28}H_{30}Cl_2N_7O_3$ $(M + H)^+$ calcd: 582.2/584.2/586.2 ^{1}H NMR (400 MHz, DMSO-d_6): δ 11.82 (s, 1H), 8.99 (d, $J = 2.0$ Hz, 1H), 8.94 (d, $J = 2.2$ Hz, 1H), 8.74 (t, $J = 5.7$ Hz, 1H), 8.40 (t, $J = 2.2$ Hz, 1H), 8.36 (d, $J = 1.8$ Hz, 1H), 8.30 (s, 1H), 7.65 (s, 1H), 7.58 (dd, $J = 8.2$ and 1.8 Hz, 1H), 7.35–7.26 (m, 2H), 7.22 (d, $J = 8.2$ Hz, 1H), 7.12 (dd, $J = 5.8$ and 3.9 Hz, 1H), 3.39–3.32 (m, 2H), 2.98 (br s, 4H), 2.60–2.50 (m, 4H), 2.39 (br s, 2H), 1.69–1.46 (m, 4H). General procedure G was followed using the isolated free base (0.031g, 0.053 mmol) and HCl (1.25 N) in CH_3OH (0.43 mL) in CH_3OH (1.68 mL), affording the pure salt **3** (32.0 mg, 87 % yield) as a light beige powder. ^{1}H NMR (600 MHz, DMSO-d_6): δ 11.93 (s, 1H), 10.72 (br s, 1H), 9.05 (br s, 2H), 8.78 (t, $J = 5.9$ Hz, 1H), 8.59 (br s, 1H), 8.43 (br s, 1H), 8.39 (d, $J = 1.8$ Hz, 1H), 7.77 (br s, 1H), 7.64 (dd, $J = 8.1$ and 1.8 Hz, 1H), 7.39–7.33 (m, 2H), 7.25 (d, $J = 8.2$ Hz, 1H), 7.20 (dd, $J = 7.6$ and 2.0 Hz, 1H), 3.58 (d, $J = 8.9$ Hz, 2H), 3.45–3.37 (m, 4H), 3.22–3.14 (m, 6H), 1.85–1.77 (m, 2H), 1.65 (q, $J = 7.3$ Hz, 2H). ^{13}C NMR (151 MHz, DMSO-d_6): δ 165.4, 153.7, 151.4, 149.6, 146.9, 144.6, 136.9, 135.5, 132.8, 130.9, 129.2, 128.9, 128.7, 128.3, 126.1, 125.4, 123.1, 119.9, 112.9, 110.2, 55.2, 51.2 (2C), 47.8 (2C), 38.7, 26.4, 20.6. UPLC-MS purity (UV at 215 nm): 99.2 %; $t_R = 3.23$ min (method D). MS (ESI) *m/z*: 582.29/584.29/586.29 $(M + H)^+$. HRMS (ESI) *m/z*: calcd for $C_{28}H_{30}Cl_2N_7O_3$ $(M + H)^+$ 582.1773; found: 582.1782.

3.1.1.7.63. 6-(5-Cyanopyridin-3-yl)-N-(4-(4-(2,3-dichlorophenyl)piperazin-1-yl)butyl)-2-oxo-2,3-dihydro-1H-benzo[d]imidazole-1-carboxamide trihydrogen chloride (4). General procedure F was followed treating *N*-Boc protected urea **40** (0.089 g, 0.134 mmol) with TFA (0.10 mL) in CH_2Cl_2 (2.0 mL) for 4 h to give the corresponding free base (61.0 mg, 81 %) as a pale-yellow powder. UPLC-MS: $t_R = 2.06$ min (method A). MS (ESI) *m/z*: 564.2/566.2/568.2 $(M + H)^+$; $C_{28}H_{28}Cl_2N_7O_2$ $(M + H)^+$ calcd: 564.2/566.2/568.2. ^{1}H NMR (400 MHz, DMSO-d_6): δ 9.09 (d, $J = 2.3$ Hz, 1H), 8.97 (d, $J = 1.9$ Hz, 1H), 8.80 (t, $J = 4.93$ Hz, 1H), 8.55 (t, $J = 2.1$ Hz, 1H), 8.33 (d, $J = 1.8$ Hz, 1H), 7.58 (dd, $J = 8.2$ and 1.9 Hz, 1H), 7.36–7.24 (m, 2H), 7.20 (d, $J = 8.2$ Hz, 1H), 7.12 (dd, $J = 6.0$ and 3.6 Hz, 1H), 3.38–3.31 (m, 2H), 2.55–2.51 (m, 4H), 2.97 (br s, 4H), 2.38 (t, $J = 6.9$ Hz, 2H), 1.61–1.51 (m, 4H). General procedure G was followed using the isolated free base (0.060 g, 0.106 mmol) and HCl (4 N) in dioxane (0.25 mL) in 1,4-dioxane (0.25 mL), affording the pure salt **4** (60.0 mg, 84 %) as a yellow powder. ^{1}H NMR (400 MHz, DMSO-d_6): δ 11.95 (s, 1H), 11.03 (br s, 1H), 9.08 (d, $J = 2.3$ Hz, 1H), 8.97 (d, $J = 1.9$ Hz, 1H), 8.76 (t, $J = 5.8$ Hz, 1H), 8.55 (t, $J = 2.1$ Hz, 1H), 8.33 (d, $J = 1.8$ Hz, 1H), 7.59 (dd, $J = 8.2$ and 1.9 Hz, 1H), 7.38–7.32 (m, 2H), 7.23 (d, $J = 8.2$ Hz, 1H), 7.19 (dd, $J = 6.9$ and 2.7 Hz, 1H), 3.57 (d, $J = 10.2$ Hz, 2H), 3.42–3.36 (m, 4H) 3.26–3.13 (m, 6H), 1.91–1.78 (m, 2H), 1.70–1.59 (m, 2H). ^{13}C NMR (101 MHz, DMSO-d_6): δ 153.6, 151.3, 150.9, 150.4, 149.6, 137.5, 136.2, 132.8, 128.9, 128.8, 128.7, 128.2, 126.1, 125.3, 123.1, 119.8, 117.0, 112.9, 110.2, 109.4, 55.1, 51.1 (2C), 47.7 (2C), 38.7, 26.4, 20.6. UPLC-MS purity (UV at 215 nm): 95.9 %; $t_R = 4.11$ min (method D). MS (ESI) *m/z*: 564.30/566.24/568.35 $(M + H)^+$. HRMS (ESI) *m/z*: calcd for $C_{28}H_{28}Cl_2N_7O_2$ $(M + H)^+$ 564.1683; found: 564.1676.

3.1.1.7.64. N-(4-(4-(2,3-Dichlorophenyl)piperazin-1-yl)butyl)-6-(5-(hydroxymethyl)pyridin-3-yl)-2-oxo-2,3-dihydro-1H-benzo[d]imidazole-1-carboxamide trihydrogen chloride (5). General procedure F was followed three times in parallel using each time *N*-Boc protected urea **41** (0.333 g, 0.497 mmol) and TFA (0.766 mL) in CH_2Cl_2 (5.0 mL) for 3 h and 30 min to give the corresponding free base (714.0 mg, 84 %) as a white powder. UPLC-MS: $t_R = 1.72$ min (method A). MS (ESI) *m/z*: 569.1/571.1/573.1 $(M + H)^+$; $C_{28}H_{31}Cl_2N_6O_3$ $(M + H)^+$ calcd: 569.2/571.2/573.2. ^{1}H NMR (400 MHz, DMSO-d_6): δ 8.84 (br s, 1H), 8.69 (d, $J = 2.2$ Hz, 1H), 8.48 (d,

J = 2.0 Hz, 1H), 8.30 (d, J = 1.9 Hz, 1H), 7.91 (t, J = 2.21 Hz, 1H), 7.49 (dd, J = 8.1 and 2.0 Hz, 1H), 7.33–7.24 (m, 2H), 7.18 (d, J = 8.2 Hz, 1H), 7.12 (dd, J = 5.8 and 3.8 Hz, 1H), 5.41 (s, 1H), 4.61 (d, J = 3.6 Hz, 2H), 3.38–3.33 (br s, 2H), 2.97 (br s, 4H), 2.55–2.51 (m, 4H), 2.38 (t, J = 6.9 Hz, 2H), 1.62–1.51 (m, 4H). General procedure G was followed using the isolated free base (0.712 g, 1.250 mmol) and HCl (3 N) solution in CH_3OH (4.17 mL) in CH_3OH (8.00 mL), affording the pure salt **5** (760.0 mg, 90 % yield) as light-yellow powder. ^{1}H NMR (600 MHz, DMSO-d_6): δ 12.04 (s, 1H), 11.40 (br s, 1H), 9.02 (d, J = 2.1 Hz, 1H), 8.74 (t, J = 5.8 Hz, 1H), 8.72 (d, J = 1.7 Hz, 1H), 8.61 (t, J = 1.9 Hz, 1H), 8.40 (d, J = 1.8 Hz, 1H), 7.66 (dd, J = 8.2 and 1.9 Hz, 1H), 7.37–7.32 (m, 2H), 7.27 (d, J = 8.2 Hz, 1H), 7.18 (dd, J = 7.0 and 2.6 Hz, 1H), 4.77 (s, 2H), 3.56 (d, J = 11.8 Hz, 2H), 3.45–3.35 (m, 4H), 3.27 (t, J = 11.8 Hz, 2H), 3.19–3.13 (m, 4H), 1.87–1.82 (m, 2H), 1.64 (q, J = 7.3 Hz, 2H). ^{13}C NMR (151 MHz, DMSO-d_6): δ 153.5, 151.2, 149.5, 142.0, 139.1, 138.7, 138.5, 138.3, 132.7, 129.3, 128.6, 128.2, 127.8, 126.0, 125.2, 123.0, 119.7, 112.8, 110.2, 59.6, 55.1, 51.0 (2C), 47.5 (2C), 38.7, 26.4, 20.5. UPLC-MS purity (UV at 215 nm): 99.6 %; t_R = 3.40 min (method D). MS (ESI) *m/z*: 569.10/571.13/573.11 $(M + H)^+$. HRMS (ESI) *m/z*: calcd for $C_{28}H_{31}Cl_2N_6O_3$ $(M + H)^+$ 569.1829; found: 569.1829.

3.1.1.7.65. N-(4-(4-(2,3-Dichlorophenyl)piperazin-1-yl)butyl)-2-oxo-6-(pyridin-4-yl)-2,3-dihydro-1H-benzo[d]imidazole-1-carboxamide trihydrogen chloride (6). General procedure F was followed treating *N*-Boc protected urea **42** (0.119 g, 0.186 mmol) with TFA (0.23 mL) in CH_2Cl_2 (2.0 mL) for 2 h to give the corresponding free base (91.0 mg, 91 %) as a white powder. UPLC-MS: t_R = 1.93 min (method A). MS (ESI) *m/z*: 539.3/541.3/543.2 $(M + H)^+$; $C_{27}H_{29}Cl_2N_6O_2$ $(M + H)^+$ calcd: 539.2/540.2/542.2. ^{1}H NMR (400 MHz, DMSO-d_6): δ 9.24 (br s, 1H), 8.59–8.53 (m, 2H), 8.30 (d, J = 1.9 Hz, 1H), 7.59 (dd, J = 4.50 and 1.62 Hz, 2H), 7.49 (d, J = 8.1 Hz, 1H), 7.34–7.26 (m, 2H), 7.12 (dd, J = 5.9 and 3.8 Hz, 1H), 7.08 (d, J = 8.1 Hz, 1H), 3.57–3.55 (m, 2H), 2.97 (t, J = 5.47 Hz, 4H), 2.50–2.51 (m, 4H), 2.38 (t, J = 6.8 Hz, 2H), 1.60–1.51 (m, 4H). General procedure G was followed using the isolated free base (0.090 g, 0.167 mmol) and HCl (4 N) in 1,4-dioxane (0.42 mL) in 1,4-dioxane (0.42 mL), affording the pure salt **6** (87.0 mg, 80 %) as light-yellow powder after lyophilization. ^{1}H NMR (400 MHz, DMSO-d_6): δ 12.19 (s, 1H), 11.18 (br s, 1H), 8.84 (d, J = 6.4 Hz, 2H), 8.72 (t, J = 5.9 Hz, 1H), 8.53 (d, J = 1.6 Hz, 1H), 8.20 (d, J = 6.6 Hz, 2H), 7.83 (dd, J = 8.3 and 1.8 Hz, 1H), 7.37–7.28 (m, 3H), 7.18 (dd, J = 6.5 and 3.0 Hz, 1H), 3.57–3.55 (m, 2H, confirmed by ^{1}H–^{13}C HSQC), 3.42–3.36 (m, 4H), 3.27–3.16 (m, 6H), 1.87–1.79 (m, 2H), 1.63 (p, J = 7.2 Hz, 2H). ^{13}C NMR (101 MHz, DMSO-d_6): δ 153.7, 151.3, 149.6, 143.1 (2C), 132.8, 131.1, 128.7, 128.5, 128.2, 126.1, 125.4, 124.1, 123.0 (2C), 119.9, 113.2, 110.5, 55.2, 51.1 (2C), 47.7 (2C), 38.8, 26.4, 20.6. UPLC-MS purity (UV at 215 nm): >99.5 %; t_R = 3.70 min (method D). MS (ESI) *m/z*: 537.25/539.21/541.32 $(M - H)^-$. HRMS (ESI) *m/z*: calcd for $C_{27}H_{29}Cl_2N_6O_2$ $(M + H)^+$ 539.1729; found: 539.1724.

3.1.1.7.66. N-(4-(4-(2,3-Dichlorophenyl)piperazin-1-yl)butyl)-2-oxo-6-(pyrimidin-5-yl)-2,3-dihydro-1H-benzo[d]imidazole-1-carboxamide trihydrogen chloride (7). General procedure F was followed treating *N*-Boc protected urea **43** (0.145 g, 0.226 mmol) with TFA (0.17 mL) in CH_2Cl_2 (2.3 mL) overnight to give the corresponding free base (106.0 mg, 87 %) as a white powder. UPLC-MS: t_R = 1.81 min (method A). MS (ESI) *m/z*: 540.1/542.0/544.0 $(M + H)^+$; $C_{26}H_{28}Cl_2N_7O_2$ $(M + H)^+$calcd: 540.2/542.2/544.2. ^{1}H NMR (400 MHz, DMSO-d_6): δ 9.15 (s, 1H), 9.04 (s, 2H), 8.87 (br s, 1H), 8.30 (d, J = 1.8 Hz, 1H), 7.54 (dd, J = 8.1 and 1.8 Hz, 1H), 7.34–7.24 (m, 2H), 7.20 (d, J = 8.1 Hz, 1H), 7.12 (dd, J = 6.0 and 3.6 Hz, 1H), 3.35–3.32 (m, 2H), 2.97 (t, J = 4.80 Hz, 4H), 2.53 (br s, 4H), 2.38 (t, J = 6.9 Hz, 2H), 1.62–1.53 (m, 4H). General procedure G was followed using the isolated free base (0.105 g, 0.194 mmol) and HCl (4 N) in 1,4-dioxane (0.49 mL) in 1,4-dioxane (0.97 mL), affording the pure salt **7** (103.0 mg, 82 %) as a light-yellow powder after lyophilization. ^{1}H NMR (400 MHz, DMSO-d_6): δ 11.94 (s, 1H), 10.96 (br s, 1H), 9.16 (s, 1H), 9.04 (s, 2H), 8.77 (t, J = 5.8 Hz, 1H), 8.31 (d, J = 1.8 Hz, 1H), 7.58 (dd, J = 8.1 and 1.8 Hz, 1H), 7.38–7.32 (m, 2H), 7.24 (d, J = 8.1 Hz, 1H), 7.19 (dd, J = 7.0 and 2.6 Hz, 1H), 3.57 (d, J = 10.1 Hz, 2H), 3.38–3.33 (m, 4H), 3.24–3.12 (m, 6H), 1.83–1.78 (m, 2H), 1.66–1.59 (m, 2H). ^{13}C NMR (101 MHz, DMSO-d_6): δ 156.9, 154.5 (2C), 153.6, 151.3, 149.6, 133.8, 132.8, 128.8, 128.7, 128.3, 127.5, 126.1, 125.3, 122.8, 119.8, 112.6, 110.3, 55.1, 51.1 (2C), 47.7 (2C), 38.7, 26.4, 20.6. UPLC-MS purity (UV at 215 nm): >99.5 %; t_R = 3.62 min (method D). MS (ESI) *m/z*: 540.32/542.35/544.28 $(M + H)^+$. HRMS (ESI) *m/z*: calcd for $C_{26}H_{28}Cl_2N_7O_2$ $(M + H)^+$ 540.1674; found: 540.1676.

3.1.1.7.67. N-(4-(4-(2,3-Dichlorophenyl)piperazin-1-yl)butyl)-6-(1-methyl-1H-imidazole-5-yl)-2-oxo-2,3-dihydro-1H-benzo[d]imidazole-1-carboxamide trihydrogen chloride (8). General procedure F was followed treating *N*-Boc protected urea **44** (0.157 g, 0.244 mmol) with TFA (0.19 mL) in CH_2Cl_2 (3.0 mL) for 4 h and 30 min to give the corresponding free base (72.0 mg, 54 %) as a white powder. UPLC-MS: t_R = 1.79 min (method A). MS (ESI) *m/z*: 542.2/544.2/546.2 $(M + H)^+$; $C_{26}H_{30}Cl_2N_7O_2$ $(M + H)^+$ calcd: 542.2/544.2/546.2. ^{1}H NMR (400 MHz, DMSO-d_6): δ 8.74 (br s, 1H), 8.07 (d, J = 1.7 Hz, 1H), 7.68 (s, 1H), 7.32–7.23 (m, 3H), 7.18–7.08 (m, 2H), 6.96 (d, J = 1.2 Hz, 1H), 3.63 (s, 3H), 3.36–3.32 (s, 2H), 2.97 (br s, 4H), 2.53 (br s, 4H), 2.38 (t, J = 6.9 Hz, 2H), 1.66–1.47 (m, 4H). General procedure G was followed using the isolated free base (0.071 g, 0.131 mmol) and HCl (1.25 N) in CH_3OH (1.05 mL) in CH_3OH (1.05 mL), affording the pure salt **8** (62.5 mg, 73 %) as a white powder. ^{1}H NMR (400 MHz, DMSO-d_6): δ 12.00 (s, 1H), 9.11 (br s, 1H), 8.75 (t, J = 5.7 Hz, 1H), 8.15 (d, J = 1.7 Hz, 1H), 7.78 (s, 1H), 7.40–7.33 (m, 3H), 7.26 (d, J = 8.1 Hz, 1H), 7.20 (dd, J = 7.2 and 2.4 Hz, 1H), 3.78 (3H), 3.56 (br s, 2H), 4.40–3.36 (m, 4H, confirmed by ^{1}H–^{13}C HSQC), 3.21–3.16 (m, 6H), 1.83–1.75 (m, 2H), 1.63–1.60 (m, 2H). ^{13}C NMR (101 MHz, DMSO-d_6): δ 153.6, 151.2, 149.6, 136.4, 134.5, 132.8, 129.3, 128.7, 127.7, 126.1, 125.4, 125.0, 119.8, 119.1, 117.6, 115.1, 110.0, 55.15, 51.1 (2C), 47.7 (2C), 38.8, 34.2, 26.4, 20.6. UPLC-MS purity (UV at 215 nm): >99.5 %; t_R = 3.35 min (method D). MS (ESI) *m/z*: 542.33/544.35/546.33 $(M + H)^+$. HRMS (ESI) *m/z*: calcd for $C_{26}H_{30}Cl_2N_7O_2$ $(M + H)^+$ 542.1842; found: 542.1833.

3.1.1.7.68. N-(4-(4-(2,3-Dichlorophenyl)piperazin-1-yl)butyl)-6-(1-methyl-1H-pyrazol-4-yl)-2-oxo-2,3-dihydro-1H-benzo[d]imidazole-1-carboxamide trihydrogen chloride (9). General procedure F was followed treating *N*-Boc protected urea **45** (0.161 g, 0.251 mmol) with TFA (0.19 mL) in CH_2Cl_2 (2.5 mL) for 3 h and 30 min to give the corresponding free base (82.0 mg, 60 %) as a light pink powder. UPLC-MS: t_R = 1.94 min (method A). MS (ESI) *m/z*: 542.2/544.1/546.1 $(M + H)^+$ $C_{26}H_{30}Cl_2N_7O_2$ $(M + H)^+$ calcd: 542.2/544.2/546.2. ^{1}H NMR (600 MHz, DMSO-d_6): δ 8.99 (s, 1H), 8.11 (d, J = 2.0 Hz, 1H), 8.01 (d, J = 2.6 Hz, 1H), 7.70 (d, J = 1.6 Hz, 1H), 7.34–7.19 (m, 3H), 7.18–7.06 (m, 1H), 7.00 (d, J = 8.1 Hz, 1H), 3.85 (s, 3H), 3.36–3.32 (br s, 2H), 2.97 (br s, 4H), 2.54–2.51 (m, 4H), 2.37 (t, J = 6.8 Hz, 2H), 1.61–1.50 (m, 4H). General procedure G was followed using the isolated free base (0.081 g, 0.149 mmol) and HCl (1.25 N) solution in CH_3OH (1.19 mL) in CH_3OH (1.19 mL), affording the pure salt **9** (79.0 mg, 81 %) as white powder. ^{1}H NMR (400 MHz, DMSO-d_6): δ 11.67 (s, 1H), 10.75 (br s, 1H), 8.79 (t, J = 5.9 Hz, 1H), 8.15 (br s, 1H), 8.03 (d, J = 3.3 Hz, 1H), 7.72 (s, 1H), 7.38–7.32 (m, 3H), 7.19 (dd, J = 7.1 and 2.5 Hz, 1H), 7.06 (d, J = 8.1 Hz, 1H), 3.85 (s, 3H), 3.57 (d, J = 8.8 Hz, 2H), 3.47–3.42 (m, 4H, confirmed by ^{1}H–^{13}C HSQC), 3.23–3.05 (m, 6H), 1.80 (br s, 2H), 1.62 (p, J = 7.2 Hz, 2H). ^{13}C NMR (101 MHz, DMSO-d_6): δ 153.7, 151.6, 149.6, 135.6, 132.8, 128.8, 128.0, 127.5, 126.7, 126.3, 126.2, 125.4, 122.4, 120.7, 119.9, 111.0, 109.9, 55.3, 51.2 (2C), 47.8 (2C), 38.7 (2C), 26.4, 20.7. UPLC-MS purity (UV at 215 nm): >99.5 %; t_R = 3.75 min (method D). MS (ESI) *m/z*: 542.22/544.19/546.19 $(M + H)^+$. HRMS (ESI) *m/z*: calcd for $C_{26}H_{30}Cl_2N_7O_2$ $(M + H)^+$ 542.1824; found: 542.1833.

3.1.1.7.69. N-(4-(4-(2,3-Dichlorophenyl)piperazin-1-yl)butyl)-6-(3-methyl-2,5-dioxoimidazolidin-1-yl)-2-oxo-2,3-dihydro-1H-benzo[d]imidazole-1-carboxamide dihydrogen chloride (10). To a mixture of *N*-Boc protected urea **46** (0.057 g, 0.084 mmol) in 1,4-dioxane (1.00 mL), cooled down to 0 °C, HCl (4 N) in dioxane (0.42 mL, 1.69 mmol) was added dropwise. The ice bath was removed and the resulting mixture was allowed to stir at rt overnight. The next morning, extra 60 mol equiv of HCl in dioxane (1.26 mL) were added to the reaction mixture, cooled

down to 0 °C. The resultant mixture was stirred at rt for 72 h; then, 1,4-dioxane was evaporated under reduced pressure to give a residue, which was treated with Et_2O (2 mL). The obtained solid was filtered under *vacuum*, washed with fresh Et_2O (2x4 mL) and lyophilized, affording the pure salt **10** (43.0 mg, 79 %) as white powder. UPLC-MS: $t_R = 1.90$ min (method A). MS (ESI) *m/z*: 574.1/576.0/578.1 $(M + H)^+$; $C_{26}H_{30}Cl_2N_7O_4$ $(M + H)^+$ calcd: 574.2/576.2/578.2. ^{1}H NMR (400 MHz, DMSO-d_6): δ 11.85 (s, 1H), 10.55 (br s, 1H), 8.75 (t, $J = 5.8$ Hz, 1H), 7.96 (d, $J = 1.9$ Hz, 1H), 7.38–7.33 (m, 2H), 7.20 (dd, $J = 7.1$ and 2.5 Hz, 1H), 7.16 (d, $J = 8.3$ Hz, 1H), 7.10 (dd, $J = 8.3$ and 2.0 Hz, 1H), 4.09 (s, 2H), 3.60–3.52 (m, 2H), 3.45–3.37 (m, 4H, confirmed by ^{1}H–^{13}C HSQC), 3.25–3.09 (m, 6H), 2.92 (s, 3H), 1.76 (br s, 2H), 1.64–1.57 (m, 2H). ^{13}C NMR (101 MHz, DMSO-d_6): δ 169.8, 155.9, 153.8, 151.3, 149.7, 132.8, 128.7, 127.6, 127.2, 126.2, 126.1, 125.3, 122.7, 119.9, 113.6, 109.3, 55.4, 51.5, 51.4 (2C), 48.0 (2C), 38.7, 29.5, 26.4, 20.8. UPLC-MS purity (UV at 215 nm): 98.2 %; $t_R = 3.43$ min (method D). MS (ESI) *m/z*: 574.23/576.23/578.28 $(M + H)^+$.

3.1.1.7.70. N-(3-(4-(2,3-Dichlorophenyl)piperazin-1-yl)propyl)-2-oxo-6-(pyridin-3-yl)-2,3-dihydro-1H-benzo[d]imidazole-1-carboxamide trihydrogen chloride (11). General procedure F was followed treating *N*-Boc protected urea **47** (0.097 g, 0.155 mmol) with TFA (0.12 mL) in CH_2Cl_2 (1.6 mL) for 6 h to give the title free base (65.0 mg, 80 %) as an off-white powder. UPLC-MS: $t_R = 2.01$ min (method A). MS (ESI) *m/z*: 525.0/527.1/529.1 $(M + H)^+$; $C_{26}H_{27}Cl_2N_6O_2$ $(M + H)^+$ calcd: 525.2/527.2/529.2. ^{1}H NMR (400 MHz, DMSO-d_6): δ 8.91 (br s, 1H), 8.81 (d, $J = 2.8$ Hz, 1H), 8.54 (dd, $J = 5.0$ and 1.6 Hz, 1H), 8.29 (t, $J = 1.8$ Hz, 1H), 7.99 (dt, $J = 7.9$ and 2.0 Hz, 1H), 7.52–7.44 (m, 2H), 7.35–7.25 (m, 2H), 7.17 (dd, $J = 8.0$ and 1.8 Hz, 1H), 7.12 (dd, $J = 6.5$ and 3.1 Hz, 1H), 3.40 (q, $J = 6.5$ Hz, 2H), 2.99 (t, $J = 5.5$ Hz, 4H), 2.55 (br s, 4H), 2.44 (t, $J = 6.8$ Hz, 2H), 1.81–1.72 (m, 2H). General procedure G was followed using the isolated free base (0.063 g, 0.120 mmol) and HCl (4 N) in 1,4-dioxane (0.30 mL) in 1,4-dioxane (3.00 mL), affording the pure salt **11** (58.0 mg, 76 %) as a white powder. ^{1}H NMR (400 MHz, DMSO-d_6): δ 12.03 (s, 1H), 11.28 (br s, 1H), 9.11 (s, 1H), 8.84–8.80 (m, 2H), 8.64 (d, $J = 8.2$ Hz, 1H), 8.40 (s, 1H), 8.00–7.97 (m, 1H), 7.66 (d, $J = 8.2$ Hz, 1H), 7.39–7.33 (m, 2H), 7.28 (d, $J = 8.1$ Hz, 1H), 7.20 (dd, $J = 7.0$ and 2.6 Hz, 1H), 3.60 (d, $J = 11.2$ Hz, 2H), 3.49–3.41 (m, 4H), 3.29–3.17 (m, 6H), 2.11–2.07 (m, 2H). ^{13}C NMR (101 MHz, DMSO-d_6): δ 153.5, 151.4, 149.5, 141.8, 141.4, 140.9, 138.5, 132.7, 129.2, 128.7, 128.3, 126.5, 126.0, 125.3, 123.2, 119.8, 113.0, 110.2, 53.3, 51.1 (2C), 47.7 (2C), 36.9, 23.7. UPLC-MS purity (UV at 215 nm): 99.0 %; $t_R = 4.00$ min (method D). MS (ESI) *m/z*: 525.17/527.13 $(M + H)^+$. HRMS (ESI) *m/z*: calcd for $C_{26}H_{27}Cl_2N_6O_2$ $(M + H)^+$ 525.1559; found: 525.1567.

3.1.1.7.71. (E)-N-(4-(4-(2,3-Dichlorophenyl)piperazin-1-yl)but-2-en-1-yl)-2-oxo-6-(pyridin-3-yl)-2,3-dihydro-1H-benzo[d]imidazole-1-carboxamide trihydrogen chloride (12). General procedure F was followed treating *N*-Boc protected urea **48** (0.074 g, 0.116 mmol) with TFA (0.09 mL) in CH_2Cl_2 (1.2 mL) for 4 h and 15 min to give the corresponding free base (52.0 mg, 83 %) as a white powder. UPLC-MS: $t_R = 2.00$ min (method A). MS (ESI) *m/z*: 537.0/538.8/541.0 $(M + H)^+$; $C_{27}H_{27}Cl_2N_6O_2$ $(M + H)^+$ calcd: 537.2/539.2/541.2. ^{1}H NMR (400 MHz, DMSO-d_6): δ 8.97 (br s, 1H), 8.80 (d, $J = 2.4$ Hz, 1H), 8.53 (d, $J = 5.0$ Hz, 1H), 8.26 (s, 1H), 8.04–7.92 (m, 1H), 7.54–7.43 (m, 2H), 7.38–7.24 (m, 2H), 7.17 (d, $J = 8.9$ Hz, 1H), 7.12 (dd, $J = 6.2$ and 3.4 Hz, 1H), 5.81–5.62 (m, 2H), 3.97 (t, $J = 5.2$ Hz, 2H), 3.02 (d, $J = 5.5$ Hz, 2H), 2.97 (br s, 4H), 2.53 (br s, 4H). General procedure G was followed using the isolated free base (0.052 g, 0.097 mmol) and HCl (4 N) in 1,4-dioxane (0.24 mL) in 1,4-dioxane (2.42 mL), affording the pure salt **12** (48.0 mg, 77 %) as white powder after lyophilization. ^{1}H NMR (600 MHz, DMSO-d_6): δ 12.03 (s, 1H), 11.25 (br s, 1H), 9.07 (d, $J = 2.3$ Hz, 1H), 8.90 (t, $J = 5.8$ Hz, 1H), 8.76 (d, $J = 5.3$ Hz, 1H), 8.56 (d, $J = 8.1$ Hz, 1H), 8.37 (d, $J = 1.8$ Hz, 1H), 7.91 (dd, $J = 8.2$, 5.3 Hz, 1H), 7.64 (dd, $J = 8.2$ and 1.9 Hz, 1H), 7.37–7.32 (m, 2H), 7.27 (d, $J = 8.2$ Hz, 1H), 7.18 (dd, $J = 7.6$ and 2.0 Hz, 1H), 6.09 (dt, $J = 15.5$ and 5.3 Hz, 1H), 5.88–5.83 (m, 1H), 4.05 (t, $J = 5.7$ Hz, 2H), 3.83 (d, $J = 7.2$ Hz, 2H), 3.52–3.47 (m, 2H, confirmed by ^{1}H–^{13}C HSQC), 3.42–3.39 (m, 2H, confirmed by ^{1}H–^{13}C HSQC), 3.19–3.11 (m, 4H). ^{13}C NMR (151 MHz, DMSO-d_6): δ 153.6, 151.2, 149.5, 142.4, 142.0, 140.3, 138.3, 137.5, 132.7, 129.2, 128.7, 128.5, 128.2, 126.3, 126.1, 125.3, 123.2, 119.9, 119.7, 112.9, 110.3, 56.3, 50.5 (2C), 47.8 (2C), 40.6. UPLC-MS purity (UV at 215 nm): 97.7 %; $t_R = 4.08$ min (method D). MS (ESI) *m/z*: 537.32/539.25/541.29 $(M + H)^+$. HRMS (ESI) *m/z*: calcd for $C_{27}H_{27}Cl_2N_6O_2$ $(M + H)^+$ 537.1564; found: 537.1567.

3.1.1.7.72. 2-Oxo-N-(4-(4-phenylpiperazin-1-yl)butyl)-6-(pyridin-3-yl)-2,3-dihydro-1H-benzo[d]imidazole-1-carboxamide trihydrogen chloride (13). General procedure F was followed treating *N*-Boc protected urea **49** (0.078 g, 0.137 mmol) with TFA (0.11 mL) in CH_2Cl_2 (1.5 mL) for 4 h and 15 min to give the corresponding free base (55.0 mg, 85 %) as a white powder. UPLC-MS: $t_R = 1.65$ min (method A). MS (ESI) *m/z*: 471.1 $(M + H)^+$; $C_{27}H_{31}N_6O_2$ $(M + H)^+$ calcd: 471.3. ^{1}H NMR (400 MHz, DMSO-d_6): δ 8.81 (dd, $J = 2.5$ and 0.8 Hz, 1H), 8.78 (s, 1H), 8.55 (dd, $J = 4.7$ and 1.6 Hz, 1H), 8.29 (d, $J = 1.8$ Hz, 1H), 7.99 (ddd, $J = 7.9$, 2.5 and 1.6 Hz, 1H), 7.55–7.44 (m, 2H), 7.22–7.14 (m, 3H), 6.90 (d, $J = 7.8$ Hz, 2H), 6.75 (tt, $J = 7.1$ and 1.1 Hz, 1H), 3.39–3.32 (m, 2H), 3.11 (t, $J = 5.0$ Hz, 4H), 2.52–2.50 (m, 4H), 2.36 (t, $J = 7.0$ Hz, 2H), 1.62–1.51 (m, 4H). General procedure G was followed using the isolated free base (0.053 g, 0.113 mmol) and HCl (4 N) in 1,4-dioxane (0.28 mL) in 1,4-dioxane (1.13 mL), affording the pure salt **13** (45.0 mg, 69 %) as a light-yellow powder after lyophilization. ^{1}H NMR (400 MHz, DMSO-d_6): δ 12.00 (s, 1H), 10.75 (br s, 1H), 9.12 (d, $J = 2.2$ Hz, 1H), 8.81 (dd, $J = 5.5$ and 1.4 Hz, 1H), 8.76 (t, $J = 5.8$ Hz, 1H), 8.66 (dt, $J = 8.2$ and 1.8 Hz, 1H), 8.40 (d, $J = 1.8$ Hz, 1H), 7.99 (dd, $J = 8.2$ and 5.4 Hz, 1H), 7.65 (dd, $J = 8.2$ and 1.9 Hz, 1H), 7.35–7.19 (m, 3H), 7.08–6.93 (m, 2H), 6.86 (t, $J = 7.2$ Hz, 1H), 3.79 (d, $J = 9.9$ Hz, 2H), 3.55 (d, $J = 8.9$ Hz, 2H), 3.39 (q, $J = 6.6$ Hz, 2H), 3.14 (t, $J = 9.3$ Hz, 6H), 1.87–1.76 (m, 2H), 1.63 (p, $J = 7.1$ Hz, 2H). ^{13}C NMR (101 MHz, DMSO-d_6): δ 153.8, 151.4, 149.8, 141.5 (2C), 138.8, 129.4, 129.3 (2C), 128.5, 128.3, 126.9, 123.4, 120.2, 116.1 (2C), 113.2, 110.4, 55.2, 50.8 (2C), 45.6 (2C), 38.9, 26.6, 20.8. UPLC-MS purity (UV at 215 nm): >99.5 %; $t_R = 3.03$ min (method D). MS (ESI) *m/z*: 471.39 $(M + H)^+$. HRMS (ESI) *m/z*: calcd for $C_{27}H_{31}N_6O_2$ $(M + H)^+$ 471.2499; found: 471.2503.

3.1.1.7.73. N-(4-(4-(2-Methoxyphenyl)piperazin-1-yl)butyl)-2-oxo-6-(pyridin-3-yl)-2,3-dihydro-1H-benzo[d]imidazole-1-carboxamide trihydrogen chloride (14). General procedure F was followed treating *N*-Boc protected urea **50** (0.22 g, 0.366 mmol) with TFA (0.42 mL) in CH_2Cl_2 (1.5 mL) for 10 h to give the corresponding free base (161.0 mg, 88 %) as an off-white powder. UPLC-MS: $t_R = 1.66$ min (method A). MS (ESI) *m/z*: 501.3 $(M + H)^+$; $C_{28}H_{33}N_6O_3$ $(M + H)^+$ calcd: 501.3. ^{1}H NMR (400 MHz, DMSO-d_6): δ 8.81 (dd, $J = 2.5$ and 0.9 Hz, 1H), 8.76 (t, $J = 5.7$ Hz, 1H), 8.55 (dd, $J = 4.7$ and 1.6 Hz, 1H), 8.29 (d, $J = 1.8$ Hz, 1H), 7.99 (ddd, $J = 8.0$, 2.5 and 1.6 Hz, 1H), 7.56–7.46 (m, 2H), 7.19 (d, $J = 8.2$ Hz, 1H), 6.95–6.88 (m, 2H), 6.85 (dd, $J = 3.9$ and 1.6 Hz, 2H), 3.75 (s, 3H), 3.40 (br s, 2H), 2.94 (br s, 4H), 2.51 (br s, 4H), 2.35 (t, $J = 7.0$ Hz, 2H), 1.62–1.51 (m, 4H). General procedure G was followed using the isolated free base (0.160 g, 0.320 mmol) and HCl (4 N) in 1,4-dioxane (1.19 mL) in 1,4-dioxane (1.19 mL), affording the pure salt **14** (155.0 mg, 79 %) as pale-yellow powder after lyophilization. ^{1}H NMR (400 MHz, DMSO-d_6): δ 12.02 (s, 1H), 10.87 (br s, 1H), 9.10 (d, $J = 2.2$ Hz, 1H), 8.79 (d, $J = 5.4$ Hz, 1H), 8.76 (t, $J = 5.8$ Hz, 1H), 8.64 (d, $J = 8.2$ Hz, 1H), 8.39 (d, $J = 1.8$ Hz, 1H), 7.98 (dd, $J = 8.2$ and 5.4 Hz, 1H), 7.65 (dd, $J = 8.2$ and 1.9 Hz, 1H), 7.05–6.95 (m, 2H), 6.95–6.87 (m, 2H), 3.78 (s, 3H), 3.54–3.48 (m, 4H, confirmed by 1H–^{13}C HSQC), 3.40–3.36 (m, 2H, confirmed by 1H–^{13}C HSQC), 3.18–3.05 (m, 6H), 1.88–1.75 (m, 2H), 1.63 (p, $J = 7.2$ Hz, 2H). ^{13}C NMR (101 MHz, DMSO-d_6): δ 153.6, 151.8, 151.3, 141.3, 141.1 (confirmed by 1H–^{13}C HSQC), 140.5 (confirmed by 1H–^{13}C HSQC), 139.4, 129.2, 128.3 (2C), 126.6, 123.5, 123.2, 120.9, 118.2, 112.0, 111.8 (confirmed by ^{1}H–^{13}C HSQC), 110.2, 55.4, 55.1, 51.1 (2C), 46.8 (2C), 38.9, 26.4, 20.6. UPLC-MS purity (UV at 215 nm): >99.5 %; $t_R = 3.29$ min (method D). MS (ESI) *m/z*: 501.26 $(M + H)^+$. HRMS (ESI) *m/z*: calcd for $C_{28}H_{33}N_6O_3$ $(M + H)^+$ 501.2602; found: 501.2607.

3.1.1.7.74. 2-Oxo-6-(pyridin-3-yl)-N-(4-(4-(o-tolyl)piperazin-1-yl) butyl)-2,3-dihydro-1H-benzo[d]imidazole-1-carboxamide (15). To a suspension of *N*-Boc protected urea **51** (0.245 g, 0.419 mmol) in dry 1,4-dioxane (4.2 mL), cooled down to 0 °C, HCl (4 N) in 1,4-dioxane (8.38 ml, 33.521 mmol) was added dropwise. The ice bath was removed and EtOH (4.2 mL) was added to improve the solubility of the reaction mixture, which was allowed to stir at rt for 12 h. Extra 110 mol equiv of HCl in 1,4-dioxane (11.52 mL, 46.09 mmol) were added and the reaction mixture was allowed to stir at rt for an additional 48 h. The solvent was evaporated under reduced pressure to give a residue, which was triturated with Et_2O (2x5 mL). The obtained solid was filtered under *vacuum*, was suspended in EtOAc (50 mL) and washed with a saturated aqueous solution of $NaHCO_3$ (2x50 mL). The separated organic phase was dried over Na_2SO_4 and concentrated to dryness affording **15** (150.0 mg, 74 %) as a white powder. UPLC-MS: t_R = 1.75 min (method A). MS (ESI) *m/z*: 485.3 $(M + H)^+$; $C_{28}H_{33}N_6O_2$ $(M + H)^+$ calcd: 485.3. ^{1}H NMR (400 MHz, DMSO-d_6): δ 8.81 (d, *J* = 1.8 Hz, 1H), 8.74 (t, *J* = 5.7 Hz, 1H), 8.55 (dd, *J* = 4.7 and 1.5 Hz, 1H), 8.30 (d, *J* = 1.7 Hz, 1H), 8.01–7.95 (m, 1H), 7-52-7.46 (m, 2H), 7.19 (d, *J* = 8.2 Hz, 1H), 7.14–7.08 (m, 2H), 6.97 (d, *J* = 7.3 Hz, 1H), 6.92 (td, *J* = 7.3 and 1.2 Hz, 1H), 3.38–3.35 (m, 2H, confirmed by ^{1}H–^{13}C HSQC), 2.81 (t, *J* = 4.6 Hz, 4H), 2.53–2.50 (m, 4H, confirmed by ^{1}H–^{13}C HSQC), 2.37 (t, *J* = 7.0 Hz, 2H), 2.21 (s, 3H), 1.65–1.48 (m, 4H). ^{13}C NMR (101 MHz, DMSO-d_6): δ 153.8, 151.3, 151.2, 148.1, 147.4, 136.0, 134.0, 131.7, 130.9, 130.8, 128.2, 128.1, 126.5, 123.9, 122.7, 122.5, 118.6, 112.6, 110.0, 57.4, 53.2 (2C), 51.4 (2C), 38.9, 27.1, 23.6, 17.5. UPLC-MS purity (UV at 215 nm): 97.9 %; t_R = 3.48 min (method D). MS (ESI) *m/z*: 485.13 $(M + H)^+$. HRMS (ESI) *m/z*: calcd for $C_{28}H_{33}N_6O_2$ $(M + H)^+$ 485.2659; found: 485.2660.

3.1.1.7.75. 2-Oxo-N-(3-(4-phenylpiperazin-1-yl)propyl)-6-(pyridin-3-yl)-2,3-dihydro-1H-benzo[d]imidazo-le-1-carboxamide trihydrogen chloride (16). General procedure F was followed treating *N*-Boc protected urea **52** (0.966 g, 1.735 mmol) with TFA (1.34 mL) in CH_2Cl_2 (17.4 mL) overnight to give the corresponding free base (727.0 mg, 92 %) as a light pink powder. UPLC-MS: t_R = 1.69 min (method A). MS (ESI) *m/z*: 457.1 $(M + H)^+$; $C_{26}H_{29}N_6O_2$ $(M + H)^+$ calcd: 457.2. ^{1}H NMR (400 MHz, DMSO-d_6) δ 11.77 (s, 1H), 8.83 (t, *J* = 5.6 Hz, 1H), 8.81 (d, *J* = 2.5 Hz, 1H), 8.55 (dd, *J* = 4.8 and 1.6 Hz, 1H), 8.30 (d, *J* = 1.8 Hz, 1H), 8.00 (dt, *J* = 8.0 and 1.9 Hz, 1H), 7.58–7.39 (m, 2H), 7.22–7.17 (m, 3H), 6.92 (d, *J* = 8.2 Hz, 2H), 6.76 (t, *J* = 7.2 Hz, 1H), 3.41 (q, *J* = 6.5 Hz, 2H), 3.14 (br s, 4H), 2.54 (br s, 4H), 2.44 (br s, 2H), 1.77 (t, *J* = 6.9 Hz, 2H). General procedure G was followed using the isolated free base (726.0 mg, 1.590 mmol) and HCl (1.25 N) solution in CH_3OH (12.72 mL) in CH_3OH (12.72 mL), affording the pure salt **16** (810.0 mg, 90 % yield) as a light-yellow powder. ^{1}H NMR (400 MHz, DMSO-d_6): δ 12.04 (s, 1H), 11.02 (br s, 1H), 9.14 (d, *J* = 2.2 Hz, 1H), 8.86–8.76 (m, 2H), 8.73 (d, *J* = 7.1 Hz, 1H), 8.41 (d, *J* = 1.8 Hz, 1H), 8.05 (dd, *J* = 8.2 and 5.5 Hz, 1H), 7.67 (dd, *J* = 8.2 and 1.9 Hz, 1H), 7.38–7.18 (m, 3H), 7.10–6.94 (m, 2H), 6.86 (t, *J* = 7.3 Hz, 1H), 3.80 (d, *J* = 10.7 Hz, 2H), 3.57 (d, *J* = 9.7 Hz, 2H), 3.45 (q, *J* = 6.5 Hz, 2H), 3.25–3.06 (m, 6H), 2.08 (t, *J* = 8.1 Hz, 2H).^{13}C NMR (151 MHz, DMSO-d_6): δ 153.6, 151.4, 149.6, 142.6, 140.3, 139.9, 139.1, 129.5, 129.2 (2C), 128.3, 127.6, 127.3, 123.4, 120.1, 116.0 (2C), 113.1, 110.4, 53.3, 50.7 (2C), 45.4 (2C), 37.0, 23.8. UPLC-MS purity (UV at 215 nm): >99.5 %; t_R = 3.05 min (method D). MS (ESI) *m/z*: 457.11 $(M + H)^+$. HRMS (ESI) *m/z*: calcd for $C_{26}H_{29}N_6O_2$ $(M + H)^+$ 457.2344; found: 457.2347.

3.1.1.7.76. (E)-2-Oxo-N-(4-(4-phenylpiperazin-1-yl)but-2-en-1-yl)-6-(pyridin-3-yl)-2,3-dihydro-1H-benzo[d]imidazole-1-carboxamide trihydrogen chloride (17). General procedure F was followed treating *N*-Boc protected urea **53** (0.068 g, 0.120 mmol) with TFA (0.09 mL) in CH_2Cl_2 (1.2 mL) for 3 h to give the corresponding free base (37.0 mg, 66 %) as a beige powder. UPLC-MS: t_R = 1.65 min (method A). MS (ESI) *m/z*: 469.1 $(M + H)^+$; $C_{27}H_{29}N_6O_2$ $(M + H)^+$ calcd: 469.2. ^{1}H NMR (400 MHz, DMSO-d_6): δ 8.94 (br s, 1H), 8.81 (dd, *J* = 2.5 and 0.9 Hz, 1H), 8.54 (dd, *J* = 4.7 and 1.6 Hz, 1H), 8.27 (d, *J* = 1.9 Hz, 1H), 7.99 (ddd, *J* = 7.9, 2.6 and 1.6 Hz, 1H), 7.52–7.43 (m, 2H), 7.24–7.13 (m, 3H), 6.95–6.84 (m, 2H), 6.75 (tt, *J* = 7.3 and 1.1 Hz, 1H), 5.83–5.64 (m, 2H), 3.97 (t, *J* = 5.1 Hz, 2H), 3.11 (t, *J* = 5.0 Hz, 4H), 2.99 (d, *J* = 5.3 Hz, 2H), 2.51 (br s, 4H). General procedure G was followed using the isolated free base (0.036 g, 0.077 mmol) and HCl (4 N) in 1,4-dioxane (0.19 mL) in 1,4-dioxane (1.92 mL), affording the pure salt **17** (31.0 mg, 70 %) as a light-yellow powder. ^{1}H NMR (400 MHz, DMSO-d_6): δ 12.05 (s, 1H), 11.14 (br s, 1H), 9.13 (d, *J* = 2.2 Hz, 1H), 8.90 (t, *J* = 5.8 Hz, 1H), 8.82 (dd, *J* = 5.5 and 1.4 Hz, 1H), 8.69 (d, *J* = 8.1 Hz, 1H), 8.39 (d, *J* = 1.8 Hz, 1H), 8.01 (dd, *J* = 8.2 and 5.4 Hz, 1H), 7.67 (dd, *J* = 8.2 and 1.9 Hz, 1H), 7.34–7.19 (m, 3H), 7.05–6.92 (m, 2H), 6.85 (t, *J* = 7.3 Hz, 1H), 6.08 (dt, *J* = 15.5 and 5.3 Hz, 1H), 5.85 (dt, *J* = 15.0 and 7.2 Hz, 1H), 4.05 (d, *J* = 5.8 Hz, 2H), 3.81 (d, *J* = 8.4 Hz, 4H), 3.47 (d, *J* = 9.2 Hz, 2H), 3.17–2.99 (m, 4H). ^{13}C NMR (151 MHz, DMSO-d_6): δ 153.6, 151.1, 149.6, 142.2, 140.7, 140.4, 138.9, 137.3, 129.5, 129.1 (2C), 128.3, 127.8, 127.0, 123.4, 120.1, 119.8, 116.0 (2C), 113.0, 110.3, 56.2, 50.0 (2C), 45.4 (2C), 40.6. UPLC-MS purity (UV at 215 nm): >99.5 %; t_R = 3.12 min (method D). MS (ESI) *m/z*: 469.34 $(M + H)^+$. HRMS (ESI) *m/z*: calcd for $C_{27}H_{29}N_6O_2$ $(M + H)^+$ 469.2332; found: 469.2347.

3.1.1.7.77. N-(4-(4-(2,3-Dichlorophenyl)piperazin-1-yl)-4-oxobutyl)-2-oxo-6-(pyridin-3-yl)-2,3-dihydro-1H-benzo[d]imidazole-1-carboxamide hydrogen chloride (18). General procedure F was followed treating *N*-Boc protected urea **54** (0.095 g, 0.145 mmol) with TFA (0.11 mL) in CH_2Cl_2 (1.5 mL) for 3 h to give the corresponding free base (60.0 mg, 75 %) as a white powder. UPLC-MS: t_R = 2.10 min (method A): MS (ESI) *m/z*: 553.0/555.0/557.0 $(M + H)^+$; $C_{27}H_{27}Cl_2N_6O_3$ $(M + H)^+$ calcd: 553.2/555.2/557.2. ^{1}H NMR (400 MHz, DMSO-d_6): δ 11.76 (br s, 1H), 8.80 (d, *J* = 2.4 Hz, 1H), 8.74 (t, *J* = 5.6 Hz, 1H), 8.54 (d, *J* = 4.8 Hz, 1H), 8.29 (s, 1H), 7.98 (dt, *J* = 8.0 and 2.0 Hz, 1H), 7.50 (d, *J* = 8.2 Hz, 1H), 7.47 (dd, *J* = 8.0 and 4.7 Hz, 1H), 7.33–7.23 (m, 2H), 7.19 (d, *J* = 8.2 Hz, 1H), 7.07 (dd, *J* = 7.7 and 1.8 Hz, 1H), 3.61 (t, *J* = 5.0 Hz, 4H), 3.40–3.37 (m, 2H), 3.00–2.86 (m, 4H), 2.45 (t, *J* = 7.2 Hz, 2H), 1.83 (p, *J* = 7.0 Hz, 2H). General procedure G was followed using the isolated free base (0.059 g, 0.107 mmol) and HCl (4 N) in 1,4-dioxane (0.27 mL) in 1,4-dioxane (1.00 mL), affording the pure salt **18** (54.0 mg, 86 %) as a light-yellow powder after lyophilization. ^{1}H NMR (400 MHz, DMSO-d_6): δ 11.96 (s, 1H), 9.09 (d, *J* = 2.2 Hz, 1H), 8.78 (dd, *J* = 5.4 and 1.4 Hz, 1H), 8.71 (t, *J* = 5.8 Hz, 1H), 8.60 (dt, *J* = 8.4 and 1.9 Hz, 1H), 8.38 (d, *J* = 1.8 Hz, 1H), 7.94 (dd, *J* = 8.2 and 5.4 Hz, 1H), 7.63 (dd, *J* = 8.2 and 1.9 Hz, 1H), 7.36–7.18 (m, 3H), 7.07 (dd, *J* = 7.6 and 2.0 Hz, 1H), 3.66–3.58 (m, 4H), 3.38 (q, *J* = 6.6 Hz, 2H), 2.96 (t, *J* = 4.9 Hz, 2H), 2.91 (t, *J* = 5.0 Hz, 2H), 2.45 (t, *J* = 7.3 Hz, 2H), 1.83 (p, *J* = 7.1 Hz, 2H). ^{13}C NMR (101 MHz, DMSO-d_6): δ 170.3, 153.6, 151.2, 150.8, 142.0, 141.6, 140.7, 138.4, 132.6, 129.1, 128.5, 128.3, 126.4, 126.2, 124.7, 123.1, 119.8, 112.9, 110.2, 51.2, 50.8, 45.1, 41.2, 38.9 (confirmed by ^{1}H–^{13}C HSQC), 29.5, 24.8. UPLC-MS purity (UV at 215 nm): 95.7 %; t_R = 4.44 min (method D). MS (ESI) *m/z*: 553.32/555.29/557.33 $(M + H)^+$. HRMS (ESI) *m/z*: calcd for $C_{27}H_{27}Cl_2N_6O_3$ $(M + H)^+$ 553.1513; found: 553.1516.

3.2. Biology

3.2.1. D3R dopamine receptor cellular assays

Both agonistic and antagonistic activities on D3R were evaluated with a cAMP HTRF (cyclic adenosine 3′,5′-monophosphate) functional assay (cAMP dynamic 2, CISBIO) on stably transfected human-DRD3 expressing CHO–K1 cells. The assays (agonist and antagonist) measure the intracellular cAMP modulation (decrease and increase, respectively) following compounds' treatment. D3R assays were run in 384 well microplates (384 Well Small Volume™ HiBase Polystyrene Microplates, Greiner) in a total reaction volume of 20 μL. Briefly, the cells are suspended in HBSS buffer (Life Technologies) complemented with 20 mM Hepes/NaOH (pH 7.4), 0.1 % BSA and 200 μM IBMX. Cells are then seeded in 384 multiwell microplates at a density of 10^4 cells/well in the presence of either the HBSS (basal control), the reference agonist or antagonist (stimulated control) or various concentrations of the test compounds. After 10 min of pre-incubation at rt, 10 nM DA is added to antagonist reaction mix for further 10 min. Thereafter, to increase

intracellular cAMP levels, the adenylyl cyclase activator NKH 477 (N3290, Sigma) is added at a final concentration of 0.5 or 1.5 μM, for agonist and antagonist assay, respectively. Following 45 min incubation at rt, the cells are lysed and the fluorescence acceptor (D2-labeled cAMP) and fluorescence donor (anti-cAMP antibody labeled with europium cryptate) are added. After 1 h at rt, the fluorescence transfer is measured at $\lambda_{ex} = 320$ nm and $\lambda_{em} = 620$ and 665 nm using EnVision 2014 Multilabel Reader (PerkinElmer, Massachusetts, USA) and the cAMP concentration was determined by dividing the signal measured at 665 nm by that measured at 620 nm (ratio). The compounds were tested at 10 different concentrations ranging from 100 pM up to 10 μM in technical triplicates. The results were expressed as a percent of the control response to 300 nM or 10 nM DA, for agonist and antagonist assay, respectively.

3.2.2. GSK-3β kinase assay

The inhibitory potency against human recombinant GSK-3β (Carna Biosciences) was evaluated using the LANCE® Ultra time-resolved fluorescence resonance energy transfer (TR-FRET) (PerkinElmer), by measuring the phosphorylation of the specific substrate human muscle glycogen synthase (ULight-GS (Ser641/pSer657)), according to the manufacturer's instructions. Briefly, test compounds, staurosporine (reference compound) or DMSO (control) are mixed with the enzyme (2 nM) in a buffer containing 50 mM Hepes (pH 7.5), 1 mM EGTA, 10 mM $MgCl_2$, 2 mM DTT and 0.01 % Tween-20. The reaction is initiated by adding 50 nM of the substrate ULight-PASVPPSPSLSRHSSPHQ(pS)ED and 0.7 μM ATP, and the mixture is incubated for 1 h at 23 °C. Following incubation, the reaction is stopped by adding 8 mM EDTA. After 5 min, the anti-phospho-GS antibody labeled with europium chelate is added. After 1 more hour, the kinase reaction is monitored by irradiation at 320 nm, and the fluorescence measured at 615 and 665 nm, using EnVision 2014 Multilabel Reader (PerkinElmer). The calculated signal ratio at 665/615 nm is proportional to the extent of ULight-GS phosphorylation. The compounds were tested at 11 concentrations ranging from 1 nM up to 100 μM in technical triplicates. For a few compounds with poor solubility or potency, percentage of inhibition at one concentration (1 μM and 100 μM, respectively) were determined. The results were expressed as a percent inhibition of the control enzyme activity.

3.3. ADME profiling studies

3.3.1. Microsomal stability study

10 mM DMSO stock solution of test compound was pre-incubated at 37 °C for 15 min with mouse/human liver microsomes (0.5 mL at 20 mg protein/mL) added 0.1 M Tris-HCl buffer (pH 7.4). The final concentration was 4.6 μM. After pre-incubation, the cofactors (NADPH, G6P, G6PDH and $MgCl_2$ pre-dissolved in 0.1 M Tris-HCl) were added to the incubation mixture (final concentration 1 mg protein/mL) and the incubation was continued at 37 °C for 1 h. At each time point (0.5, 15, 30, 60 min), 30 μL of incubation mixture was diluted with 200 μL cold CH_3CN spiked with 200 nM of internal standard, followed by centrifugation at 3.270*g* for 15 min. The supernatant was further diluted with H_2O (1:1) for analysis. The concentration of test compound was quantified by LC-MS/MS on a Waters ACQUITY UPLC-MS system consisting of a triple quadrupole detector (TQD) mass spectrometer equipped with an electrospray ionization interface (ESI) and a photodiode array detector (PDA) from Waters Inc. (Milford, MA, USA). The analyses were run on an ACQUITY UPLC BEH C_{18} (50 × 2.1 mm ID, particle size 1.7 μm) with a VanGuard BEH C_{18} pre-column (5 × 2.1 mm ID, particle size 1.7 μm) at 40 °C, using H_2O + 0.1 % HCOOH (A) and CH_3CN + 0.1 % HCOOH (B) as mobile phase. Electrospray ionization was applied in positive mode. Compound-dependent parameters as MRM transitions and collision energy were developed for each compound. The percentage of test compound remaining at each time point relative to t = 0 was calculated by the response factor on the basis of the internal standard peak area. The percentage of test compound versus time was plotted and fitted by GraphPad Prism (GraphPad Software, Version 5 for Windows, CA, USA, www.graphpad.com) to estimate the compounds half-life (t½) which was reported as mean value along with the standard deviation (*n = 3*).

3.3.2. Plasma stability study

10 mM DMSO stock solution of test compound was diluted 50-fold with DMSO-H_2O (1:1) and incubated at 37 °C for 2 h with mouse plasma added 5 % DMSO (pre-heated at 37 °C for 10 min). The final concentration was 2 μM. At each time point (0.5, 15, 30, 60, 120 min), 50 μL of incubation mixture was diluted with 200 μL cold CH_3CN spiked with 200 nM of internal standard, followed by centrifugation at 3500*g* for 20 min. The supernatant was further diluted with H_2O (1:1) for analysis. The concentration of test compound was quantified by LC-MS/MS on a Waters ACQUITY UPLC-MS TQD system as described above. The analyses were run on an ACQUITY UPLC BEH C_{18} (50 × 2.1 mm ID, particle size 1.7 μm) with a VanGuard BEH C_{18} pre-column (5 × 2.1 mm ID, particle size 1.7 μm) at 40 °C, using H_2O + 0.1 % HCOOH (A) and CH_3CN + 0.1 % HCOOH (B) as mobile phase. Electrospray ionization - was applied in positive mode. Compound-dependent parameters as MRM transitions and collision energy were developed for each compound. The percentage of test compound remaining at each time point relative to t = 0 was calculated by the response factor on the basis of the internal standard peak area. The percentage of test compound versus time was plotted and fitted by GraphPad Prism (GraphPad Software, Version 5 for Windows, CA, USA, www.graphpad.com) to estimate the compounds half-life (t½) which was reported as mean value along with the standard deviation (*n = 3*).

3.3.3. ADME-tox study

P-gp inhibition (MDR1-MDCKII, calcein AM substrate, 2 μM) assay was carried out by Eurofins Cerep SA France (Celle l'Evescault France), using previously described methods [26,60]. The selected compound (**16**) was tested at two concentrations (1 and 10 μM) in duplicate on human recombinant MDCKII cells. In each experiment, Verapamil was used as reference compound. The percent of control activity was calculated by comparing the signal obtained in the presence of the test compound to the vehicle control. Subsequently, the percent inhibition was calculated by subtracting the percent control activity from 100.

3.3.4. MetID and HLM stability

Samples of test compound at 5 μM were incubated for 0, 5, 15, 30 and 60 min at 37 °C in a 0.1 M phosphate buffer (pH 7.4) containing HLM (0.5 mg/mL, pool of 50 donors; Gibco cat. HMMCPL, Lot #PL050E-A). The reactions were started by addition of 1 mM NADPH. At each time points an aliquot of reactions mixture was taken and quenched with ice-cold acetonitrile 2:1 (containing internal standard). Proteins were precipitated by centrifugation at 21000*g* for 10 min at 4 °C. Blank sample was prepared by incubating cell solution without any compound for 60 min. Metabolite identification was performed for all analyses on an UHPLC system interfaced with an Agilent mass spectrometer (Agilent, US). Chromatographic separation of metabolites was carried out on an Agilent 1290 Infinity Series with a Waters Acquity UPLC BEH C_{18} column (1.7 μm, 2.1 × 100 mm). The mobile phases consisted of 0.1 % formic acid in water (A) and acetonitrile + 0.1 % formic acid (B), respectively. The LC gradient was as follow: 0–8 min 0–95 % B, 8–10 min 95-95 % and (post time) 10–12 min 95-5 % B, at a flow rate of 0.65 mL/min. The Agilent Technology 6540 UHD Accurate Mass Q-TOF LC/MS system was operated under positive conditions with Dual JetStream source (ESI family) in the following conditions: Gas Temp 250 °C, Drying Gas: 9 L/min, Nebulizer: 35 psi, Sheath Gas Temp: 250 °C, Sheath Gas Flow: 9 L/min, Vcap: 4000 V, Nozzle Voltage: 0 V, Fragmentor: 120 V, Skimmer: 65 V, OCT RF Vpp: 750 V. The acquisition was performed in AutoMSMS mode using a mass list to trigger the MSMS acquisition based on the accurate masses computed by Mass-MetaSite. The conditions were: MS range: 100–1700 *m/z*, rate 3 spectra/s; MS/

MS range: 100–1000 *m/z*, Rate 8 spectra/s; Isolation Width: "medium (4 *m/z*); Fixed Collision energy 30 V, max 1 precursor Per Cycle, Abs. Precursor threshold 100 counts, Rel Threshold 0.01 %. The MS/MS data were processed using MassMetaSite **4.5.0–2** in the WebMetabase application encapsulated in the web platform Oniro version 1.4.2 (MassAnalytica™).

3.4. Cellular assays in neuronal SH-SY5Y cells

3.4.1. Cell cultures

Human neuronal SH-SY5Y cells (Sigma Aldrich, St. Louis, MO, USA) were routinely grown in Dulbecco's modified Eagle's Medium supplemented with 10 % fetal bovine serum, 2 mM L-glutamine, 50 U/mL penicillin and 50 μg/mL streptomycin at 37 °C in a humidified incubator with 5 % CO_2.

3.4.2. Neuronal viability

SH-SY5Y cells were seeded in a 96-well plate at 2×10^4 cells/well, incubated for 24 h and then treated with various concentrations (1.25–40 μM) of compound **5** (ARN25297) or **16** (ARN25657) for 24 h. Cell viability, in terms of mitochondrial activity, was evaluated by 3-(4,5-dimethylthiazol-2-yl)-2,5-diphenyltetrazolium bromide (MTT) colorimetric assay, as previously described [61].

3.4.3. Western blotting

SH-SY5Y cells were seeded in 60 mm dishes at 2×10^6 cells/dish, incubated for 24 h and subsequently treated with compound **5** (ARN25297) (0.5–1 μM) or **16** (ARN25657) (1–5 μM) for 3 h at 37 °C in 5 % CO_2. At the end of the incubation, cells were trypsinized and the cellular pellet was resuspended in complete lysis buffer containing leupeptin (2 μg/mL), PMSF (100 μg/mL) and cocktail of protease/phosphatase inhibitors (100 ×). Protein concentration was determined using the Bradford method. The samples (30 μg proteins) were run on 4–15 % SDS polyacrylamide gels (Bio-rad Laboratories S.r.L., Hercules, CA, USA) and electroblotted onto 0.45 μm nitrocellulose membranes. The membrane was incubated at 4 °C overnight with primary antibody recognizing phospho-GSK-3α/β (Ser21/9), (1:1000; Cell Signaling Technology Inc, Danvers, MA, USA). After washing with TBS-T (TBS + 0.05 % Tween20), the membrane was incubated with secondary antibody (1:2000; GE Healthcare). Enhanced chemiluminescence was used to visualize the bands (ECL; Bio-rad Laboratories). The membrane was then reprobed with GSK-3β (1:1000; Cell Signaling Technology Inc.) and β-Actin (1:1000; Sigma Aldrich, St. Louis, MO, USA) antibodies. Data were analyzed by densitometry, using Quantity One software (Bio-Rad Laboratories® S.r.L.). The values were normalized and expressed as mean ± SD of densitometry in each experimental group.

3.4.4. Statistical analysis

Results are shown as mean ± standard deviation (SD) of three independent experiments. Statistical analysis was performed using one-way ANOVA with Bonferroni post-hoc test. Differences were considered significant at $p < 0.05$. Analyses were performed using GraphPad PRISM software (version 5.0; GraphPad Software, La Jolla, CA, USA) on a Windows platform.

3.5. In vivo pharmacokinetic studies

3.5.1. Animals models

Male C57B6/J mice, 8 weeks old were used (Charles River). All procedures were performed in accordance with the Ethical Guidelines of European Communities Council (Directive 2010/63/EU of September 22, 2010) and accepted by the Italian Ministry of Health (N.322/2021-PR). All efforts were made to minimize animal suffering and to use the minimal number of animals required to produce reliable results, according to the "3Rs concept". Animals were group-housed in ventilated cages and had free access to food and water. They were maintained under a 12-h light/dark cycle (lights on at 8:00 a.m.) at controlled temperature (21 °C ± 1 °C) and relative humidity (55 % ± 10 %).

3.5.2. Administration and experimental design

ARN25297 (**5**) and ARN25657 (**16**) were administered P.O. and I.V. to C57BL/6 male mice at 10 and 3 mg/kg. The vehicle used was PEG400/Tween 80/saline solution at 10/10/80 % in volume, respectively. Three animals per each time point were treated. Blood samples at 0, 15, 30, 60, 120, 240, and 480 min after administration were collected for the P.O. arm. Blood samples at 0, 5, 15, 30, 60, 120, and 240 min after administration were collected for the I.V. arm. Plasma was separated from blood by centrifugation for 15 min at 1500 rpm a 4 °C, transferred to Eppendorf tubes, and frozen (−80 °C). Control animals treated with vehicle only were also included in the experimental protocol.

3.5.3. In vivo pharmacokinetic measurements

Plasma samples were centrifuged at 21100×*g* for 15 min at 4 °C. An aliquot of each plasma sample was extracted (1:3) with cold CH_3CN containing 200 nM of an appropriate internal standard. A calibration curve was prepared in blank mouse plasma over a 1 nM to 10 μM range. Three quality control samples were prepared by spiking the parent compound in blank mouse plasma to 20, 200 and 2000 nM as final concentrations. The calibrators and quality control samples were extracted (1:3) with the same extraction solution as the plasma samples. The plasma samples, calibrators and quality control samples were centrifuged at 3270×*g* for 15 min at 4 °C.

Whole brains were homogenized in 4 vol (v/w) homogenizing solution (Phosphate Buffer Saline:Protease inhibitor (100:1). An aliquot of each brain homogenate was extracted (1:3) with cold CH_3CN containing 200 nM of an appropriate internal standard. A calibration curve was prepared in naïve mouse brain homogenate over a 1 nM to 10 μM range. Three quality control samples were prepared by spiking the parent compound in naïve mouse brain homogenate to 20, 200 and 2000 nM as final concentrations. The calibrators and quality control samples were extracted (1:3) with the same extraction solution as the brain homogenates. The brain homogenates, calibrators and quality control samples were centrifuged at 3270×*g* for 20 min at 4 °C.

The supernatants of the extracted plasma samples, brain homogenates and respective calibrators and quality controls were further diluted (1:1) with H_2O, and analyzed by LC-MS/MS on a Waters ACQUITY UPLC-MS/MS system as defined above. The analyses were run on an ACQUITY UPLC BEH C_{18} (50 × 2.1 mm ID, particle size 1.7 μm) with a VanGuard BEH C_{18} pre-column (5 × 2.1 mm ID, particle size 1.7 μm) at 40 °C, using H_2O + 0.1 % HCOOH (A) and CH_3CN + 0.1 % HCOOH (B) as mobile phase. All samples were quantified by MRM peak area response factor in order to determine the levels of the parent compound in both plasma and brain. The plasma concentrations versus time were plotted, and the profiles were fitted using PK Solutions Excel Application (Summit Research Service, USA) in order to determine the pharmacokinetic parameters.

3.6. Selectivity studies

3.6.1. Binding assays

ARN25657 (**16**) was tested at 10 and 100 nM in duplicate in GPCRs binding assays at Eurofins Cerep (Celle l'Evescault France). Activity was assessed as inhibition of the binding of a radioactively labeled ligand specific for each target.

3.6.2. Kinome selectivity panel

ARN25657 (**16**) was tested at 0.1 and 10 μM in duplicate by using KinaseProfiler kinase activity radiometric assays [Km ATP] at Eurofins Cerep (Celle l'Evescault France). The results were expressed as a percent of inhibition of control specific activity obtained in the presence of the tested compounds.

3.7. Molecular modelling

3.7.1. Molecular dynamics

Systems were prepared according to the standard protein preparation protocol as implemented in Schrödinger (Schrödinger, Inc., USA). Only a single copy of protein and ligand atoms were retained from the crystallographic coordinates. Hydrogens were added by the software, optimizing the hydrogen-bonding pattern, with protonation states and tautomers assigned at pH 7.4. The force field used was OPLS4 [62]. The system was solvated in an orthorhombic box whose dimensions were automatically calculated assigning a 12 Å buffer in each direction. The system was neutralized considering a 0.15 M salt concentration. Each system encompassed roughly 52000 atoms. The system was first minimized by means of a 100 ps Brownian motion simulation and then thermalized according to the NPT relax protocol implemented in Schrödinger. Simulations were carried out for 1000 ns, using a RESPA integrator with 2 fs timestep in an NPT ensemble. Temperature was set at 300 K and regulated by a Nose-Hoover chain thermostat; pressure was set at 1.01 bar using the Martyna-Tobias-Klein barostat. Coordinates were written every 100 ps collecting 10000 frames from each trajectory.

pKa predictions. Empirical pKa predictions were performed using Epik as implemented in Schrödinger [63].

3.8. GSK-3β purification, crystallization, diffraction data collection on protein crystals

Human full-length GSK-3β sequence was overexpressed in High Five insect cells and purified as previously described [64].

GSK-3β protein was concentrated to 3–4 mg/mL. Drops were prepared by mixing 1 μL of protein solution with 1 μL of reservoir solution (20 mM Hepes pH 7.5, 50 mM $MgCl_2$, 15–20 % polyethylene glycol 3350). Crystals were grown with the hanging drop vapor diffusion method and protein crystals appeared within 1–2 days. Apo crystals were soaked in the reservoir buffer supplemented with 6–8 % glycerol and 1 mM final concentration of each compound (**1**, **11** and **16**). Crystals were then flash-frozen in liquid nitrogen, after 5–6 h of soaking.

X-ray diffraction data were collected at the XRD2 beamline in Elettra Synchrotron, Trieste, Italy (see Table S1 in the Supporting Information). For all the crystals, total 720 diffraction images were collected each corresponding to 0.5 degree rotation, finally covering entire 360 degree of reciprocal space. Data integration was performed using XDS [65]. Data scaling is performed using AIMLESS [66].

Structures were solved by molecular replacement with PHASER and refined using PHENIX.REFINE in PHENIX [67]. The structure 7U36 has been used as starting model for molecular replacement. Model modification, visualization and evaluation was performed using Coot [68]. The structures have been deposited in the PDB with accession codes 9HUK (**1**), 9HUL (**11**) and 9HV3 (**16**) and will be released upon publication.

CRediT authorship contribution statement

R.M.C. Di Martino: Writing – review & editing, Writing – original draft, Project administration, Methodology, Formal analysis, Data curation, Conceptualization. **D. Russo:** Writing – review & editing, Methodology, Formal analysis, Data curation. **I. Penna:** Writing – review & editing, Methodology, Formal analysis, Data curation. **S. Demuro:** Writing – review & editing, Methodology, Data curation. **A. Dalle Vedove:** Writing – review & editing, Methodology, Formal analysis, Data curation. **R. Spagnuolo:** Writing – review & editing, Methodology, Data curation. **G. Ottonello:** Writing – review & editing, Methodology, Data curation. **S.M. Bertozzi:** Writing – review & editing, Methodology, Data curation. **M. Summa:** Writing – review & editing, Methodology. **J. Desantis:** Writing – review & editing, Methodology. **A. Valeri:** Writing – review & editing, Methodology, Data curation. **L. Pruccoli:** Data curation, Formal analysis, Methodology, Writing – review & editing. **S.K. Tripathi:** Methodology. **A. Tarozzi:** Data curation, Formal analysis, Methodology, Supervision, Writing – review & editing. **P. Storici:** Writing – review & editing, Supervision, Formal analysis. **S. Girotto:** Writing – review & editing, Supervision, Formal analysis. **R. Bertorelli:** Writing – review & editing, Supervision, Formal analysis, Data curation. **A. Armirotti:** Writing – review & editing, Supervision, Formal analysis. **G. Cruciani:** Writing – review & editing, Supervision, Formal analysis, Data curation. **T. Bandiera:** Writing – review & editing, Supervision, Formal analysis. **A. Cavalli:** Writing – review & editing, Supervision, Resources, Formal analysis, Conceptualization, project administration. **G. Bottegoni:** Writing – review & editing, Writing – original draft, Supervision, Project administration, Methodology, Formal analysis, Data curation, Conceptualization.

Notes

The authors declare no competing financial interest.

Declaration of competing interest

The authors declare that they have no known competing financial interests or personal relationships that could have appeared to influence the work reported in this paper.

Acknowledgments

The authors thank Silvia Venzano for compound handling and Dr. Luca Goldoni for his support with 2D NMR experiments (both from the Istituto Italiano di Tecnologia Genova, Italy); Dr. Barbara Giabbai for human full-length GSK-3β sequence expression, and the staff of XRD2 beamline of Elettra Sincrotrone Trieste (Trieste, Italy). The graphical abstract has been created with BioRender.com.

Appendix A. Supplementary data

Supplementary data to this article can be found online at https://doi.org/10.1016/j.ejmech.2025.117899.

Abbreviations

BD	bipolar disorder
CDK5	cyclin dependent kinase 5
CHO	Chinese hamster ovary
CL	clearance
DYRK	dual-specificity tyrosine-regulated kinases
F	fraction absorbed (bioavailability)
FYN	FYN proto-oncogene, Src family tyrosine kinase
GSK-3	glycogen synthase kinase-3
HLM	human liver microsomes

(*continued on next page*)

(*continued*)

HTRF	homogeneous time resolved fluorescence
MD	molecular dynamics
MDCKII	Madin-Darby canine kidney strain II
MetID	metabolite identification
MLM	mouse liver microsomes
MTDL	multi-target-directed ligand
OBP	orthosteric binding pocket
PP	primary pharmacophore
RMSD	root mean square deviation
SBP	specificity binding pocket
SCX	strong cation exchange
SQD	single quadrupole detector
TR-FRET	time-resolved fluorescence energy transfer
V_D	volume of distribution

Data availability

Data will be made available on request.

References

[1] E. Vieta, M. Berk, T.G. Schulze, A.F. Carvalho, T. Suppes, J.R. Calabrese, K. Gao, K. W. Miskowiak, I. Grande, Bipolar disorders, Nat. Rev. Dis. Primers 4 (1) (2018) 18008.

[2] J. Guzman-Parra, F. Streit, A.J. Forstner, J. Strohmaier, M.J. González, S. Gil Flores, F.J. Cabaleiro Fabeiro, F. del Río Noriega, F. Perez Perez, J. Haro González, G. Orozco Diaz, Y. de Diego-Otero, B. Moreno-Kustner, G. Auburger, F. Degenhardt, S. Heilmann-Heimbach, S. Herms, P. Hoffmann, J. Frank, J.C. Foo, L. Sirignano, S. H. Witt, S. Cichon, F. Rivas, F. Mayoral, M.M. Nöthen, T.F.M. Andlauer, M. Rietschel, Clinical and genetic differences between bipolar disorder type 1 and 2 in multiplex families, Transl. Psychiatry 11 (1) (2021) 31.

[3] P. Magioncalda, M. Martino, A unified model of the pathophysiology of bipolar disorder, Mol. Psychiatry 27 (1) (2022) 202–211.

[4] A.H. Ashok, T.R. Marques, S. Jauhar, M.M. Nour, G.M. Goodwin, A.H. Young, O. D. Howes, The dopamine hypothesis of bipolar affective disorder: the state of the art and implications for treatment, Mol. Psychiatry 22 (5) (2017) 666–679.

[5] M.P. Dandekar, S.S. Valvassori, G.C. Dal-Pont, J. Quevedo, Glycogen synthase Kinase-3β as a putative therapeutic target for bipolar disorder, Curr. Drug Metab. 19 (8) (2018) 663–673.

[6] G. Furlotti, M.A. Alisi, N. Cazzolla, P. Dragone, L. Durando, G. Magarò, F. Mancini, G. Mangano, R. Ombrato, M. Vitiello, A. Armirotti, V. Capurro, M. Lanfranco, G. Ottonello, M. Summa, A. Reggiani, Hit optimization of 5-Substituted-N-(piperidin-4-ylmethyl)-1H-indazole-3-carboxamides: potent glycogen synthase Kinase-3 (GSK-3) inhibitors with in vivo activity in model of mood disorders, J. Med. Chem. 58 (22) (2015) 8920–8937.

[7] F. Prati, R. Buonfiglio, G. Furlotti, C. Cavarischia, G. Mangano, R. Picollo, L. Oggianu, A. di Matteo, S. Olivieri, G. Bovi, P.F. Porceddu, A. Reggiani, B. Garrone, F.P. Di Giorgio, R. Ombrato, Optimization of indazole-based GSK-3 inhibitors with mitigated hERG issue and in vivo activity in a mood disorder model, ACS Med. Chem. Lett. 11 (5) (2020) 825–831.

[8] Y. Gao, S. Peterson, B. Masri, M.T. Hougland, N. Adham, I. Gyertyán, B. Kiss, M. G. Caron, R.S. El-Mallakh, Cariprazine exerts antimanic properties and interferes with dopamine D2 receptor β-arrestin interactions, Pharmacol. Res. Perspect. 3 (1) (2015) e00073.

[9] J.M. Beaulieu, R.R. Gainetdinov, M.G. Caron, The Akt-GSK-3 signaling Cascade in the actions of dopamine, Trends Pharmacol. Sci. 28 (4) (2007) 166–172.

[10] B. Masri, A. Salahpour, M. Didriksen, V. Ghisi, J.M. Beaulieu, R.R. Gainetdinov, M. G. Caron, Antagonism of dopamine D2 receptor/beta-arrestin 2 interaction is a common property of clinically effective antipsychotics, Proc. Natl. Acad. Sci. U. S. A. 105 (36) (2008) 13656–13661.

[11] J.M. Azorin, N. Simon, Dopamine receptor partial agonists for the treatment of bipolar disorder, Drugs 79 (15) (2019) 1657–1677.

[12] C. Volkmann, T. Bschor, S. Köhler, Lithium treatment over the lifespan in bipolar disorders, Front. Psychiatry 11 (2020) 377.

[13] G.S. Malhi, C. McAulay, S. Gershon, D. Gessler, K. Fritz, P. Das, T. Outhred, The lithium battery: assessing the neurocognitive profile of lithium in bipolar disorder, Bipolar Disord. 18 (2) (2016) 102–115.

[14] E. Beurel, S.F. Grieco, R.S. Jope, Glycogen synthase kinase-3 (GSK3): regulation, actions, and diseases, Pharmacol. Ther. 148 (2015) 114–131.

[15] S.M. Stahl, Drugs for psychosis and mood: unique actions at D3, D2, and D1 dopamine receptor subtypes, CNS Spectr. 22 (5) (2017) 375–384.

[16] R.M.C. Di Martino, A. Cavalli, G. Bottegoni, Dopamine D3 receptor ligands: a patent review (2014-2020), Expert Opin. Ther. Pat. 32 (6) (2022) 605–627.

[17] I. Gyertyán, B. Kiss, K. Sághy, J. Laszy, G. Szabó, T. Szabados, L.I. Gémesi, G. Pásztor, M. Zájer-Balázs, M. Kapás, E. Csongor, G. Domány, K. Tihanyi, Z. Szombathelyi, Cariprazine (RGH-188), a potent D3/D2 dopamine receptor partial agonist, binds to dopamine D3 receptors in vivo and shows antipsychotic-like and procognitive effects in rodents, Neurochem. Int. 59 (6) (2011) 925–935.

[18] A. Edinoff, M.T. Ruoff, Y.T. Ghaffar, A. Rezayev, D. Jani, A.M. Kaye, E.M. Cornett, A.D. Kaye, O. Viswanath, I. Urits, Cariprazine to treat schizophrenia and bipolar disorder in adults, Psychopharmacol. Bull. 50 (4) (2020) 83–117.

[19] F. Calabrese, F.I. Tarazi, G. Racagni, M.A. Riva, The role of dopamine D(3) receptors in the mechanism of action of cariprazine, CNS Spectr. 25 (3) (2020) 343–351.

[20] K. Levenberg, Z.A. Cordner, Bipolar depression: a review of treatment options, Gen. Psychiatr. 35 (4) (2022) e100760.

[21] B.T. Zhu, Rational design of receptor partial agonists and possible mechanisms of receptor partial activation: a theory, J. Theor. Biol. 181 (3) (1996) 273–291.

[22] E.S. Gogarnoiu, C.D. Vogt, J. Sanchez, A. Bonifazi, E. Saab, A.B. Shaik, O. Soler-Cedeño, G.-H. Bi, B. Klein, Z.-X. Xi, J.R. Lane, A.H. Newman, Dopamine D3/D2 receptor ligands based on cariprazine for the treatment of psychostimulant use disorders that may be dual diagnosed with affective disorders, J. Med. Chem. 66 (3) (2023) 1809–1834.

[23] M.L. Bolognesi, Harnessing polypharmacology with medicinal chemistry, ACS Med. Chem. Lett. 10 (3) (2019) 273–275.

[24] M.L. Bolognesi, A. Cavalli, Multitarget drug discovery and polypharmacology, ChemMedChem 11 (12) (2016) 1190–1192.

[25] V. Lembo, G. Bottegoni, Systematic investigation of dual-target-directed ligands, J. Med. Chem. 67 (12) (2024) 10374–10385.

[26] R.M.C. Di Martino, G. Bottegoni, F. Seghetti, D. Russo, I. Penna, A. De Simone, G. Ottonello, S. Mandrup Bertozzi, A. Armirotti, T. Bandiera, F. Belluti, A. Cavalli, Multitarget compounds for bipolar disorder: from rational design to preliminary pharmacokinetic evaluation, ChemMedChem 15 (11) (2020) 949–954.

[27] P. Grundt, E.E. Carlson, J. Cao, C.J. Bennett, E. McElveen, M. Taylor, R.R. Luedtke, A.H. Newman, Novel heterocyclic trans olefin analogues of N-{4-[4-(2,3-dichlorophenyl)piperazin-1-yl]butyl}arylcarboxamides as selective probes with high affinity for the dopamine D3 receptor, J. Med. Chem. 48 (3) (2005) 839–848.

[28] A.H. Newman, J. Cao, C.J. Bennett, M.J. Robarge, R.A. Freeman, R.R. Luedtke, N-(4-[4-(2,3-dichlorophenyl)piperazin-1-yl]butyl, butenyl and butynyl) arylcarboxamides as novel dopamine D(3) receptor antagonists, Bioorg. Med. Chem. Lett. 13 (13) (2003) 2179–2183.

[29] M. Pilla, S. Perachon, F. Sautel, F. Garrido, A. Mann, C.G. Wermuth, J.C. Schwartz, B.J. Everitt, P. Sokoloff, Selective inhibition of cocaine-seeking behaviour by a partial dopamine D3 receptor agonist, Nature 400 (6742) (1999) 371–375.

[30] G. Stemp, T. Ashmeade, C.L. Branch, M.S. Hadley, A.J. Hunter, C.N. Johnson, D. J. Nash, K.M. Thewlis, A.K. Vong, N.E. Austin, P. Jeffrey, K.Y. Avenell, I. Boyfield, J.J. Hagan, D.N. Middlemiss, C. Reavill, G.J. Riley, C. Routledge, M. Wood, Design and synthesis of trans-N-[4-[2-(6-cyano-1,2,3, 4-tetrahydroisoquinolin-2-yl)ethyl] cyclohexyl]-4-quinolinecarboxamide (SB-277011): a potent and selective dopamine D(3) receptor antagonist with high oral bioavailability and CNS penetration in the rat, J. Med. Chem. 43 (9) (2000) 1878–1885.

[31] R. Ando, K. Aritomo, A. Shoda, K. Watanabe, F. Uehara, K.-I. Saito, Carboxyamido Derivatives, 2001. WO01/42224A1.

[32] G. Bottegoni, M. Veronesi, P. Bisignano, P. Kacker, A.D. Favia, A. Cavalli, Development and application of a virtual screening protocol for the identification of multitarget fragments, ChemMedChem 11 (12) (2016) 1259–1263.

[33] M. Ferraro, S. Decherchi, A. De Simone, M. Recanatini, A. Cavalli, G. Bottegoni, Multi-target dopamine D3 receptor modulators: actionable knowledge for drug design from molecular dynamics and machine learning, Eur. J. Med. Chem. 188 (2020) 111975.

[34] A. Bonifazi, E. Saab, J. Sanchez, A.L. Nazarova, S.A. Zaidi, K. Jahan, V. Katritch, M. Canals, J.R. Lane, A.H. Newman, Pharmacological and physicochemical properties optimization for dual-target dopamine D(3) (D(3)R) and μ-Opioid (MOR) receptor ligands as potentially safer analgesics, J. Med. Chem. 66 (15) (2023) 10304–10341.

[35] A. Bonifazi, F.O. Battiti, J. Sanchez, S.A. Zaidi, E. Bow, M. Makarova, J. Cao, A. B. Shaik, A. Sulima, K.C. Rice, V. Katritch, M. Canals, J.R. Lane, A.H. Newman, Novel dual-target μ-Opioid receptor and dopamine D(3) receptor ligands as potential nonaddictive pharmacotherapeutics for pain management, J. Med. Chem. 64 (11) (2021) 7778–7808.

[36] T.T. Wager, X. Hou, P.R. Verhoest, A. Villalobos, Central nervous system multiparameter optimization desirability: application in drug discovery, ACS Chem. Neurosci. 7 (6) (2016) 767–775.

[37] A. Seelig, P-Glycoprotein: one mechanism, many tasks and the consequences for pharmacotherapy of cancers, Front. Oncol. 10 (2020) 576559.
[38] C. Jorgensen, M.B. Ulmschneider, P.C. Searson, Modeling substrate entry into the P-Glycoprotein efflux pump at the blood–brain barrier, J. Med. Chem. 66 (24) (2023) 16615–16627.
[39] J.-U. Peters, Polypharmacology – Foe or friend? J. Med. Chem. 56 (22) (2013) 8955–8971.
[40] R. Morphy, Z. Rankovic, Designed multiple ligands. An emerging drug discovery paradigm, J. Med. Chem. 48 (21) (2005) 6523–6543.
[41] A. De Simone, D. Russo, G.F. Ruda, A. Micoli, M. Ferraro, R.M. Di Martino, G. Ottonello, M. Summa, A. Armirotti, T. Bandiera, A. Cavalli, G. Bottegoni, Design, synthesis, structure-activity relationship studies, and three-dimensional quantitative structure-activity relationship (3D-QSAR) modeling of a series of O-Biphenyl carbamates as dual modulators of dopamine D3 receptor and fatty acid amide hydrolase, J. Med. Chem. 60 (6) (2017) 2287–2304.
[42] A. De Simone, G.F. Ruda, C. Albani, G. Tarozzo, T. Bandiera, D. Piomelli, A. Cavalli, G. Bottegoni, Applying a multitarget rational drug design strategy: the first set of modulators with potent and balanced activity toward dopamine D3 receptor and fatty acid amide hydrolase, Chem. Commun. 50 (38) (2014) 4904–4907.
[43] G. Cruciani, E. Carosati, B. De Boeck, K. Ethirajulu, C. Mackie, T. Howe, R. Vianello, MetaSite: understanding metabolism in human cytochromes from the perspective of the chemist, J. Med. Chem. 48 (22) (2005) 6970–6979.
[44] I. Zamora, F. Fontaine, B. Serra, G. Plasencia, High-throughput, computer assisted, specific MetID. A revolution for drug discovery, Drug Discov. Today Technol. 10 (1) (2013) e199–e205.
[45] A.H. Newman, T. Beuming, A.K. Banala, P. Donthamsetti, K. Pongetti, A. LaBounty, B. Levy, J. Cao, M. Michino, R.R. Luedtke, J.A. Javitch, L. Shi, Molecular determinants of selectivity and efficacy at the dopamine D3 receptor, J. Med. Chem. 55 (15) (2012) 6689–6699.
[46] E. Kirino, Profile of aripiprazole in the treatment of bipolar disorder in children and adolescents, Adolesc. Health Med. Ther. 5 (2014) 211–221.
[47] T. Hirose, Y. Uwahodo, S. Yamada, T. Miwa, T. Kikuchi, H. Kitagawa, K.D. Burris, C.A. Altar, T. Nabeshima, Mechanism of action of aripiprazole predicts clinical efficacy and a favourable side-effect profile, J. Psychopharmacol. 18 (3) (2004) 375–383.
[48] D.K. Grandy, M.A. Marchionni, H. Makam, R.E. Stofko, M. Alfano, L. Frothingham, J.B. Fischer, K.J. Burke-Howie, J.R. Bunzow, A.C. Server, et al., Cloning of the cDNA and gene for a human D2 dopamine receptor, Proc. Natl. Acad. Sci. U. S. A 86 (24) (1989) 9762–9766.
[49] R.G. MacKenzie, D. VanLeeuwen, T.A. Pugsley, Y.H. Shih, S. Demattos, L. Tang, R. D. Todd, K.L. O'Malley, Characterization of the human dopamine D3 receptor expressed in transfected cell lines, Eur. J. Pharmacol. 266 (1) (1994) 79–85.
[50] M. Rinaldi-Carmona, B. Calandra, D. Shire, M. Bouaboula, D. Oustric, F. Barth, P. Casellas, P. Ferrara, G.L. Fur, Characterization of two cloned human CB1 cannabinoid receptor isoforms, J. Pharmacol. Exp. Ther. 278 (2) (1996) 871–878.
[51] J.G. Mulheron, S.J. Casañas, J.M. Arthur, M.N. Garnovskaya, T.W. Gettys, J. R. Raymond, Human 5-HT1A receptor expressed in insect cells activates endogenous G(o)-like G protein(s), J. Biol. Chem. 269 (17) (1994) 12954–12962.
[52] H.U. Bryant, D.L. Nelson, D. Button, H.W. Cole, M.B. Baez, V.L. Lucaites, D. B. Wainscott, C. Whitesitt, J. Reel, R. Simon, G.A. Koppel, A novel class of 5-HT2A receptor antagonists: aryl aminoguanidines, Life Sci. 59 (15) (1996) 1259–1268.
[53] F. Ahmad, H. Marzook, A. Gupta, A. Aref, K. Patil, A.A. Khan, M.A. Saleh, W. J. Koch, J.R. Woodgett, R. Qaisar, GSK-3α aggravates inflammation, metabolic derangement, and cardiac injury post-ischemia/reperfusion, J. Mol. Med. (Berl) 101 (11) (2023) 1379–1396.
[54] T. Neumann, L. Benajiba, S. Göring, K. Stegmaier, B. Schmidt, Evaluation of improved glycogen synthase Kinase-3α inhibitors in models of acute myeloid leukemia, J. Med. Chem. 58 (22) (2015) 8907–8919.
[55] Y. Yang, X. Fan, Y. Liu, D. Ye, C. Liu, H. Yang, Z. Su, Y. Zhang, Y. Liu, Function and inhibition of DYRK1A: emerging roles of treating multiple human diseases, Biochem. Pharmacol. 212 (2023) 115521.
[56] E. Lana-Elola, R. Aoidi, M. Llorian, D. Gibbins, C. Buechsenschuetz, C. Bussi, H. Flynn, T. Gilmore, S. Watson-Scales, M. Haugsten Hansen, D. Hayward, O. R. Song, V. Brault, Y. Herault, E. Deau, L. Meijer, A.P. Snijders, M.G. Gutierrez, E. M.C. Fisher, V.L.J. Tybulewicz, Increased dosage of DYRK1A leads to congenital heart defects in a mouse model of Down syndrome, Sci. Transl. Med. 16 (731) (2024) eadd6883.
[57] S. Demuro, R.M.C. Di Martino, J.A. Ortega, A. Cavalli, GSK-3β, FYN, and DYRK1A: master regulators in neurodegenerative pathways, Int. J. Mol. Sci. 22 (16) (2021).
[58] J.L. Barr, E.M. Unterwald, Glycogen synthase kinase-3 signaling in cellular and behavioral responses to psychostimulant drugs, Biochim. Biophys. Acta Mol. Cell Res. 1867 (9) (2020) 118746.
[59] X. Shi, J.S. Miller, L.J. Harper, R.L. Poole, T.J. Gould, E.M. Unterwald, Reactivation of cocaine reward memory engages the Akt/GSK3/mTOR signaling pathway and can be disrupted by GSK3 inhibition, Psychopharmacology (Berl) 231 (16) (2014) 3109–3118.
[60] J.W. Polli, S.A. Wring, J.E. Humphreys, L. Huang, J.B. Morgan, L.O. Webster, C. S. Serabjit-Singh, Rational use of in vitro P-glycoprotein assays in drug discovery, J. Pharmacol. Exp. Ther. 299 (2) (2001) 620–628.
[61] L. Pruccoli, F. Morroni, G. Sita, P. Hrelia, A. Tarozzi, Esculetin as a bifunctional antioxidant prevents and counteracts the oxidative stress and neuronal death induced by amyloid protein in SH-SY5Y cells, Antioxidants 9 (6) (2020) 551.
[62] C. Lu, C. Wu, D. Ghoreishi, W. Chen, L. Wang, W. Damm, G.A. Ross, M.K. Dahlgren, E. Russell, C.D. Von Bargen, R. Abel, R.A. Friesner, E.D. Harder, OPLS4: improving force field accuracy on challenging regimes of chemical space, J. Chem. Theor. Comput. 17 (7) (2021) 4291–4300.
[63] J.C. Shelley, A. Cholleti, L.L. Frye, J.R. Greenwood, M.R. Timlin, M. Uchimaya, Epik: a software program for pK(a) prediction and protonation state generation for drug-like molecules, J. Comput. Aided Mol. Des. 21 (12) (2007) 681–691.
[64] S. Demuro, C. Sauvey, S.K. Tripathi, R.M.C. Di Martino, D. Shi, J.A. Ortega, D. Russo, B. Balboni, B. Giabbai, P. Storici, S. Girotto, R. Abagyan, A. Cavalli, ARN25068, a versatile starting point towards triple GSK-3β/FYN/DYRK1A inhibitors to tackle tau-related neurological disorders, Eur. J. Med. Chem. 229 (2022) 114054.
[65] W. Kabsch, XDS. Acta Crystallogr. D Biol. Crystallogr. 66 (Pt 2) (2010) 125–132.
[66] P.R. Evans, G.N. Murshudov, How good are my data and what is the resolution? Acta Crystallogr. D Biol. Crystallagr. 69 (Pt 7) (2013) 1204–1214.
[67] D. Liebschner, P.V. Afonine, M.L. Baker, G. Bunkóczi, V.B. Chen, T.I. Croll, B. Hintze, L.W. Hung, S. Jain, A.J. McCoy, N.W. Moriarty, R.D. Oeffner, B.K. Poon, M.G. Prisant, R.J. Read, J.S. Richardson, D.C. Richardson, M.D. Sammito, O. V. Sobolev, D.H. Stockwell, T.C. Terwilliger, A.G. Urzhumtsev, L.L. Videau, C. J. Williams, P.D. Adams, Macromolecular structure determination using X-rays, neutrons and electrons: recent developments in phenix, Acta Crystallogr. D Struct. Biol. 75 (Pt 10) (2019) 861–877.
[68] P. Emsley, B. Lohkamp, W.G. Scott, K. Cowtan, Features and development of coot, Acta Crystallogr. D Biol. Crystallogr. 66 (Pt 4) (2010) 486–501.